5-2011

Wave Reflection Characteristics of Permeable and Impermeable Submerged Trapezoidal Breakwaters

Mathew Hornack
Clemson University, mhornack@gmail.com

WAVE REFLECTION CHARACTERISTICS OF PERMEABLE AND IMPERMEABLE SUBMERGED TRAPEZOIDAL BREAKWATERS

A Thesis
Presented to
the Graduate School of
Clemson University

In Partial Fulfillment
of the Requirements for the Degree
Master of Science
Civil Engineering

---

by
Mathew Carter Hornack
May 2011

Accepted by:
Dr. Firat Testik, Committee Chair
Dr. Abdul Khan
Dr. Nigel Kaye

ABSTRACT

The present study aims to quantify reflection coefficients in the vicinity of impermeable and permeable submerged trapezoidal breakwaters. Three impermeable breakwater models are tested, each with a unique side slope for the breakwater faces. Two permeable models are tested, one made of PVC pipe and the other consisting of golf balls contained within a mesh cage, to provide two separate porosities. Testing is carried out at the Clemson University Flow Physics Laboratory in a laboratory wave tank with the inclusion of a 1:20 sloping sandy beach to simulate natural environmental conditions. Wave elevations are collected during experiments by two capacitance wave gages. A dimensional analysis is conducted to identify the governing dimensionless parameters in this study. Based on experimental results, the relative submergence depth, h_c/H_i, is found to be of primary importance (h_c - depth of submergence, H_i - incident wave height). Breakwaters remain submerged throughout testing and gathered reflection coefficient values are compared to the parameter, h_c/H_i. The relationship between the reflection coefficient and the relative submergence depth of the breakwater is found to evolve through several stages as h_c/H_i increases. Initially, for plunging breakers occurring on the offshore breakwater face (corresponding to h_c/H_i values between 0.0 and roughly 0.5, depending on the breakwater face slope), the reflection coefficient is observed to strongly decay, without an explicit regard to varying breakwater slopes. From h_c/H_i values of roughly 0.5 to approximately 1.0, the reflection coefficient bulges in response to a shift in breaker types (from plunging to spilling), resulting in less energy

dissipation from wave-breaking and additional energy available for reflection from the structure. After the bulge, reflection coefficients generally decay as h_c/H_i increases. This region is associated with waves that do not break over the breakwater. Detailed discussions on reflection coefficient behavior with changing wave conditions are provided based upon our experimental observations. Predictive capabilities of reflection coefficient equations available in literature were tested using a large set of experimental data. The results from this study will assist those designing breakwaters by providing additional insight to further detail the hydrodynamic processes surrounding submerged breakwaters.

DEDICATION

This thesis is dedicated to my wonderful parents, Dr. and Mrs. Frederick Mathew Hornack, Jr. As I have grown and matured through the years I have learned to appreciate them more and more, and I thank them for their constant support and trust in all of my decisions and, above all, teaching me how to be a man. I only hope that this thesis will make them proud.

ACKNOWLEDGMENTS

Special thanks must be given to my advisor, Dr. Firat Y Testik, for his constant insight and guidance throughout this project as well as my other committee members, Dr. Nigel B Kaye and Dr. Abdul A Khan, for their input. I also would like to thank Dr. Paul B Zielinski for his design of the permeable breakwaters and for working with Mr. John Calabria of TaylorMade – Adidas Golf Co., who graciously donated the golf balls used in this study. Thanks must be given as well to the Department of Civil Engineering as a whole for their excellent staff, notably the support given by Mr. Danny Metz to all of the graduate students during their research. Finally, I would like to thank my best friend, Samuel Harrill, for constantly encouraging me throughout this assignment and being open to assist in reading and commenting on the content contained herein.

TABLE OF CONTENTS

Page

TITLE PAGE i

ABSTRACT ii

DEDICATION iv

ACKNOWLEDGMENTS v

LIST OF TABLES viii

LIST OF FIGURES ix

LIST OF PARAMETERS xii

CHAPTER

I. INTRODUCTION 1

Motivation 1
Submerged Breakwaters 1
Reflection vs. Transmission 3
Organization of Thesis 4

II. LITERATURE REVIEW 6

Introduction 6
Breakwater Types and Applications 6
Wave Kinematics Around a Breakwater 19
Breakwater Design Considerations 42
Environmental Impacts of Breakwaters 50

III. EXPERIMENTAL SETUP AND METHODOLOGY 53

Introduction 53
Experimental Setup 53
Experimental Procedure 59
Data Analysis 65
Experimental Parameters 65

Table of Contents (Continued)

Page

IV. WAVE REFLECTION ANALYSIS 69

Introduction 69
Dimensionless Parameters Governing Wave Reflection 69
Experimental Results 78
Evaluation of Reflection Coefficient Equations 96
Design Considerations 102

V. CONCLUSIONS 108

Conclusions 108
Future Work 111

APPENDICES 114

A: Permissions for Reuse 114

REFERENCES 121

LIST OF TABLES

Table		Page
2.1	Summary table of reflection coefficient parameterizations	31
3.1	Breakwater dimensions	56
3.2	Experimental conditions	65
4.1	Compilation of available C_r equations for permeable and impermeable breakwaters	99
4.2	Parameters of testing	104

LIST OF FIGURES

Figure		Page
2.1	Fixed emerged vertical breakwater diagram	7
2.2	Examples of concrete armour units	12
2.3	Cross section of in-place reefs at Sea Palling	16
2.4	Shoreline response to offshore breakwater placement	17
2.5	Beach volume change in the center of the bay at Sea Palling	17
2.6	Standing wave field description	20
2.7	Partial standing wave field schematic	21
2.8	Effect of surf similarity parameter on C_r	24
2.9	Breakwater parameter schematic	24
2.10	Reflection coefficient vs. wave height, water depth, and wave period	29
2.11	Phase shift versus χ for 2-D wave tank tests	34
2.12	Common forms of wave-breaking as a function of ξ	42
2.13	Comparison between the Hudson Formula and the van der Meer formulas for a permeable core	45
2.14	Segmented breakwater system parameter definitions	47
2.15	Site description of Lido di Dante	51
3.1	Wave tank schematic	54
3.2	Wave maker assembly	55
3.3	Breakwaters	57
3.4	Schematics for BW-4	58

List of Figures (Continued)

Figure Page

3.5 Experimental parameter schematic 59

3.6 Reflection coefficients at different relative gage spacings 61

3.7 Reflection coefficients at varying distances from barrier 62

3.8 Wave gage criteria 63

3.9 Barrier test comparison of a flat vs. sloped sandy beach 64

4.1 Dimensional analysis parameter definitions 70

4.2 Comparison of dimensionless groups and their effect on the reflection coefficient 73

4.3 C_r versus ξ for submerged structures 75

4.4 Effect of seawall slope on C_r for different wave periods (H_i/h = 0.21) 76

4.5 Effect of seawall slope on C_r for different wave heights (h/L = 0.45) 77

4.6 Effect of seawall slope on C_r for different wave heights (h/L = 0.09) 77

4.7 Reflection coefficients of impermeable breakwater tests 79

4.8 Comparison of experimental reflection coefficient values of impermeable submerged breakwaters with the Young and Testik (2011) parameterization 81

4.9 Breaker type of each experiment as observed at the impermeable breakwater 83

4.10 Enhanced presentation of bulge region for each breakwater 84

4.11 Visualization of bulge in reflection coefficient data 86

4.12 Comparison of BW-1 reflection coefficients measured from tests with exposed breakwater width reduction with Young and Testik (2011) parameterization 89

List of Figures (Continued)

Figure Page

4.13 Comparison of BW-2 reflection coefficients measured from tests with exposed breakwater width reduction with Young and Testik (2011) parameterization 90

4.14 Reflection coefficients of permeable breakwater tests 92

4.15 Comparison of reflection coefficients from impermeable (BW-2) and permeable (BW-4 and 5) breakwaters of the same shape 94

4.16 Breaker type of each experiment as observed at the permeable breakwaters 95

4.17 Breaker type regime diagram 96

4.18 Predictions of the reflection coefficient values by the equations tabulated in Table 4.1 compared to C_r values measured in the experiments conducted for submerged trapezoidal breakwaters 98

LIST OF PARAMETERS

a	Typical Coefficient
A	Breakwater Height
b	Typical Coefficient
B	Crest Width
β	Beach Slope Angle
C_c	Contraction Coefficient
C_r	Reflection Coefficient
C_t	Transmission Coefficient
C_d	Dissipation Coefficient
D_{50a}	Breakwater Armour Dimension
D_{n50}	Nominal Diameter
ρ_r	Mass Density of Rock
ρ_w	Mass Density of Water
Δ	Relative Buoyant Density
ΔL	Distance Between Wave Gages
Δx	Horizontal Distance From Barrier
E_i	Energy Component of Incident Wave
E_r	Energy Component of Reflected Wave
E_t	Energy Component of Transmitted Wave
E_d	Energy Component of Dissipated Wave
ε	Amplitude of Wave Paddle Excursion
f	Local Frequency Within a Wave Spectrum
F	Breakwater Length
Fr	Froude Number
g	Gravitational Acceleration
G	Breakwater Gap Length
γ	Phase Shift Angle
γ_b	Wave-Breaking Criteria
γ_s	Phase Shift for a Submerged Breakwater
h	Water Depth
h_b	Wave-Breaking Depth
h_c	Water Depth Above Breakwater Crest
h_t	Water Depth at Toe of Slope
h_x	Water Depth at Position x

List of Parameters (Continued)

H_b	Wave-Breaking Height
H_i	Incident Wave Height
$H_{i,crit}$	Critical Incident Wave Height
H_r	Reflected Wave Height
H_t	Transmitted Wave Height
H_s	Significant Wave Height
$H_{\max}$	Maximum Elevation Difference in Wave Envelope
$H_{\min}$	Minimum Elevation Difference in Wave Envelope
k	Wave Number
k_s	Shallow Water Wave Number
K_D	Stability Coefficient
K_{LOSS}	Loss Coefficient
L	Local Wavelength
L_o	Deep Water Wavelength
L_s	Linear Theory Shallow-Water Wavelength
M_{50}	Median Mass of Armour Unit
n	Represents an Arbitrary Integer
N	Maximum Number of Waves
P	Porosity of Structure
P_f	Permeability Factor
ϕ	Function
R_c	Relative Crest Height
Ri	Richardson Number
Re_{bw}	Breakwater Reynolds Number
s	Wave Steepness (H/L)
S	Damage Level
ξ	Surf Similarity Parameter
ξ_f	Frequency-Dependent Surf Similarity Parameter
ξ_h	Hughes and Fowler (1995) Parameter
ξ_m	Surf Similarity Parameter Determined From Mean Period
ξ_{mc}	Critical Mean Period Surf Similarity Parameter
ξ_o	Deep Water Surf Similarity Parameter
T	Wave Period
T_m	Mean Wave Period
T_t	Transmission Function

List of Parameters (Continued)

θ	Angle of Structure Slope
u	Velocity Term
W	Breakwater Face Slope Horizontal Width
x	Horizontal Position Along Breakwater Slope
x_c	Horizontal Position of Breakwater Crest
$x_{\max}$	Location of $H_{\max}$ in Wave Envelope
$x_{\min}$	Location of $H_{\min}$ in Wave Envelope
$X_{1,2}$	Descriptive Lengths for Wave Tank Setup (Figure 3.8)
X	Offshore Distance of Breakwater
X_c	Distance From Center of Breakwater to Wave Paddle
X_s	Salient Length
χ	Dimensionless Phase Shift Parameter
Y	Function

CHAPTER ONE

INTRODUCTION

1.1 MOTIVATION

The intent of this study is to quantify wave reflection characteristics around submerged trapezoidal breakwaters, providing additional insight to the hydrodynamic processes surrounding submerged breakwaters. A laboratory wave tank is employed to simulate the coastal wave environment. Breakwater parameters of interest are: slope of structure, porosity, relative submergence depth, and many more. Combining the laboratory findings of this research with field experience will assist those proposing future breakwater constructions. This will enable them to streamline their design for executing successful coastal protection projects.

1.2 SUBMERGED BREAKWATERS

As waves approach a shoreline, the breaking forces as well as other wave actions can suspend sediment particles. Suspended particles are then washed out to sea or drift alongshore. Beaches usually experience periods of accretion and erosion throughout their tidal cycles due to these sediment transport processes. A diminished beach is the result of the total erosion outweighing the total accretion. Eroding shorelines eliminate beaches and pose a threat to not only existing real estate, but also to the tourism industry of that coastal community.

Breakwaters are typical structures engaged within a coastal zone to alleviate the damage of destructive waves to nearby shorelines. As waves approach a breakwater, wave energy is reflected back to sea by the structure and may also be dissipated through the processes of wave-breaking. General concern and protest often arise in a community when placing such large structures into a coastal zone. Some common complaints are a contamination of the view from coastal real estate and a reduction of the water quality in the lee of an emerged structure. Submerged breakwaters, structures that are completely submerged beneath the mean water level, provide an alternative that addresses these concerns. A submerged breakwater offers the aesthetic benefit of eliminating any protrusion along the horizon. Also, the transmission of waves permits natural wave motions to continue past the structure, yielding a recirculation of water along the shoreline and preventing cases where pollution could build up and collect. Considering biological impacts, waves that break and spill over the structure allow oxidation throughout the water column which retains suitable environments for the development of marine life.

Submerged breakwaters are beneficial in more ways than simply protecting a shoreline. As previously stated, they have the ability to sustain the tourism industry within a coastal community while still offering adequate beach protection. Submerged breakwaters can also be used for several recreational purposes. Companies have designed submerged breakwaters, referred to as multi-purpose artificial surfing reefs, which harness a portion of wave energy while also creating desirable conditions for surfing, as described by ASR

Limited (2008). Another intriguing benefit of a multi-purpose artificial surfing reef is its resemblance to a natural habitat which will encourage marine biodiversity. Submerged breakwaters are also useful in preserving pre-existing structures which may experience excessive, damaging waves or be in danger of failure due to natural wear and tear.

1.3 REFLECTION VS. TRANSMISSION

Reflection coefficients from breakwaters quantify the amount of energy that a breakwater can reflect from an approaching wave. The energy that is not reflected or dissipated through the process of wave-breaking is transmitted past the breakwater. Wave transmission is a major factor in the design and placement of coastal structures. However, quantifying the transmitted wave energy past a structure can be a daunting task. One issue in defining transmission coefficients is ensuring the scale from field to laboratory studies is correct. Also, transmission coefficients cannot be accurately determined in instances where waves break, as the waves lose their sinusoidal form and become a distorted train of waves.

As a result of the limits to determining transmission coefficients accurately, reflection coefficients can be used for a more accurate understanding of the processes around a structure. Reflection coefficients depend upon, and therefore incorporate, all hydraulic processes occurring at a breakwater (Muttray et al., 2006). For instance, a wave with a plunging breaker will dissipate more energy than one with a spilling breaker, and this increase in energy dissipation reduces the available energy to be reflected from a

breakwater. Likewise, overtopping waves, and those that penetrate through the structure, reduce the reflection potential of a structure. Reflection coefficients can also give an idea of incident wave conditions, and have been used in previous studies (Sumer and Fredsøe, 2000) to understand structural stability issues involving scour.

Knowing the wave reflection coefficients induced by a coastal structure can also be of importance when considering longshore sediment transport. Structures placed offshore may still be in the path of longshore currents and, as sediment moves with the currents along the shore, turbulence occurring at areas where waves break and reflect off such structures may result in the deposition and build-up of sediment on the offshore side of the structure. In such instances, ignoring the reflection coefficients when designing a coastal structure could result in a depleted beach.

1.4 ORGANIZATION OF THESIS

The following thesis is separated into five chapters: the present Introduction, a Literature Review, a discussion of the Experimental Setup and Methodology, a presentation of the Experimental Results, and Conclusions which include a portion covering Future Work. The Literature Review (Chapter 2) gives an overview of breakwaters and relevant studies that have been performed. Wave envelopes, wave reflection, phase shifting, and wave transmission are topics contained therein. Chapter 3 presents the Experimental Setup and Methodology used in the experiments that were performed for the present study. Finally,

Chapter 4 presents the Experimental Results and Chapter 5 offers the Conclusions from the given results and addresses Future Work proposals.

CHAPTER TWO

LITERATURE REVIEW

2.1 INTRODUCTION

This chapter provides an overview of breakwaters and their effects on a shoreline. When considering the stability of beach communities, protecting the coasts from destructive energies of crashing waves is of utmost importance. Breakwaters are structures that dissipate and reflect some portion of the energy from approaching waves away from a specific protected zone. Using this definition, a variety of structure shapes and materials can be used to reflect wave energy from the coast, fulfilling the purpose of a breakwater. Applications for breakwaters extend beyond commercial beaches to the protection of ports, marinas, and harbors, as well as roads or any erodible area of concern. Resulting from such a vast range of applications, numerous breakwater designs have originated to serve various functions.

2.2 BREAKWATER TYPES AND APPLICATIONS

Breakwater Types

Fixed and Floating Breakwaters

The typical shapes of fixed (bottom-founded) breakwater structures are vertical, semi-circular, and trapezoidal. Vertical breakwaters (Figure 2.1) are upright structures whose face is nearly perpendicular to the bed slope. These structures are typically used to protect harbors and marinas where space needs to be saved. Semi-circular breakwaters

have curved faces and provide low reflection based on their wave-like shape. Due to the natural repose of rocks used in primitive breakwaters, a trapezoidal shape was logical for these early structures. Trapezoidal breakwaters are the most commonly used shape for fixed breakwaters in shallow water; thus, this will be the model shape used in this study. However, when dealing with deeper water, sloping sides accumulate volume and become more expensive to build, lending the need for a vertical breakwater and/or a combination of a vertical wall over a rubble-mound foundation in deeper water (Dong et. al, 2008).

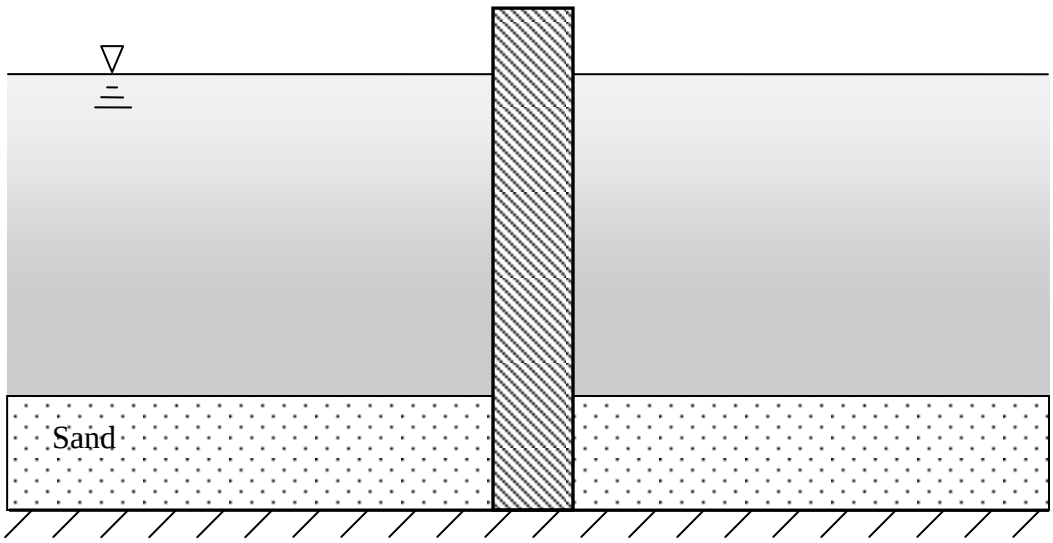

Figure 2.1. Fixed emerged vertical breakwater diagram (Sumer and Fredsøe, 1997).

Apart from fixed breakwaters, floating breakwaters are also reliable structures for protecting marinas and other areas where large waves are undesirable. In the modern world of deepwater drilling and growing technology, the need for wave sheltering is evident. Floating breakwaters are a viable option for the protection of offshore drilling structures and aquaculture. Mobility is another advantage of floating breakwaters. In

areas where a small amount of protection is needed, being able to orient the breakwater perpendicular to the approach angle of incoming waves is crucial. McCartney (1985) presents the following scenarios which support the use of a floating breakwater:

(1) Floating breakwaters might be the only option when dealing with poor foundations.

(2) Floating breakwaters are typically much cheaper in waters of depth > 20 ft (6.1 m).

(3) Floating breakwaters have less blocking of fish migration and circulation of water.

(4) Damaging ice formations can be avoided by moving the breakwater to a protected area.

(5) Floating breakwaters are aesthetically acceptable with low profiles that reduce the intrusion on the horizon, especially when an area has a high range of tides.

(6) Rearrangement of floating breakwaters into different layouts can be performed with relative ease.

McCartney (1985) describes three commonly used types of floating breakwaters: Tire Mat, Box, and Pontoon. The tire mat breakwaters are inexpensive and simple to construct, easily maneuverable, and distinguished by relatively low anchor loads and reflected waves. However, using tires to form a breakwater can attract marine growth and sediment accumulation in the bottom of the tire, and these may eventually sink the

breakwater. The design life of a tire mat breakwater is unknown and their applications are limited. Box-type breakwaters are usually constructed of reinforced-concrete units. They have a 50-year design life, a simple shape, and proven effectiveness. Box-type breakwaters can be costly to construct, though. Issues may arise if connectors are not adequately designed; due to the additional cost of docking the breakwaters for maintenance, these connectors must be well designed and time tested. Pontoon breakwaters have the same advantages and disadvantages of a box-type breakwater, but can be built either as a single pontoon, or with two pontoons (catamaran style).

Emerged and Submerged Breakwaters

In relation to the mean water level, breakwaters can be either emerged or submerged. Emerged breakwaters have been experimentally analyzed by several researchers (Hughes and Fowler, 1995; Sutherland and O'Donoghue, 1998b; Muttray et al., 2006; Zanuttigh and Van der Meer, 2008). Utilized in Long Beach, CA and Grand Isle, LA, emerged breakwaters are popular for coastal protection. Discussion of the Long Beach breakwater can be found later in this section and those in Grand Isle are located on the gulf coast, experiencing hurricane attacks almost annually. Their use primarily stems from a dire need to protect against historically dangerous and costly storms or wave action. While providing more protection than submerged breakwaters, emerged breakwaters have their drawbacks when considering aesthetics or environmental quality. For emerged rubble-mound breakwaters, their porosity allows for transmission of wave motion through the voids. This transmission may provide natural wave conditions in the lee of the structure,

after the installment of the breakwater. However, emerged structures are typically looked at as a last option for beach protection. Property owners and tourists alike want to see a natural beach and dislike the obstruction along the horizon. Effective submerged breakwaters can alleviate the concerns of a beach community looking to shelter the shoreline.

The crest of a submerged breakwater lies below the surface of the water. This configuration is not only aesthetically pleasing, but also useful in allowing mobility for boats or marine life across the breakwater. Such exchanges across the structure are a beneficial aspect of submerged breakwaters, enhancing their appeal in comparison to emerged breakwaters. The aesthetics of a breakwater are important because of the financial benefits that increased tourism brings to areas with clean beaches (Johnson, 2006). There are also smaller material requirements for the construction of submerged breakwaters, and they provide the opportunity to extend the life of existing structures by reducing the energy of approaching waves (Seabrook and Hall, 1998).

When designing a breakwater, upholding the existing longshore littoral transport (sediment transport along the intertidal zone) must be taken into consideration. Submerged breakwaters provide the benefit of protecting an erosive shoreline, while still allowing longshore transport by incoming waves. Having a system of efficient, submerged breakwaters will not only cut down on dredging costs for beach restoration, but will also sustain the aesthetic value of the beach. This keeps tourism levels high,

while hopefully reducing the cost of maintenance. In this study, submerged structures are investigated. However, to ensure the completeness of this literature review, findings of previous studies on emerged structures are also discussed.

Impermeable and Permeable Breakwaters

All breakwaters can be classified as either impermeable or permeable. Seawalls are a type of impermeable breakwater put in place to fix a point where the shoreline will stop retreating. Adversely, seawalls tend to increase erosion at the toe of the seawall and at any adjacent unprotected beaches. An interesting use of seawalls has appeared recently in the form of a seawall buried under a sand dune near Dam Neck, Virginia, preventing any excess damage from successive storms in the same season (Basco, 2000). Impermeable breakwaters in the form of pre-cast concrete units have been tested in Florida, Georgia, and New Jersey. These units may be preferred for their ease of removal or mobility in instances where they produce unexpected adverse effects or down drift impacts. Martin and Smith (1997) studied the effects of pre-cast wedge-shaped concrete units that were installed near Palm Beach, Florida. Overall, a "ponding" effect increased erosion in the lee of the breakwater due to higher water elevations and stronger currents, depositing sediment at the southern end of the structures. A similar response as a result of wave setup was observed by Ranasinghe et al. (2010) for submerged breakwaters under high tidal ranges.

Permeable breakwaters include a certain porosity which allows energy dissipation throughout the width of the breakwater. The most common of these is a rubble-mound structure, comprised of a core underlayer of fine material covered with an armour layer of larger stone. Examples of various concrete armour units, including CORE-LOC® studied by Melito and Melby (2002), are shown in Figure 2.2. Figure 2.2 comes from The Coastal Engineering Manual (CEM) prepared by the U.S. Army Corps of Engineers (2006). At a porous structure, energy dissipation occurs through wave breaking, friction from the sea bed, and percolation within the structure (Johnson, 2006). Wave energy dissipation is a major benefit of porous breakwaters as it reduces the amount of energy reflected and transmitted. High wave reflection should be avoided to prevent erosion at the base of a structure, and therefore porous structures are typically selected over solid ones (Twu and Chieu, 2000).

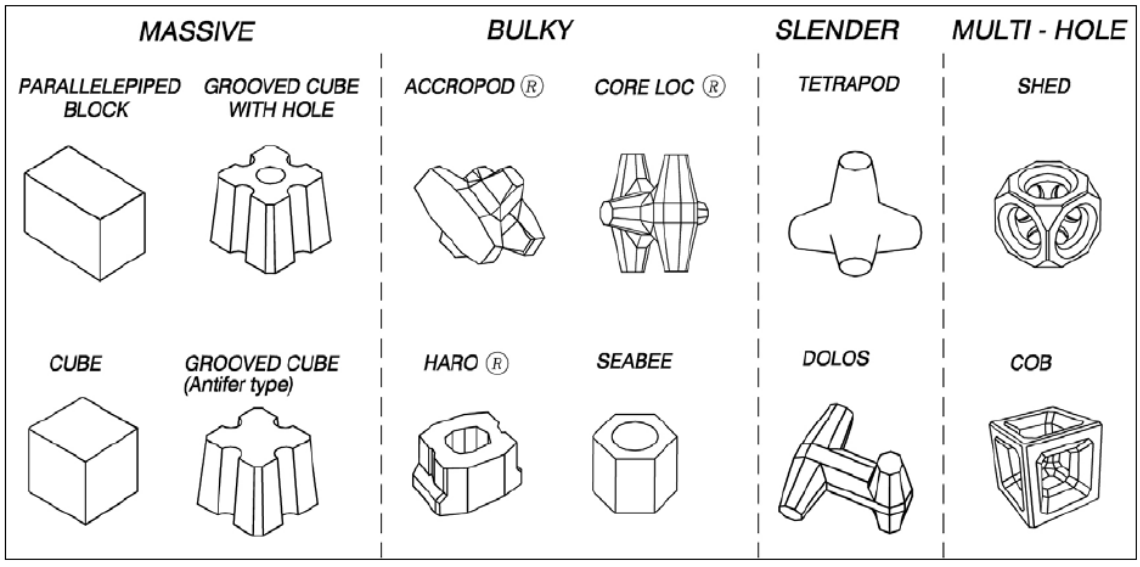

Figure 2.2. Examples of concrete armour units (CEM, 2006).

Artificial reefs have recently grown in popularity, providing coastal protection while also allowing a safe harbor for fish cultures to develop. Such structures combine engineering design with recreational facilities by creating new areas for snorkeling or diving. Porous breakwaters are generally constructed to imitate the function of coral reefs; however, they can take on many different forms. For example, Twu and Chieu (2000) developed theoretical and physical models for multilayer porous structures that would simultaneously dampen reflected and transmitted waves. Also, the efficacy of a zigzag porous screen breakwater on wave reflection, transmission, and forces are examined by Mani (2009). Chakrabarti, S.K. (1999) studied wood panels used for breakwaters that would lower reflection and transmission. When using such structures, the spacing between the panels can be crucial in determining the reflection and transmission values. By separating the seaward and lee-side panels based on a certain wave frequency, an optimum distance may be found to minimize the reflection and transmission of approaching waves (Chakrabarti, 1999). Physical models for emerged and submerged cylindrical permeable systems of piles were studied by Silva et al. (2003). Porous cylindrical piles are not only useful as foundations for coastal structures, but can also be applied independently as coastal defense features.

Regrettably, irresponsible practices have endangered many coral reef systems. Finding solutions to atone for these actions is necessary. Frihy et al. (2004) describe how coral reef systems act as natural coastal protection. The wave breaking that occurs on the reef dissipates the initial wave energy and provides shelter for the adjacent coastline.

Conserving our natural reef system is a key step towards protecting our coasts from erosion and saving beach communities from the financial burden of funding large projects to artificially recreate their presence.

Practical Uses of Breakwaters

Early breakwaters in the United States lacked proven design elements and essentially were experiments on their own. Some of the earliest breakwaters in the United States were built in the 1920s and 1930s near Santa Barbara and Santa Monica (Pope, 1985). These breakwaters were built with the intention of alleviating destructive waves and creating a sheltered zone on the coastline. Instead, they created low-energy areas in the lee of the breakwaters that formed either salients or tombolos. A bulge from the shoreline, not extending to an offshore barrier, is identified as a salient. Once sediment deposits accumulate to connect the bulge with the barrier, it is then referred to as a tombolo. Pope (1985) further described one of the first sets of segmented breakwaters installed in the United States near Winthrop Beach in Boston, Massachusetts in 1935. A series of five segmented breakwaters were constructed to not only shelter the shoreline, but also to protect a pre-existing seawall. Large tidal ranges of 3 m, however, resulted in mixed shoreline responses. During high tides, the breakwaters were able to act as one large breakwater, producing a single salient protruding from the shore. However, at low tides, five separate and smaller tombolos were formed behind each breakwater.

The range of applications for breakwaters is extremely varied. For example, one unique use is found in California. A rubble-mound breakwater sheltering Long Beach was completed in 1948 and initially built to protect the nearby naval harbor from submarines and torpedoes. Constructed in a water depth of 50 feet, and extending 10 feet above the water surface, the 2.5 mile-long breakwater is the largest of its kind in the world. There have been long-standing debates on the effects of this breakwater to the Long Beach Community. The sheltering from normal wave action has limited the recreational activities of the beach and has provided for little circulation within the sheltered area of the breakwater. This low-energy area has significantly reduced the aesthetic quality of the beach by allowing urban runoff to collect in the water. The Army Corps of Engineers has approved a feasibility study to determine the actions required to provide Long Beach with a solution for their problem. It is stated that restoring natural wave action to the beach would provide a 52 million dollar increase in tourism for the first year and would significantly increase the value of beachfront homes. However, some property owners are opposed to this, as they worry about potential damage to their homes if the breakwater is removed. Studies of the biological impacts of the Long Beach breakwater are discussed later in Section 2.4.

Breakwaters can also be used to protect pre-existing structures that are experiencing increased erosion and instability. One example of this is the endangered seawall at Sea Palling in Norfolk, UK. Before the Environment Agency implemented a 50-year sea defense strategy, erosion had lowered the beach level to the extent that the stability of the

seawall was in danger, which had been the only protection for the sheltered land from attack and inundation by sea waves (Thomalla and Vincent, 2003). Part of the sea defense strategy included construction of shore-parallel breakwaters to assist mainly during strong storm surges, reducing the amount of energy reaching the beach and sea wall. The breakwaters (Figure 2.3) were constructed of rocks weighing up to 16 tonne each. Large armour stones were necessary to combat the violent wave heights experienced in this area. After construction, the shoreline responded well (Figures 2.4 and 2.5) to the offshore breakwaters. Thomalla and Vincent (2003) claim that the beach has continuously increased in volume since the beach nourishment, proving that the steady state of the coastline at Sea Palling has not yet been attained.

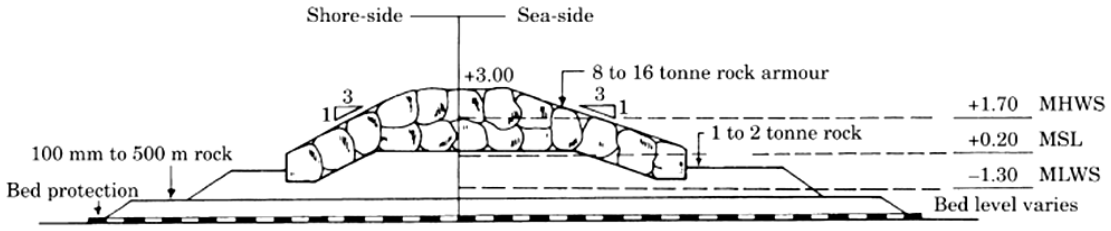

Figure 2.3. Cross section of in-place reefs at Sea Palling (Thomalla and Vincent, 2003).

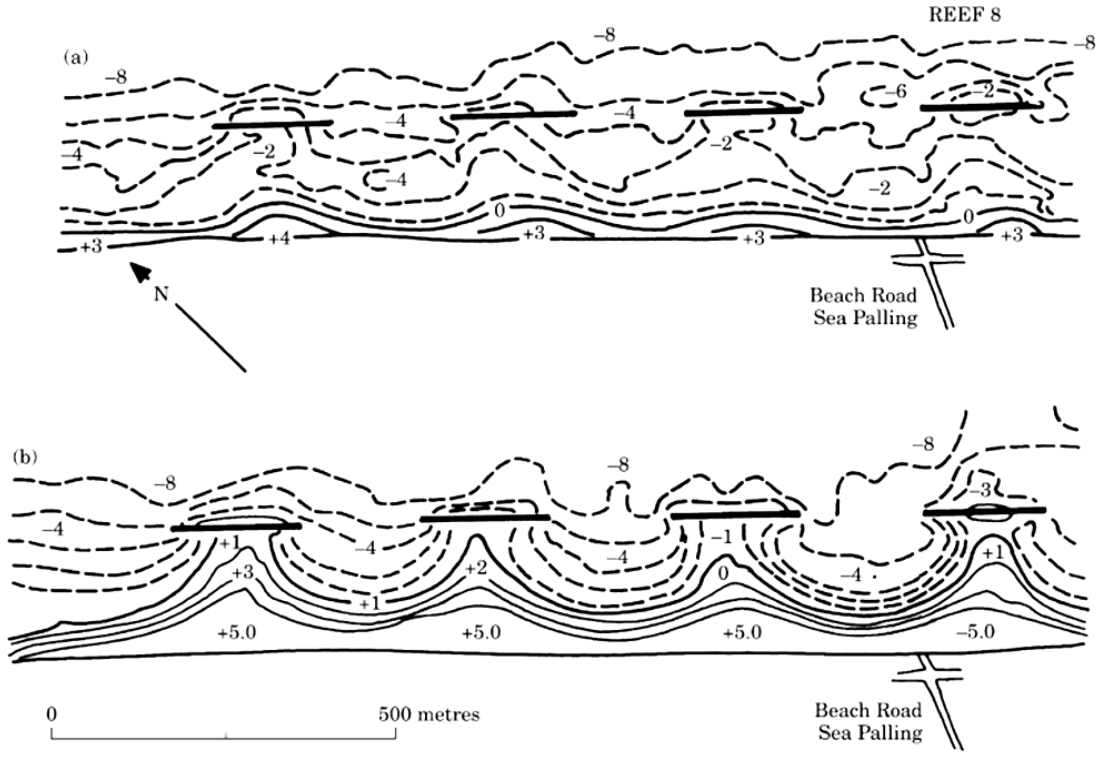

Figure 2.4. Shoreline response to offshore breakwater placement: (a) after construction; (b) one year later after two recharge operations (Thomalla and Vincent, 2003).

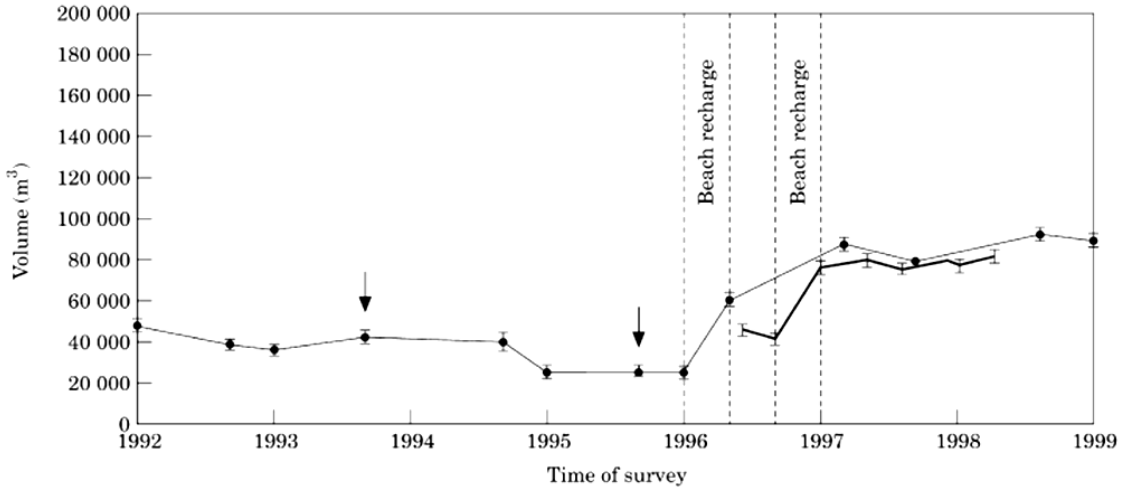

Figure 2.5. Beach volume change in the center of the bay at Sea Palling:
Environment Agency survey; Thomalla survey (Thomalla and Vincent, 2003).

At Sea Palling, high waves were penetrating to the shoreline because the sand bar between the breakwaters had eroded away. This led to the necessity of constructing sand-retaining structures and providing sediment recharge to the beach. This plan proved effective in retaining sediment at Sea Palling to the extent that tombolos formed (Figure 2.4), restricting sediment transport to adjacent beaches. In fact, beaches alongside Sea Palling have shown significant erosion, revealing the concern over placement of coastal structures. This situation appropriately demonstrates the success and dangers of using offshore breakwaters.

When attempting to mitigate costly, destructive processes in dynamic coastal zones, care must be taken to ensure that all potential consequences are properly balanced. A concept known as integrated coastal zone management includes governing developments and evaluating natural resources, while synthesizing the concerns of all relevant stakeholders. Saengsupavanich et al. (2009) discusses the integrated coastal zone management concept for a small fishing village in Southern Thailand where erosion occurred during the storm season each year. Human actions such as shrimp farming, sand mining, and ill-designed coastal structures played a key role in accelerating this process. Shrimp farmers were digging ponds between the road and the beach, leaving areas for waves to disperse into and destroy the adjacent roads. Trucks had been reported stealing sand from the beaches for commercial purposes, removing the only natural defense system of the beach. T-groins had also been placed at the beach, but were distanced such that waves penetrated the gaps and eroded away the road. To reach a solution, several parties were sought after

for input on methods to mitigate erosion: the coastal communities, shrimp farmers, Marine Department, Department of Highways, Provincial Office, and non-governmental organizations. Department of Highways had to protect their roads, and had at once put in place seawalls for protection, which prevented access of fishing boats. Structures that impeded their access to the beach were being destroyed by shrimp farmers, yet the nearby communities needed a way to protect the beach area homes which were disappearing at a rate of 10-20 per year. A Provincial Office looked after the people in their community and had put in riprap to alleviate the issues of erosion, but this also impeded boat traffic to the beach. The Marine Department funded a study to implement a design that would be publicly acceptable. Non-governmental organizations were fighting to preserve a natural beach and did not appreciate "hard" structures (or permanent, immovable structures). Large offshore, detached breakwaters were eventually installed to allow boat access but also to significantly reduce wave forces reaching the beach. This design pleased all stakeholders, and the breakwaters were even cited for having an abundant supply of fish around them. The case of Southern Thailand (Saengsupavanich et al., 2009) reveals that successful erosion management is realized not only through preventing erosion, but also by finding suitable solutions that please all participating stakeholders.

2.3 WAVE KINEMATICS AROUND A BREAKWATER

Wave Envelopes

Standing wave fields (Figure 2.6) are created by the superposition of incident and reflected waves from a fully reflective vertical barrier. The waves travel in opposite

directions and have the same frequency, giving the perception of stationary waves, oscillating about the mean water level at all non-nodal positions. At nodes, the wave elevation remains constant and does not change as a result of the passing waves. Antinodes are where the crests and troughs of each wave meet, presenting the largest changes in wave elevations.

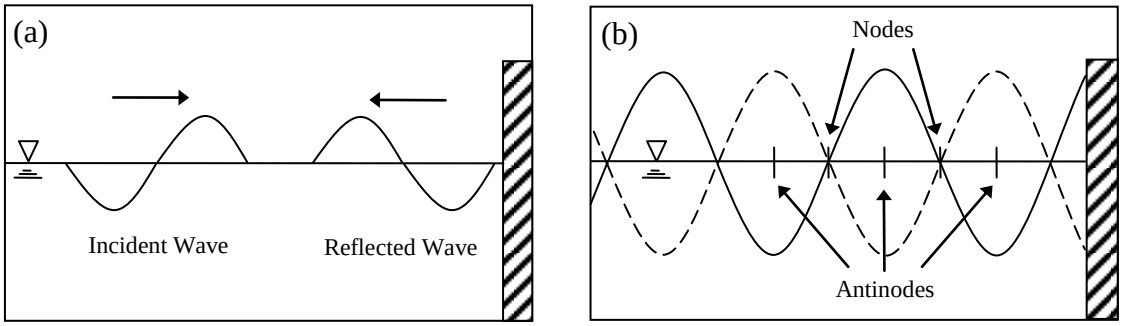

Figure 2.6. Standing wave field description.

A wave envelope (Figures 2.6.b and 2.7) depicts the maximum and minimum wave elevations at different positions offshore of the breaker for a given wave field. When the reflective surface/structure does not allow for full reflection, a partial standing wave field is created (Figure 2.7). In a partial standing wave field, nodes and antinodes are still present. Nodes become the locations of the minimum elevation difference, $H_{\min}$, and antinodes become the locations of the maximum elevation difference, $H_{\max}$, in the wave envelope, as shown in the schematic in Figure 2.7.

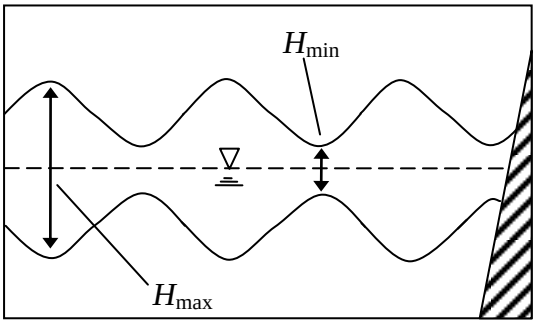

Figure 2.7. Partial standing wave field schematic.

Wave Reflection

Definition and Methods for Calculating Wave Reflection Coefficients

When waves impinge on a structure, some portion of their energy is redirected as a reflected wave. Relating this reflected wave to the incident wave can demonstrate the extent of protection a structure provides for a desired area. The basic parameter for quantifying the reflective characteristics of a coastal structure is C_r, defined as the ratio of the reflected wave height, H_r, to the incident wave height, H_i,

$$C_r = \frac{H_r}{H_i} \tag{2.1}$$

A simple method of calculating reflection coefficients is by applying Healy's formula (Equation 2.2) to wave envelope measurements for the partial standing wave field. Healy's formula is given as:

$$C_r = \frac{H_{max} - H_{min}}{H_{max} + H_{min}} \tag{2.2}$$

where C_r is the reflection coefficient. Madsen (1983), Nagashima (1971), and Koftis and Prinos (2005) are examples of studies that used this simple method to calculate reflection coefficients for their tests.

A number of methods exist to calculate reflection coefficients through wave gage measurements. Isaacson (1991) examines three separate methods for measuring reflection coefficients: (i) a two-point method from Goda and Suzuki (1976) that is used in this study and discussed further in Sections 3.3 and 3.4, (ii) a three-point method measuring three wave elevations and two phase angles at three different locations from Mansard and Funke (1980), and (iii) proposes a three-point method that only measures three wave elevations. While the second method was concluded to be the most accurate, the two-point method (i) only loses applicability when the spacing between wave gages nears an integer multiple of half wave lengths (Isaacson, 1991).

Stamos and Hajj (2001) present a model using a single wave gage to measure an incident wave and then the wave reflected by the structure before multiple reflections in the tank can occur. They separate the incident and reflected waves using the Morlet wavelet (full description found in the article of reference). Reflection coefficients can also be determined by comparing concurrent images of a wave field. Kuo et al. (2009) used three separate cameras to take simultaneous images of the wave field along a 2-D flume. After processing the images, they were able to separate the incident and reflected waves in order to obtain a reflection coefficient.

Important Parameters

There are a number of parameters that affect C_r values of a coastal structure under different wave conditions. Therefore, taking various parameters into account, many different equations are proposed to assist in the design of individual breakwaters under specific environmental conditions. Wave reflection is greatly influenced by the slope of a surface in comparison with the wave length. For example, as a wave approaches a vertical seawall, most of the energy will be reflected. However, when a wave approaches a mildly sloping beach, most of the energy dissipates through breaking and only a small amount of the energy is reflected (Kajima, 1969).

The surf similarity parameter (ξ), or Iribarren number, relates the angle of the structure slope, θ, to the relative wave steepness, s, where

$$s = \sqrt{H_i / L} \tag{2.3}$$

$$\text{and} \quad \xi = \tan\theta \Big/ \sqrt{H_i / L} = \tan\theta / s \tag{2.4}$$

with L being the incident wavelength. Neelamani and Sandhya (2003) examined C_r values from seawalls and the effect of the surf similarity parameter on the reflection coefficient from a plane seawall is presented below in Figure 2.8. In general, reflection coefficient values increase with increasing values of the surf similarity parameter. This general trend is somewhat observed in Figure 2.8, shown by a general curve fit line. However, it is clear from the figure that a C_r parameterization solely depending on ξ cannot explain the observed C_r values.

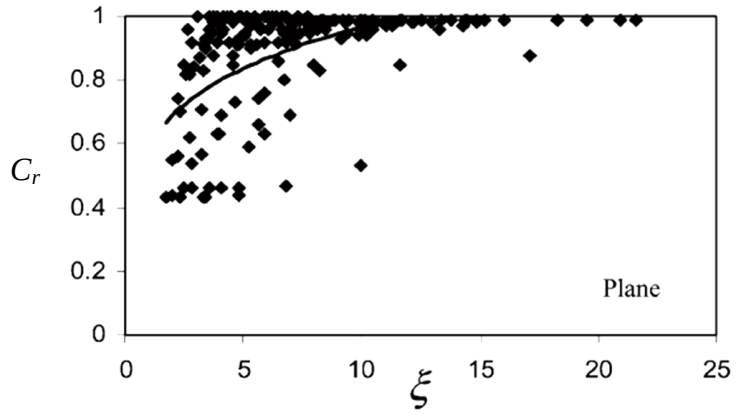

Figure 2.8. Effect of surf similarity parameter on C_r (Neelamani and Sandhya, 2003).

Reflection Coefficient Equations

For assistance in understanding some of the common used parameters in this section, Figure 2.9 is provided below.

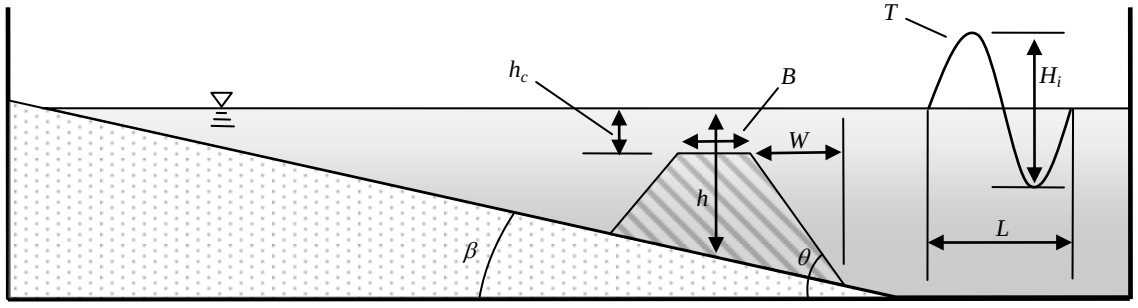

Figure 2.9. Breakwater parameter schematic: h_c – depth of submergence (freeboard), B – crest width, W – horizontal width of the offshore face of the breakwater, h – water depth at the center of breakwater, θ – angle of breakwater slope, β – angle of beach slope, H_i – incident wave height, L – incident wavelength, T – wave period.

Parameterizations for reflection coefficients have transformed over the years, but the majority of them involve some form of the surf similarity parameter. Battjes (1974) examined results from the impermeable slope tests of Moraes (1970) to give

$$C_r = 0.1\xi^2 \tag{2.5}$$

Battjes (1974) proposes that this equation can be applied to a maximum C_r value of 1. Any reflection coefficients calculated larger than 1 should be assumed as 1.

Seelig and Ahrens (1981) analyzed several data sets to introduce the following reflection coefficient parameterization:

$$C_r = \frac{a\xi^2}{\xi^2 + b} \tag{2.6}$$

The values of coefficients a and b depend on the structure type. For example, the following values can be found in Seelig and Ahrens (1981) and are also given in Table VI-5-14 of CEM (2006):

- for smooth slopes (e.g., beaches), $a = 1.0$ and $b = 5.5$
- for rough permeable slopes (e.g., rubble-mound), $a = 0.6$ and $b = 6.6$.

Postma (1989) delved into individual parameters affecting reflection coefficients and proposed several forms of equations for predicting reflection coefficients. One of the proposed equations was a modification to the previously proposed form of Battjes (1974), employing the surf similarity parameter as follows,

$$C_r = 0.14\xi^{0.73} \tag{2.7}$$

However, Postma (1989) concluded that the surf similarity parameter does not represent the effects of wave steepness sufficiently, and so suggested an equation that considers the slope angle and the wave steepness separately, given by

$$C_r = 0.071 P^{-0.082} \cot\theta^{-0.62} s^{-0.46} \tag{2.8}$$

where P is the porosity of the structure. According to this equation, increasing the porosity of a structure will reduce the reflection coefficient, supporting the trend shown later through the permeable breakwater experiments.

Hughes and Fowler (1995) analyzed a large data set of reflection coefficients that they determined using mid-depth velocity measurements near smooth and rubble-mound slopes. The reflection coefficients were found to correlate with a dimensionless parameter of similar form to an inverted surf similarity parameter,

$$\xi_h = \frac{\sqrt{\frac{h}{gT^2}}}{\tan\theta} \tag{2.9}$$

where g = gravitational acceleration, h = water depth, and T = wave period. For this parameter the water depth is substituted as the vertical length variable. Hughes and Fowler (1995) submitted the following C_r parameterizations:

for smooth slopes,

$$C_r = \frac{0.1176}{0.1176 + \xi_h^{2.6}} \tag{2.10a}$$

and for rubble-mound slopes,

$$C_r = \frac{0.1415}{0.1415 + \xi_h^{0.804}} \tag{2.10b}$$

Physical justifications do not exist for these equations (Hughes and Fowler, 1995). However, these equations satisfy the asymptotic condition that as ξ_h approaches 0, either for long waves or upright structure slopes, the reflection coefficient approaches 1. Application of Equations (2.10a) and (2.10b) is possible with little error when considering mild seaward slopes and when incident waves are analyzed at depths similar to those at the structure toe. The limits for the use of each of these equations are provided as follows (Hughes and Fowler, 1995):

- for smooth impermeable slopes: $0.14 < \xi_h < 1.2$ with slopes no less than 1:4
- for rubble-mound structures: $0.12 < \xi_h < 0.6$ with a slope of 1:2

Sutherland and O'Donoghue (1998b) implemented a larger range of tests than Hughes and Fowler (1995) in order to provide a reflection coefficient parameterization with greater range and credibility. Sutherland and O'Donoghue (1998b) found a relative dependence on a frequency-dependent surf similarity parameter, proclaiming the lack of a universally accepted reflection coefficient equation, noting that most model the form of Seelig and Ahrens (1981). The frequency-dependent surf similarity parameter is as follows:

$$\xi_f = \frac{\tan\theta}{f}\sqrt{\frac{g}{2\pi H_s}} \tag{2.11}$$

where f is the local frequency within the wave spectrum. H_s is the significant wave height, typically given as the average of the largest one-third wave heights in a system of waves. Through irregular wave tests, the following equation for impermeable walls was established:

$$C_r = \frac{\xi_f^{2.58}}{7.64 + \xi_f^{2.58}} \tag{2.12a}$$

For rubble-mound structures, a tentative equation was developed through limited testing to show that the surf similarity parameter is capable of predicting reflection coefficients, given by

$$C_r = \frac{0.82\xi_f^2}{22.85 + \xi_f^2} \tag{2.12b}$$

Muttray et al. (2006) performed large-scale tests on emerged rubble-mound structures with a steep front slope. A comparison of reflection coefficients with different parameters are presented in Figure 2.10.

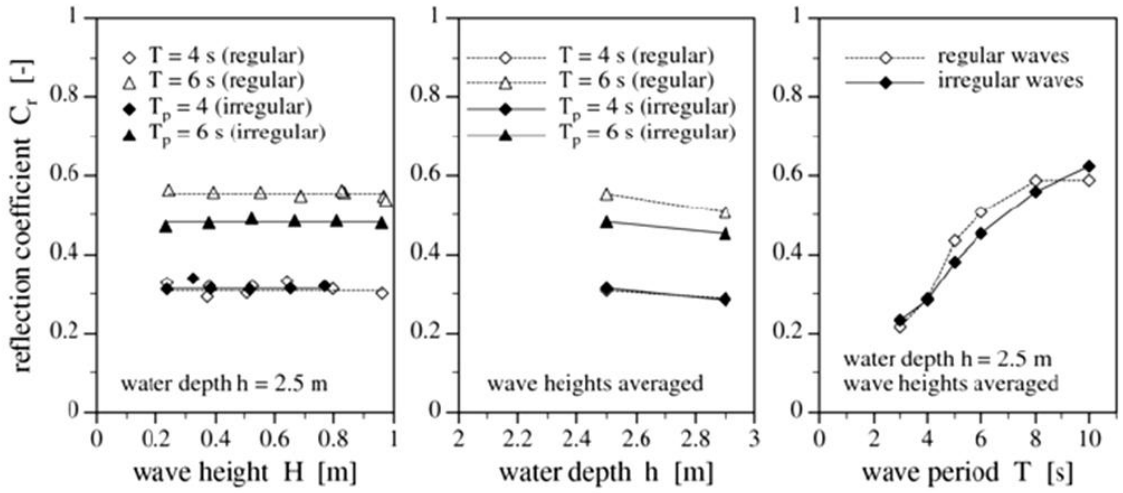

Figure 2.10. Reflection coefficient vs. wave height, water depth, and wave period. (Muttray et al., 2006). (with permission from ASCE)

From previous tests, Muttray and Oumeraci (2002) suggested the following equations for reflection from submerged impermeable slopes:

for non-breaking waves,

$$C_r = 1 - \left(\frac{H_i}{H_{i,crit}}\right)^{3/2}\left(1 - \frac{2}{\pi}\right) \text{ for } \frac{H_i}{H_{i,crit}} < 1 \tag{2.13a}$$

and for breaking waves,

$$C_r = \frac{2}{\pi}\frac{H_{i,crit}}{H_i} \text{ for } \frac{H_i}{H_{i,crit}} \geq 1 \tag{2.13b}$$

where $H_{i,crit} = L\sqrt{2\theta/\pi}\left(\sin^2\theta/\pi\right)$ with θ given in radians.

For rubble-mound structures, Muttray et al. (2006) introduced the following equation for reflection coefficients:

$$C_r = \frac{1}{1.3 + 3h\dfrac{2\pi}{L}} \tag{2.14}$$

Equation (2.14) uses an original approach, employing the wave number, $k = 2\pi/L$, to parameterize the reflection coefficient from a breakwater.

Zanuttigh and van der Meer (2008) proposed a new parameterization using a large database of over 4000 reflection coefficient values. Their new parameterization is given as

$$C_r = \tanh\left(a\xi^b\right) \tag{2.15}$$

where the coefficients a and b have the following values:

- for smooth impermeable slopes: $a = 0.16$ and $b = 1.43$
- for permeable rubble-mound slopes: $a = 0.12$ and $b = 0.87$

They also proposed an equation that is applicable for low-crested structures, given by

$$C_r = \tanh\left(a\xi^b\right)\left(0.67 + 0.37\frac{R_c}{H_i}\right) \tag{2.16}$$

for the range of $-1 \le R_c/H_i \le 0.5$ where the relative crest height, R_c, is the vertical distance of the breakwater crest to the mean water level (submerged crests have a negative value). Coefficients a and b are the same as those defined for Equation (2.15).

Table 2.1 presents a summary for all proposed reflection coefficient equations given in this section. All presented equations were derived from experimental tests with emerged

breakwaters, except for Equations (2.13a), (2.13b), and (2.16). The 4th column in Table 2.1 indicates any limits for application as suggested by the corresponding author(s).

Table 2.1. Summary table of reflection coefficient parameterizations.

Eqn. #	Reference	Equation	Applicable Limits
(2.5)	Battjes (1974)	$0.1\xi^2$	If $C_r > 1$, then $C_r = 1$
(2.6)	Seelig & Ahrens (1981)	$\frac{a\xi^2}{\xi^2 + b}$	NONE
(2.7)	Postma (1989)	$0.14\xi^{0.73}$	NONE
(2.8)	Postma (1989)	$0.071P^{-0.082}\cot\theta^{-0.62}s^{-0.46}$	NONE
(2.10a)	Hughes & Fowler (1995)	$\frac{0.1176}{0.1176 + \xi_h^{2.6}}$	$0.14 < \xi_h < 1.2$ & slope $\geq$ 1:4 $0.12 < \xi_h < 0.6$ & slope = 1:2
(2.10b)	Hughes & Fowler (1995)	$\frac{0.1415}{0.1415 + \xi_h^{0.804}}$	$0.14 < \xi_h < 1.2$ & slope $\geq$ 1:4 $0.12 < \xi_h < 0.6$ & slope = 1:2
(2.12a)	Sutherland & O'Donoghue (1998b)	$\frac{\xi_f^{2.58}}{7.64 + \xi_f^{2.58}}$	NONE
(2.12b)	Sutherland & O'Donoghue (1998b)	$\frac{0.82\xi_f^2}{22.85 + \xi_f^2}$	NONE
(2.13a)	Muttray & Oumeraci (2002)	$1 - \left(H_i / H_{i,crit}\right)^{3/2}\left(1 - \left(2/\pi\right)\right)$	$\frac{H_i}{H_{i,crit}} < 1$
(2.13b)	Muttray & Oumeraci (2002)	$\frac{2}{\pi}\frac{H_{i,crit}}{H_i}$	$\frac{H_i}{H_{i,crit}} \geq 1$
(2.14)	Muttray et al. (2006)	$\frac{1}{1.3 + 3h\frac{2\pi}{L}}$	NONE
(2.15)	Zanuttigh & van der Meer (2008)	$\tanh\left(a\xi^b\right)$	NONE
(2.16)	Zanuttigh & van der Meer (2008)	$\tanh\left(a\xi^b\right)\left(0.67 + 0.37\frac{R_c}{H_i}\right)$	$-1 \leq R_c/H_i \leq 0.5$

Phase Shift

When waves are fully reflected from a vertical, impermeable barrier (shown in Fig. 2.6) they are described as being in phase. Phase shift occurs when waves reflect through wave-breaking or contact with a sloping structure, misaligning the phase of the incident and reflected waves. The phase shift of a reflected wave is important in determining the reflection coefficients of sloped structures (Sutherland and O'Donoghue, 1998a). Taira and Nagata (1968) conclude that the absolute value of the phase angle, γ, decreases when the beach slope is held constant and the wavelength or wave period is increased. This decrease in γ can also be observed if the beach length decreases or the beach slope increases. Sutherland and O'Donoghue (1998a) proposed the following parameterization to determine the phase shift on reflection, γ, for a slope:

$$\gamma = \frac{-8\pi}{\tan\theta}\sqrt{\frac{h_t}{gT^2}} = -8\pi\chi \tag{2.17}$$

with h_t = depth at toe of slope and

$$\chi = \frac{1}{\tan\theta}\sqrt{\frac{h_t}{gT^2}} = \frac{h_t}{L_s \tan\theta} \tag{2.18}$$

with $L_s = T\sqrt{gh_t}$ = linear theory shallow-water wavelength at the toe of the slope. The dimensionless parameter χ, the ratio of the cross-shore structure length to the shallow water wavelength, is important in determining phase shift (Sutherland and O'Donoghue, 1998a). There is virtually no phase shift in the wave reflection when waves approach a vertical structure, since the cross-shore structure length is zero. However, on sloping

surfaces this parameter becomes relevant. It is interesting to note that the phase shift is independent of wave height, unlike wave reflection.

Consider the sloped face of a submerged breakwater, extending from x_c at the crest edge (with water depth = h_c) to the toe of the structure where x = 0 and the water depth = h_t. Over the slope, $h_x = h_t - x\tan\theta$ is the depth at a position x on the structure. Also, the linear theory shallow water wave number is given by $k_s = 2\pi/\sqrt{ghT^2}$ In the same manner as Sutherland and O'Donoghue (1998a), one may then derive the phase shift on reflection for a submerged breakwater, γ_s, by

$$\gamma_s = 2\int_0^{x_c} -k_s\, dx = -4\pi\int_0^{x_c}\left(gh_xT^2\right)^{-0.5} dx$$

$$= \frac{8\pi}{\sqrt{gT^2}\tan\theta}\left(\sqrt{h_c} - \sqrt{h_t}\right) \qquad (2.19)$$

Hughes and Fowler (1995) and Sutherland and O'Donoghue (1998a) both performed laboratory experiments on rubble-mound and smooth structure slopes to study phase shift phenomenon. The results of Sutherland and O'Donoghue (1998a) are shown in Figure 2.11. In the legend of Figure 2.11, 'Eq. 3' refers to the phase shift equation for a slope (2.17) while 'Eq. 17' is a best-fit line for the phase shift by the structures, given by

$$\gamma = -8.64\pi\chi^{1.22} \qquad (2.20)$$

'Eq. 11' is an explicit expression for phase shift that Sutherland and O'Donoghue (1998a) derived by matching standing waves over a slope. Smooth data points were gathered from smooth impermeable wall tests and rubble data was obtained from the rubble-mound breakwater model tests. The best-fit line, 'Eq. 17,' gives the closest approximation to the data points, while 'Eq. 11' and 'Eq. 3' over and underestimate phase shift, respectively.

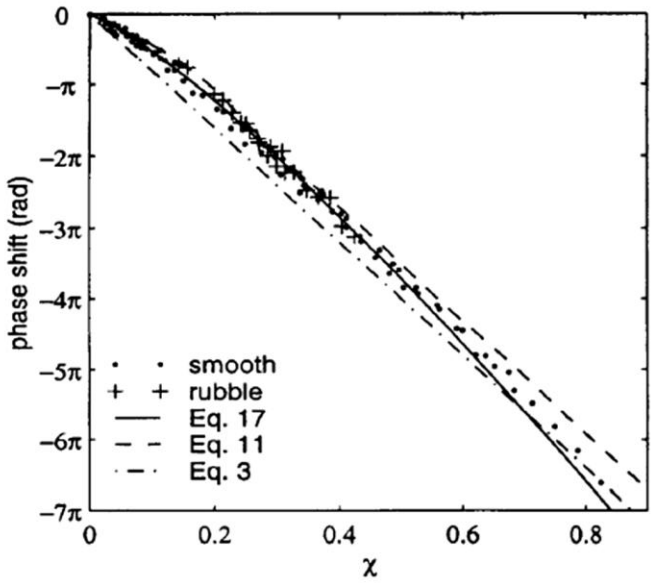

Figure 2.11. Phase shift versus χ for 2-D wave tank tests (Sutherland and O'Donoghue, 1998a).

Hughes and Fowler (1995) took a slightly different approach in measuring the phase shift. Their focus was on root mean squared velocities near coastal structures, and they used this data to determine the location of partial nodes and antinodes. Knowing that the horizontal components of water particle velocities have maximum values at nodes, Hughes and Fowler (1995) were able to calculate the reflection phase angle relative to the

structure toe. Hughes and Fowler (1995) and Taira and Nagata (1968) proposed similar semi-empirical parameterizations to estimate γ, given by:

$$\gamma = 2kx_{\max} - 2n\pi \tag{2.21a}$$

$$\gamma = 2kx_{\min} - (2n+1)\pi \tag{2.21b}$$

where $x_{\max}$ and $x_{\min}$ refer to the locations (measured from the slope toe) of maximum and minimum elevation differences in the wave envelope, respectively, while n can be any integer.

Hughes and Fowler (1995) related their phase shift data with an inverted surf similarity-type parameter, ξ_h (see Equation 2.9), of the same form as χ in Equation (2.18). The phase shift on reflection was similar for permeable and impermeable structures with the same offshore slopes and toe depths, displayed in Figure 2.11. This preliminary finding of Hughes and Fowler (1995) was later confirmed by Sutherland and O'Donoghue (1998a).

Wave Transmission

Transmission Coefficient Equations

Transmission coefficients, C_t, are used to quantify the ability of a breakwater to shelter an area from incoming waves. The transmission coefficient is defined as the ratio of the transmitted wave height to the incident wave height,

$$C_t = \frac{H_t}{H_i} \tag{2.22}$$

When considering submerged structures, it is important to note that transmission coefficients do not reach unity, even for deep crests. Melito and Melby (2002) displayed this in their laboratory tests, up to an R_c/H_i value of -8.25. Any impedance in the bottom topography can generate a reflected wave and dissipate some energy from incoming waves. However, crests near the surface can cause waves to break, dissipating a major portion of their energy. Induced-breaking is the primary objective of most breakwater placements, as this will significantly reduce transmission coefficient values.

Cokgor and Kapdasli (2005) examined the effectiveness of submerged breakwaters in harnessing wave energy and protecting shorelines from erosion through two-dimensional laboratory tests. It was determined that the breakwater slope did not affect transmission coefficients. Reduced water depths at structures can result in lower transmission coefficients, similar to increasing the width of the structure, due to the energy dissipation process by breaking waves (Cokgor and Kapdasli, 2005). Moreover, Cokgor and Kapdasli (2005) found that porosity relates directly to breakwater performance in terms of transmission coefficients. Therefore, the transmission coefficient from a coastal structure will increase as the porosity of that structure increases.

Several equations have been established over the years to predict transmission coefficients, at varying degrees of complexity. Seabrook and Hall (1998) performed two-dimensional and three-dimensional laboratory experiments using model rubble-mound structures. After analyzing the data from their 2-D tests, Seabrook and Hall (1998) found

that C_t was most affected by the depth of crest submergence, h_c, the incident wave height, H_i, and the crest width, B, and influenced to a smaller degree by wave period, T, breakwater armour dimensions, D_{50a}, and breakwater slope, θ. Based on their 2-D experiments, they proposed the following equation for the transmission coefficient with an R^2 value of 0.914:

$$C_t = 1 - \exp\left(-0.65\left(\frac{h_c}{H_i}\right) - 1.09\left(\frac{H_i}{B}\right)\right) + 0.047\left(\frac{Bh_c}{LD_{50a}}\right) - 0.067\left(\frac{h_c H_i}{BD_{50a}}\right) \quad (2.23)$$

Despite the good fit, estimations by this equation become unbounded whenever B becomes very large, and caution must be taken when applying this equation outside of the following ranges:

$$0 \le \frac{Bh_c}{LD_{50a}} \le 7.08$$

$$0 \le \frac{h_c H_i}{BD_{50a}} \le 2.14$$

D'Angremond et al. (1996) examined documented data sets on wave transmission coefficients by different researchers to determine a more robust C_t parameterization. Incorporating the surf similarity parameter, D'Angremond et al. (1996) proposed the following equation for permeable breakwaters:

$$C_t = -0.4\frac{R_c}{H_s} + \left(\frac{B}{H_s}\right)^{-0.31}\left(1 - \exp\left(-0.5\xi\right)\right) \times 0.64 \quad (2.24)$$

for the following range of C_t values:

$$0.075 < C_t < 0.80$$

D'Angremond et al. (1996) also proposed the following equation for impermeable breakwaters:

$$C_t = -0.4\frac{R_c}{H_s} + \left(\frac{B}{H_s}\right)^{-0.31}\left(1-\exp\left(-0.5\xi\right)\right)\times 0.80 \tag{2.25}$$

for the same range of C_t values. Care must be taken to ensure that positive or negative values of R_c are properly assigned.

Kriebel (1992) provided a theoretical analysis to determine the transmission coefficients of a vertical slotted breakwater by analyzing the pressure drops across the wall. This study resulted in the following transmission coefficient equation:

$$C_t = \frac{-1+\left(1+4T_t\right)^{1/2}}{2T_t} \tag{2.26}$$

with T_t being the transmission function defined as,

$$T_t = K_{LOSS}\frac{1}{6}\frac{H_i}{L}\frac{\sinh 2kh + 2kh}{\sinh^2 kh} \tag{2.27}$$

where the loss coefficient is

$$K_{LOSS} = \left(\left(1/C_c P\right)-1\right)^2 \tag{2.28}$$

where P is the porosity of the structure and C_c is the contraction coefficient that is equal to $0.6+0.4P^3$. Hence, Kriebel's (1992) equation relates the transmission coefficient to the relative water depth, wave steepness, and the porosity of the structure (indirectly

through the K_{LOSS} parameter). For deep water conditions, with $L_o = gT^2/2\pi$ representing the deep water wavelength, the following implied form of Kriebel's (1992) equation is applicable for small amplitude waves or large gap spaces:

$$C_t = 1 - T_t = 1 - K_{LOSS}\frac{1}{3}\frac{H_i}{L_o} \tag{2.29}$$

On the other hand, for large amplitude waves and narrow gap spaces, the following simplified form of Kriebel's (1992) equation is applicable:

$$C_t = \left(\frac{1}{T_t}\right)^{1/2} = \left(\frac{3}{K_{LOSS}}\frac{H_i}{L_o}\right)^{1/2} \tag{2.30}$$

Transmission coefficients for floating breakwaters have also been analyzed as this is a significant parameter in understanding how well the structure will manage wave conditions in a sheltered port or harbor. Koftis and Prinos (2005) studied differences between catamaran-shaped floating breakwaters and box-type floating breakwaters. They found that as the ratio of the immersed depths of the vertical floating breakwaters to the water depth (relative immersion depth) increases, the performance of the floating structures also increases. For relative immersion depths greater than 0.4, values of the transmission coefficient are reported as less than 0.1. Also, the influence of relative depths of immersion on wave transmission coefficients is observed to be more dominant for the catamaran-shaped floating breakwaters.

Conservation of Energy

Conservation of energy dictates the following relationship,

$$E_i = E_r + E_d + E_t \tag{2.31}$$

where the incident wave energy, E_i, is separated into reflected, dissipated, and transmitted wave energies (E_r, E_d, and E_t, respectively) and

$$C_r^2 + C_d^2 + C_t^2 = 1 \tag{2.32}$$

relating the reflection (C_r), dissipation (C_d), and transmission (C_t) coefficients with

$$C_r = \sqrt{\frac{E_r}{E_i}}, \tag{2.33}$$

$$C_d = \sqrt{\frac{E_d}{E_i}}, \tag{2.34}$$

$$\text{and} \quad C_t = \sqrt{\frac{E_t}{E_i}} \tag{2.35}$$

Each energy component can be given by the square of its corresponding wave height ($E_i \sim H_i^2$) (Muttray et al., 1992). These relationships are important in describing the connection between reflection and transmission coefficients, as well as a dissipation coefficient that includes all forms of energy dissipation (breaking, friction, percolation through the structure, etc.). Increasing the dissipation coefficient through induced wave-breaking will significantly lower the transmission coefficient of a coastal structure, increasing its overall performance.

Wave Breaking

Wave-breaking criteria, in the absence of a breakwater, is generally given in terms of the ratio of wave height to water depth at breaking,

$$\gamma_b = \frac{H_b}{h_b} \tag{2.36}$$

Battjes (1974) presented findings of several different studies, showing that γ_b tends to scatter around a value of 0.8, a standard value given for wave-breaking. Recently, experiments have been performed to determine wave-breaking limits near submerged structures. Hur et al. (2003) conducted laboratory experiments using regular waves breaking on an impermeable, submerged, vertical breakwater. Due to the effects of shoaling, the breaking wave height at a submerged breakwater over a 1:20 sloping bottom is always larger than the one over a horizontal bottom. The following equations were proposed to give breaking limits in the center of a submerged breakwater:

for a horizontal bottom,

$$H_b / L_o = 0.095 \tanh\left(2\pi\left(h_c / L_o\right)\right) \tag{2.37a}$$

and for sloping (1/20) bottom,

$$H_b / L_o = 0.106 \tanh\left(2\pi\left(h_c / L_o\right)\right) \tag{2.37b}$$

The surf similarity parameter has been used to identify wave-breaking types on a beach or structure. Common forms of wave-breaking, with relation to ξ, are depicted in Figure

2.12. The surf similarity parameter used in Figure 2.12, ξ_o, uses the deep water wave height and wavelength in determining its value.

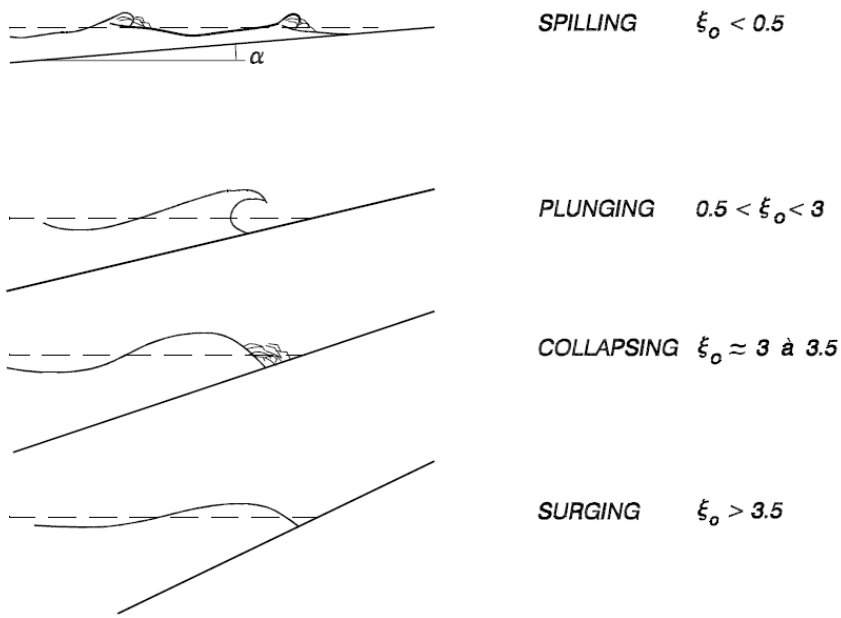

Figure 2.12. Common forms of wave-breaking as a function of ξ (CEM, 2006).

2.4 BREAKWATER DESIGN CONSIDERATIONS

van der Meer (1995) presents a functional description of design methods for rubble-mound breakwaters. Descriptions of wave run-up levels and estimates of the damage to structures can be found in the article, but will not be presented in text here. Further discussions on the actual construction process and requirements for rubble-mound breakwaters can be found in Palmer and Christian (1998).

Rubble-Mound Stability

Rubble-mound breakwaters are typically designed with at least one core underlayer of fine material, where most of the wave dissipation takes place (Madsen, 1983). Topping the underlayer, an armour layer rests on top of the core to maintain the form and stability of the structure. Stability of the armour layer is of utmost importance when designing an effective rubble-mound breakwater. van der Meer (1995) describes the well known Hudson formula, and then proposes several equations for selecting a stable rock size for armour units.

The original Hudson formula is given as

$$M_{50} = \frac{\rho_r H_i^3}{K_D \Delta^3 \cot\theta} \tag{2.38}$$

where M_{50} is the median mass of an armour unit, ρ_r is the mass density of rock, and Δ is the relative buoyant density where $\Delta = (\rho_r / \rho_w) - 1$ and ρ_w is the mass density of water. Stability coefficient, K_D, is given by the Shore Protection Manual (1984) as 4.0 for non-breaking waves and 2.0 for breaking waves. While the Hudson formula is useful in its simplicity, van der Meer (1995) discusses several limitations, including:

- most experimental tests in determining the Hudson formula were performed at a small scale
- formula applies to regular waves only
- wave period or storm duration effects are ignored
- damage level of the structure is ignored

- overtopping is ignored and only permeable core structures are used

After considering the limitations of the Hudson formula, van der Meer (1995) proposed new parameterizations for determining the rock sizes of armour units. Based on laboratory tests, van der Meer (1995) developed separate equations for plunging breakers and for surging breakers:

for plunging breakers,

$$\frac{H_s}{\Delta D_{n50}} = 6.2 P_f^{0.18} \left(\frac{S}{\sqrt{N}} \right)^{0.2} \xi_m^{-0.5} \tag{2.39a}$$

and for surging breakers,

$$\frac{H_s}{\Delta D_{n50}} = 1.0 P_f^{-0.13} \left(\frac{S}{\sqrt{N}} \right)^{0.2} \sqrt{\cot\theta}\, \xi_m^{P} \tag{2.39b}$$

ξ_m uses the mean period, T_m, to determine the deep water wave length for calculating the surf similarity parameter. The transition from plunging to surging waves is determined by a critical value of the surf similarity parameter (van der Meer, 1995):

$$\xi_{mc} = \left[6.2 P_f^{0.31} \sqrt{\tan\theta} \right] \frac{1}{P_f + 0.5} \tag{2.40}$$

When $\xi_m < \xi_{mc}$, Equation (2.39a) should be used and for $\xi_m > \xi_{mc}$, Equation (2.39b). The transition from plunging waves to surging waves does not exist for conditions where $\cot\theta \geq 4.0$, and only Equation (2.39a) should be used in this case. Damage level, S, and the permeability factor, P_f, are described in van der Meer (1995) in detail. N represents the maximum number of waves which should be used in the equations, given as 7500 by

van der Meer (1995), because after 7500 waves van der Meer (1995) assumes that the structure reaches an equilibrium. D_{n50} represents the nominal diameter, similar to D_{50a}, and can be determined by the average mass of the rock through the relationship $D_{n50} = \left(M_{50}/\rho_r\right)^{1/3}$. Figure 2.13 compares the calculations of the Hudson formula with those of the van der Meer equations, showing the limited range of applicability of the Hudson formula.

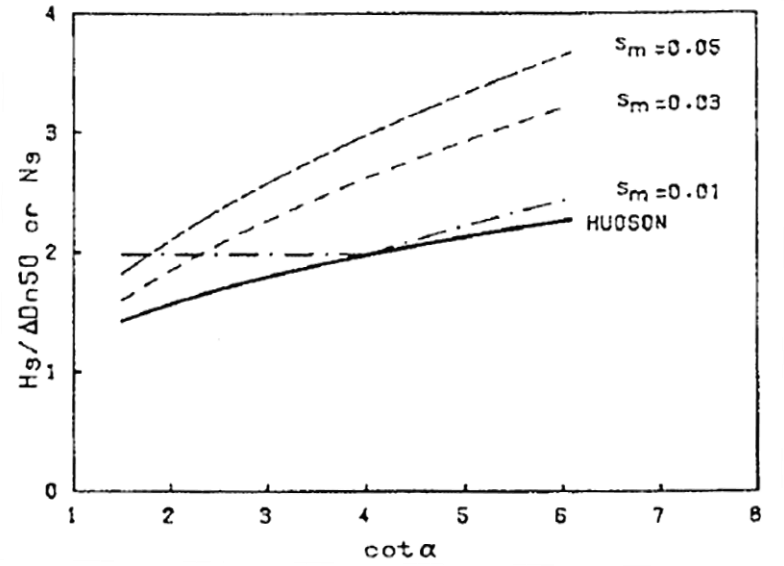

Figure 2.13. Comparison between the Hudson Formula and the van der Meer formulas for a permeable core: α is the angle of the structure slope, N_s is the stability number (equivalent to $H_s/\Delta D_{n50}$), and s_m is the wave steepness factor (van der Meer, 1995).

Vidal et al. (1992) also proposed equations for the stability of armour layers on rubble-mound breakwaters. They performed three-dimensional tests on submerged rubble-mound breakwaters to determine the stability of armour units in the whole breakwater,

and then in the front slope, crest, and back slope sections. Stability results for each section, and the equations used, are given in Vidal et al. (1992).

Placement of Breakwaters

Breakwaters are often built in systems comprised of several individual units, known as segmented breakwaters, separated by chosen gap lengths to prevent excessive amounts of sediment accumulation at the shoreline. A schematic for a segmented breakwater system with parameter definitions is given in Figure 2.14. Segmented breakwaters are not a unique concept, because their use is based on mimicking natural shore protection provided by sand bars or coral reefs (Pope, 1985). The gaps separating them not only allow accretion in the lee of the breakwaters to be manageable, but also provide for increased energy dissipation as waves diffract around the ends of the breakwaters.

When sediment accumulates in the lee of an offshore barrier, two formations are expected: a salient or a tombolo. The differences between a salient and tombolo are discussed by Dally and Pope (1986). Salients are usually preferred, but tombolos are acceptable when the accretion of sand does not affect longshore sediment transport or the stability of adjacent beaches. Tombolos can be beneficial in providing access to breakwaters if maintenance is necessary, but can be dangerous to beachgoers that decide to swim near the structures (Dally and Pope, 1986). Predicting the effect a breakwater may have on its adjacent shoreline is an essential component of breakwater design.

Birben et al. (2007) examined the effect of offshore breakwaters on sediment accumulation at the shoreline. Accretion of sand in the lee of a breakwater is highly dependent upon the distance that structure has been placed from the shoreline. If the distance of the structures from the shoreline is greater than or equal to the combined length of two structures, including the gap between them, then it becomes ineffective in reducing sediment transportation by waves (Birben et al., 2007). Selecting correct gap widths is necessary to ensure a functional system of breakwaters. The ratio of breakwater length to gap length should remain between 0.75 and 1.25 to keep the breakwater system working effectively, with a gap length equal to the breakwater length being recommended (Birben et al., 2007).

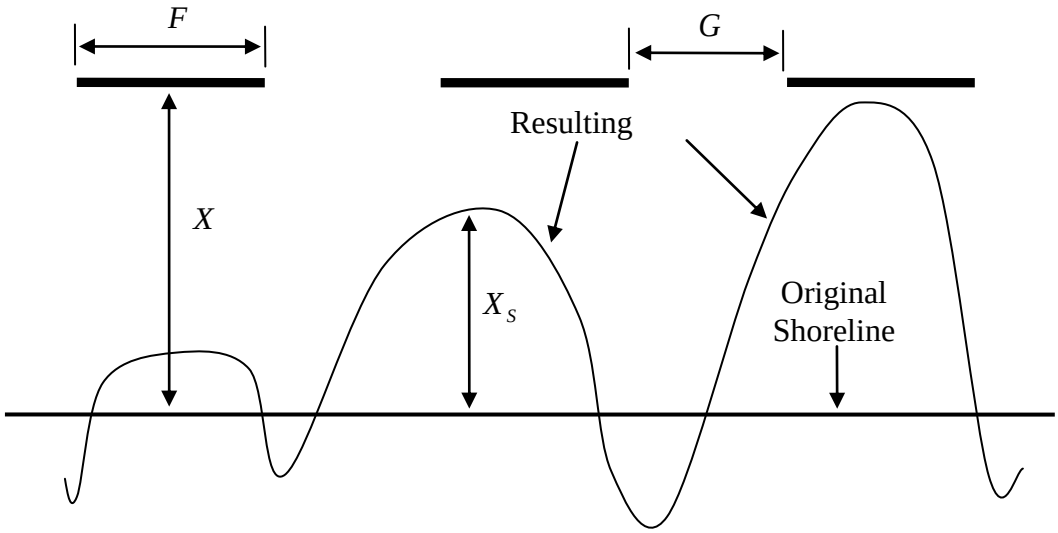

Figure 2.14. Segmented breakwater system parameter definitions: F – breakwater length, G – gap length, X – offshore distance of breakwater, X_S – salient length (Birben et al., 2007).

In order to prevent the formation of tombolos, the Shore Protection Manual (1984) recommends a structure length, F, less than the offshore distance X, such that

$$F/X < 1.0 \text{ (no tombolo)} \tag{2.41a}$$

To ensure tombolo formation, the Shore Protection Manual (1984) suggests that structure length be double the offshore distance:

$$F/X > 2.0 \text{ (guaranteed tombolo)} \tag{2.41b}$$

If diffracted wave crests do not meet before reaching the shoreline, tombolos will generally form (Dally and Pope, 1986). Studying a set of detached breakwaters in the United States, Dally and Pope (1986) concluded that tombolos tend to form when the ratio of structure length to offshore distance approaches 1.0 and tombolos may be prevented if the ratio is equal to, or less than, 0.5.

Pilarczyk (2003) presents equations for the salient and tombolo formation of emerged and submerged structures based off Dally and Pope (1986) and previous work by Pilarczyk. According to Pilarczyk (2003), shoreline responses for emerged structures are as follows: for tombolo formation,

$$F/X > (1 \sim 1.5) \tag{2.42a}$$

for salient formation,

$$F/X = (0.5 \sim 1.0) \tag{2.42b}$$

and for salients in segmented breakwater systems,

$$GX/F^2 > 0.5 \tag{2.42c}$$

For submerged structures, Pilarczyk (2003) proposes the following criteria for shoreline responses that incorporate the transmission coefficient:

for tombolo formation,

$$F/X > (1 \sim 1.5)/(1-C_t) \text{ or } X/(1-C_t) < (2/3 \sim 1)F \tag{2.43a}$$

for salient formation,

$$F/X < 1/(1-C_t) \text{ or } X/(1-C_t) > F \tag{2.43b}$$

and for salients in segmented breakwater systems,

$$GX/F^2 > 0.5(1-C_t) \tag{2.43c}$$

Ranasinghe et al. (2010) used numerical model simulations to predict shoreline responses to submerged breakwaters under different conditions. They discovered that when the submergence depth of the crest is larger than 1 m, crest width no longer plays a considerable role in shoreline transformation. However, when the crest is closer to the mean water level (< 0.5 m submergence), larger crest widths reduce the effects of erosion in the lee of a submerged breakwater. Concerning tides, only strong tidal currents affect shoreline responses to nearby submerged structures. The shoreline is expected to produce net accretion under small tidal ranges as the breakwater remains submerged throughout. For higher tidal ranges the shoreline response could be insignificant. Currents in the higher water are more erosive than those during the rest of the tidal cycle. Due to wave setup, the submerged behavior of the structure can be prolonged, even

during lower tidal elevations when the breakwater crest may become emerged, evening out the net accretion throughout the tidal range.

2.5 ENVIRONMENTAL IMPACTS OF BREAKWATERS

A study by Bertasi et al. (2007) at Lido di Dante, as part of the DELOS project, discovered a significant increase in the number of species found at the leeside of low crested structures. These increases had not been observed in previous studies, and out of four other sites investigated through the DELOS project, only one of them showed a similar increase. The main cause for an increase in species at Lido di Dante is the enclosure of the shoreline by breakwaters and groynes (Figure 2.15). In a sheltered area, current flows are reduced, and the residence time within this zone is highly increased, especially during extreme events. A reduction of hydraulic motion enables more species, normally floating along the shoreline, to settle and find shelter behind the breakwater. Organic matter may also have increased in this area in response to the accumulation of algae and seagrass debris which becomes trapped on the structures.

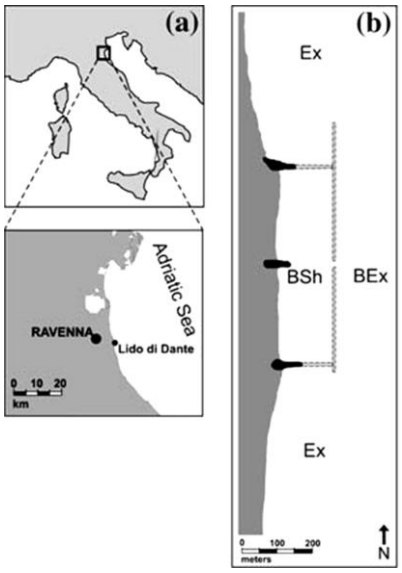

Figure 2.15. Site description of Lido di Dante: (a) geographical location; (b) sampling design. Ex – exposed shoreline; BEx – partially exposed; BSh – sheltered area (Bertasi et al., 2007).

Daniil et al. (2000) performed two-dimensional laboratory experiments with rubble-mound coastal structures and, after deoxygenating the water in the tank, generated waves to measure the dissolved oxygen concentrations resulting from wave interactions around the structure. Daniil et al. (2000) discovered that oxygenation in response to structure-induced wave-breaking is not influenced by the surface of the structure. Rubble-mound structures and smooth, plane sloping structures each have the same effect on oxygenation. Wave breaking at sloping structures produces higher oxygenation rates, increasing the water quality of the surrounding area (Daniil et al., 2000). These tests were two-dimensional and included only a two cell model, sampling dissolved oxygen concentrations at both sides of the structure.

Several experimental investigations have taken place to examine the biological conditions present in the harbor near Long Beach, California. Loi (1981) and Reish et al. (1980) both set up stations in the harbor to determine the activity and survival of organisms. Loi (1981) found that species population increases from the shoreline to the outer breakwater. Closer to the breakwater, the water quality improves because of the exposure to natural wave motions. At the shoreline, silt and oil can accumulate, making the survival of any marine organism difficult.

It is hoped that future breakwater designs will consider their potential impact on organisms living around them. This especially demands consideration as breakwaters are used to protect tourist-attracting beaches. If these structures are simultaneously creating feeding grounds for other organisms it could drive away tourists.

CHAPTER THREE

EXPERIMENTAL SETUP AND METHODOLOGY

3.1 INTRODUCTION

A series of laboratory wave tank experiments were performed to analyze the differences in the efficacy of two separate types of submerged, trapezoidal breakwaters, impermeable and permeable, in the Flow Physics Laboratory (FPL) at Clemson University. This chapter is comprised of four separate sections explaining the experimental setup and methodology: Experimental Setup, Experimental Procedure, Data Analysis, and Experimental Parameters. The Experimental Setup section describes the wave tank, the dimensions and characteristics of model breakwaters, and the characteristics of the instrumentation while the Experimental Procedure section highlights the order of operation for experiments and data analysis. Reflection coefficient and average wave elevation calculations are described in the Data Analysis section. The final section presents values of all of the experimental parameters used in our experimental campaign.

3.2 EXPERIMENTAL SETUP

Experiments were performed in a wave tank of dimensions 12 m x 0.6 m x 0.6 m (see Figure 3.1 for a schematic). The wave tank consists of a wave maker assembly, adjustable sandy beach, and 1 cm thick Plexiglas walls for visualization purposes. In all tests, a beach of 1:20 slope was formed by quartz sand, manufactured and sorted by

Foster-Dixiana. This sand has a median diameter of 0.067 cm, a mean diameter of 0.058 cm, and a density of 2.65 g/cm^3.

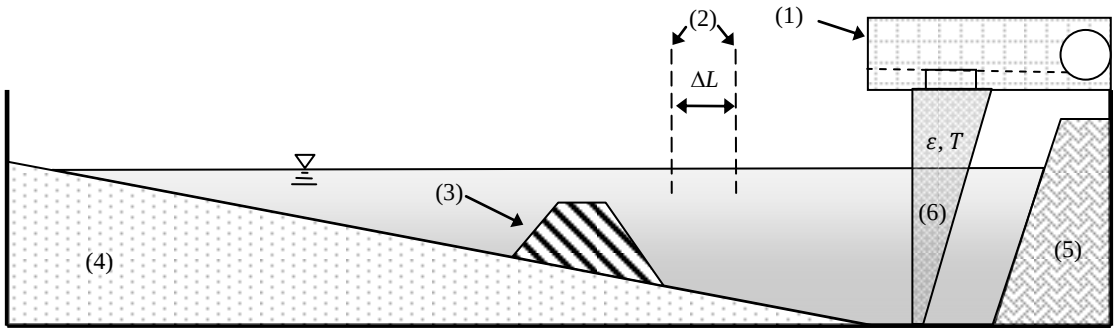

Figure 3.1. Wave tank schematic: (1) linear actuator and motor, (2) wave gages, (3) breakwater, (4) sloping beach, (5) wave absorber, (6) wave paddle. Symbols: ΔL – distance between gages, ε – amplitude of wave paddle excursion, T – wave period.

Waves were generated using a paddle that was driven by a linear actuator. The linear actuator was controlled by a Nook Industries motor (assembly shown in Figure 3.2), rated at 4000 rpm and capable of achieving a maximum allowable torque of 20.3 Nm at 10000 rpm. Wave paddle velocities up to 1.5 m/s and accelerations up to 6 m/s^2 can be achieved by the wave maker assembly. Wave maker motion has a precision of 2 micrometers and is controlled by an in-house computer code written in LabView. To record wave elevations, two RBR WG-50 capacitance-type wave gages were set up at various locations along the wave tank, depending on the specific test. Wave gages have a sampling frequency of up to 50 Hz and a measurement accuracy of 0.001 m. The measurement range of the gages is from 0.005 m to a full-length measurement of 1 m. Wave surface elevation data from the gages is acquired simultaneously by a National

Instruments data acquisition board (model #NI USB-6009), with a sampling frequency of 14000 Hz.

Figure 3.2. Wave maker assembly.

For the impermeable submerged breakwater tests, three similar models of trapezoidal breakwaters were tested. Each individual breakwater is symmetric and each has its own unique side slope. Breakwater dimensions are tabulated in Table 3.1. Permeable tests were performed with two separate models, both based on the geometric parameters of BW-2 (i.e. side slope, crest width, and height; BW-2 – Breakwater with ID # 2, see Table 3.1). Photographs of the individual breakwaters can be found in Figure 3.3. Impermeable breakwaters (Figure 3.3.a-c) were built with oriented strand board. One of

the permeable breakwaters was constructed with upright PVC pipes (Figure 3.3.d), and the other permeable breakwater consisted of golf balls collected into a trapezoidal caged compartment (Figure 3.3.e and 3.3.f), simulating a comparable set-up to a rubble-mound breakwater.

BW-4 was built with schedule 40, 1.5-inch diameter PVC pipe. This size PVC pipe has an outside diameter of 1.9 inches. These pipes were inserted into a base plate, 78 cm by 60 cm, covering a total area of 4680 cm^2. With ten pipes in each row, and 13 separate rows, the pipes cover a surface area of 2378 cm^2, leaving a void space of 2302 cm^2. The ratio of void space to total area determines the porosity for BW-4 to be 0.49. Schematics of the top and side views for BW-4 can be found in Figure 3.4 (drawings are not scaled).

Table 3.1. Breakwater dimensions. A – breakwater structural height.

Breakwater ID	***A* (cm)**	**Side Slope (V:H)**	**Crest Width, *B* (cm)**	***P***
BW-1	20	1:1	18	0.0
BW-2	20	2:3	18	0.0
BW-3	32	1:2	18	0.0
BW-4	20	2:3	18	0.49
BW-5	20	2:3	18	0.39

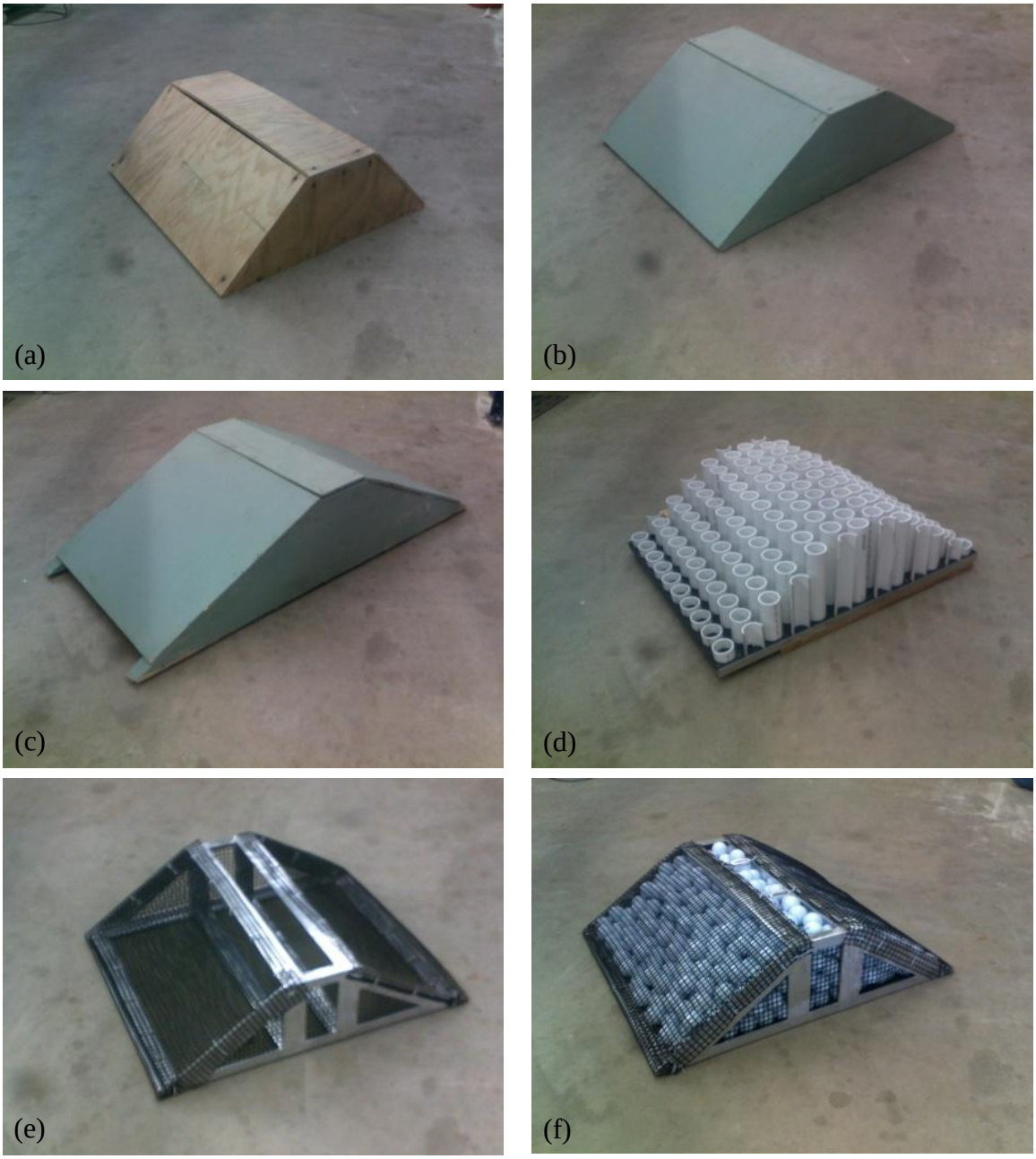

Figure 3.3. Breakwaters: (a) – BW-1; (b) – BW-2; (c) – BW-3; (d) – BW-4; (e) – BW-5(empty); (f) – BW-5(full). See Table 3.1. for the dimensions of the breakwaters.

(a)

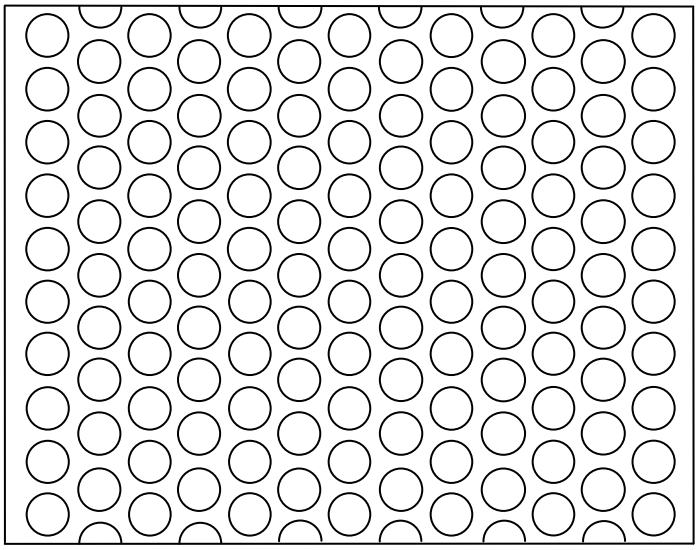

(b)

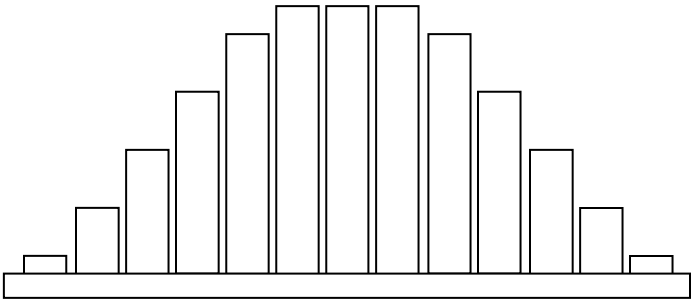

Figure 3.4. Schematics for BW-4: (a) – top view; (b) – side view.

BW-5 was constructed of an aluminum frame, covered by a plastic mesh to contain golf balls. Once golf balls were placed into the frame, a mesh lid was connected to the crest to hold the golf balls in place. 850 golf balls were inserted into BW-5 during testing, with a total golf ball volume of 35050 cm^3. The geometric shape of BW-5 has a total volume of 57600 cm^3, leaving a voids volume of 22550 cm^3. For BW-5, the ratio of volume of voids to total volume gives its porosity at 0.39.

Breakwaters were built to span the width of the tank, considering the two-dimensional nature of this study. BW-3, the largest of all the breakwater models, was always installed directly on the tank bottom. However, the other breakwaters were sometimes elevated and installed on the sandy beach. This was done to increase the width of the sloping face (W, see Figure 3.5 for notations) and the breakwater slope exposed to the incident wave. Important breakwater test parameters are displayed in Figure 3.5.

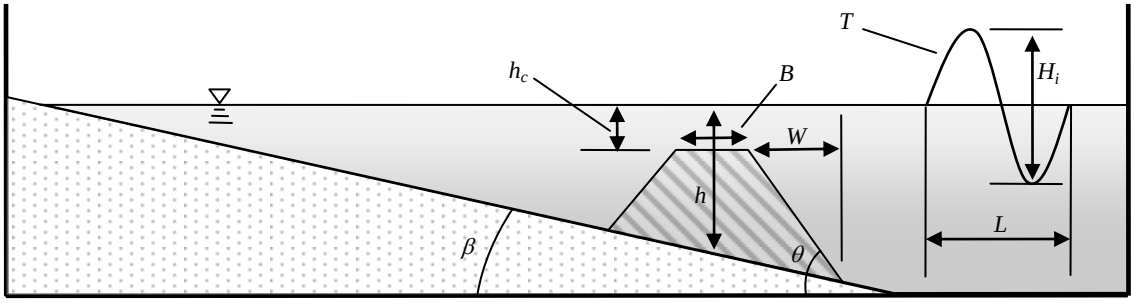

Figure 3.5. Experimental parameter schematic: h_c – depth of submergence (freeboard), B – crest width, W – horizontal width of the offshore face of the breakwater, h – water depth at the center of breakwater, θ – angle of breakwater slope, β – angle of beach slope, H_i – incident wave height, L – incident wavelength, T – wave period.

3.3 EXPERIMENTAL PROCEDURE

Prior to running a test, several tasks were performed. With the proper breakwater installed, the beach was prepared at a 1:20 slope and initial wave gage voltages were recorded (to reference the still water level) for accuracy purposes. Measurements of W and h_c were also taken before performing each test using a ruler.

Initial tests were performed with no breakwater installed, in order to determine the incident wavelengths of each generated test wave. These wavelengths were used in positioning and spacing of wave gages to satisfy the criteria described below. After completing the initial tests, background reflection tests were performed in the absence of a breakwater to obtain the reflection coefficient produced by the sloping beach and the wave tank, only. Average incident wave heights were calculated from the wave elevation data obtained in the absence of a breakwater.

Preliminary experiments are conducted to investigate the effects of spacing between two wave gages and their location, with respect to a reflective structure, on reflection coefficient measurements. With all the sand removed from the tank, the end wall of the tank acted as a rigid vertical reflective barrier that would completely reflect all the wave energy (neglecting dissipation losses). Gages were then spaced at fractions of the wavelength, with reflection coefficients being calculated at each position. As shown in Figure 3.6, reflection coefficients seem to vary at distances that fall along $0.5L$ increments. These results are similar to the ones reported by Goda and Suzuki (1976) who demonstrated that the incident and reflected wave amplitudes diverge around an integer multiple of half wavelengths. At such locations their established equation for wave amplitude obtains a null value in the devisor of $\sin k\Delta L$.

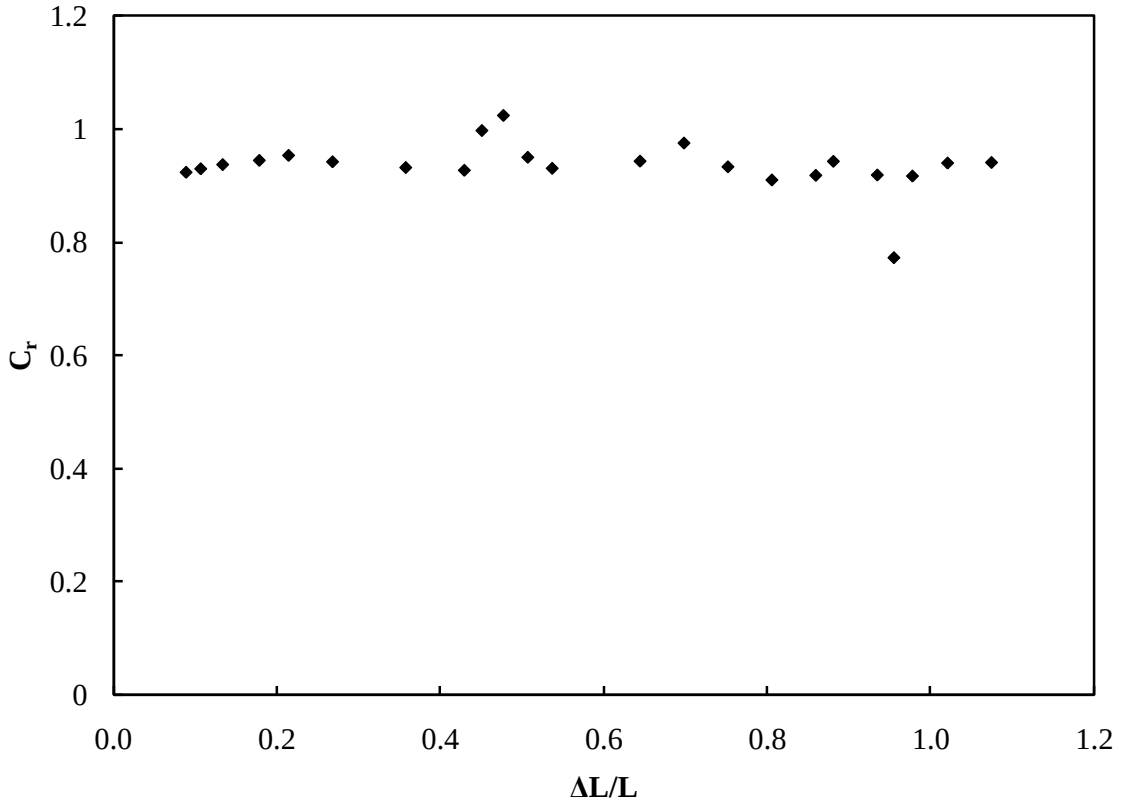

Figure 3.6. Reflection coefficients at different relative gage spacings. Experiment (80) from Table 3.2.

Once gage spacing effects were analyzed, gages were held at a constant spacing of 0.2 times the incident wavelength and then moved along the tank at different distances away from the reflective end wall. Reflection coefficient measurements for these tests are shown in Figure 3.7. Again similar to preliminary test results of Goda and Suzuki (1976), gage distance from a reflective barrier was not found to significantly affect reflection coefficients after a buffer distance of $0.1L$. A decaying trend is observed, however, so results of the tests in Figure 3.7 could indicate a source of error in tests for reflection coefficients.

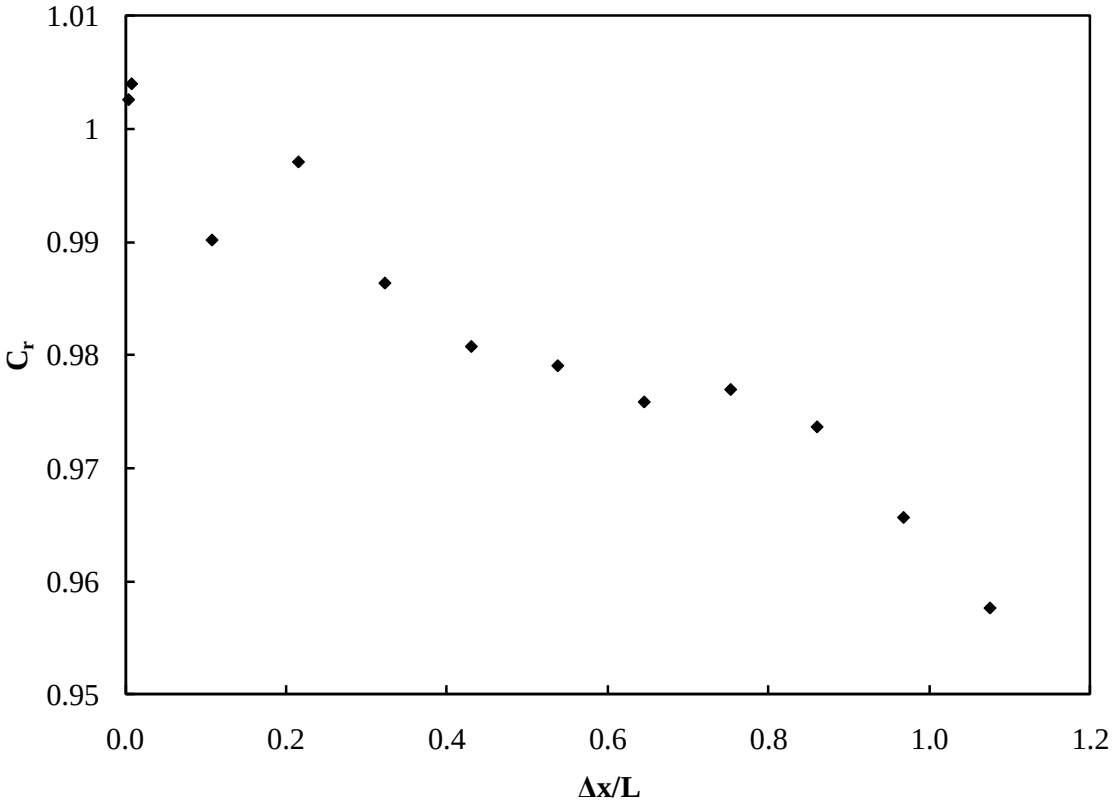

Figure 3.7. Reflection coefficients at varying distances from barrier. Experiment (80) from Table 3.2.

Based on Goda and Suzuki (1976) and the wave gage spacing tests performed as outlined above, certain criteria were established for the breakwater wave reflection experiments conducted, as follows (see Figure 3.8 for an explanation of the parameters used in these criteria):

(i) $X_1 > 1L$

(ii) $\Delta L \neq n(0.5L)(\pm 0.1L)$ where $n = 0,1,2,...,$ [typically $\Delta L = 0.2L$ is selected]

(iii) $X_2 > 0.1L$

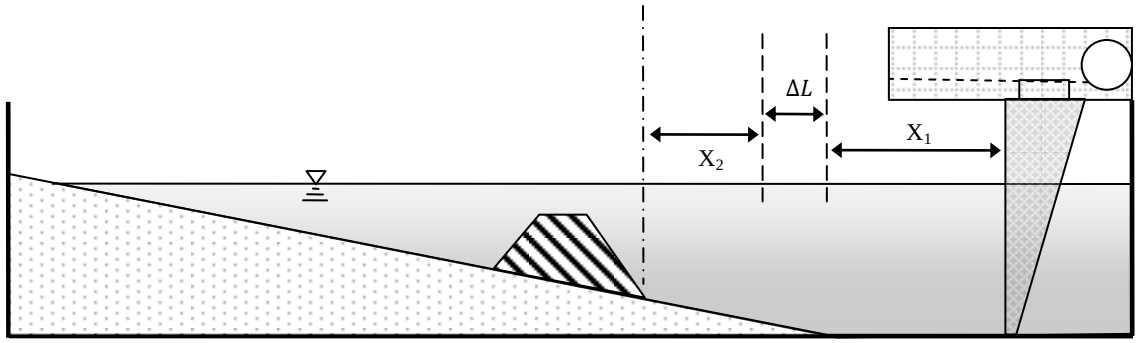

Figure 3.8. Wave gage criteria: ΔL – distance between wave gages, X_1 – distance from paddle to offshore wave gage, X_2 – distance from offshore BW toe to onshore wave gage.

Additional tests were performed to confirm the validity of using the calculations of Goda and Suzuki (1976) to obtain reflection coefficients over a sloping bed. Goda and Suzuki (1976) established their method using two fixed point gages over a horizontal bed. Their calculations did not consider effects of phase shifting due to reflection off of a sloped bottom. Therefore, similar to the validation experiments described above, rigid vertical barrier tests were performed over a horizontal and sloped sandy seabed. The sloped bed was at a slope of 1:20 and extended 3 meters from the barrier. As can be observed from Figure 3.9, the reflection coefficient values at different distances from the vertical barrier show similar values and trends, confirming the use of Goda and Suzuki's (1976) method for calculating reflection coefficients over a sloped seabed.

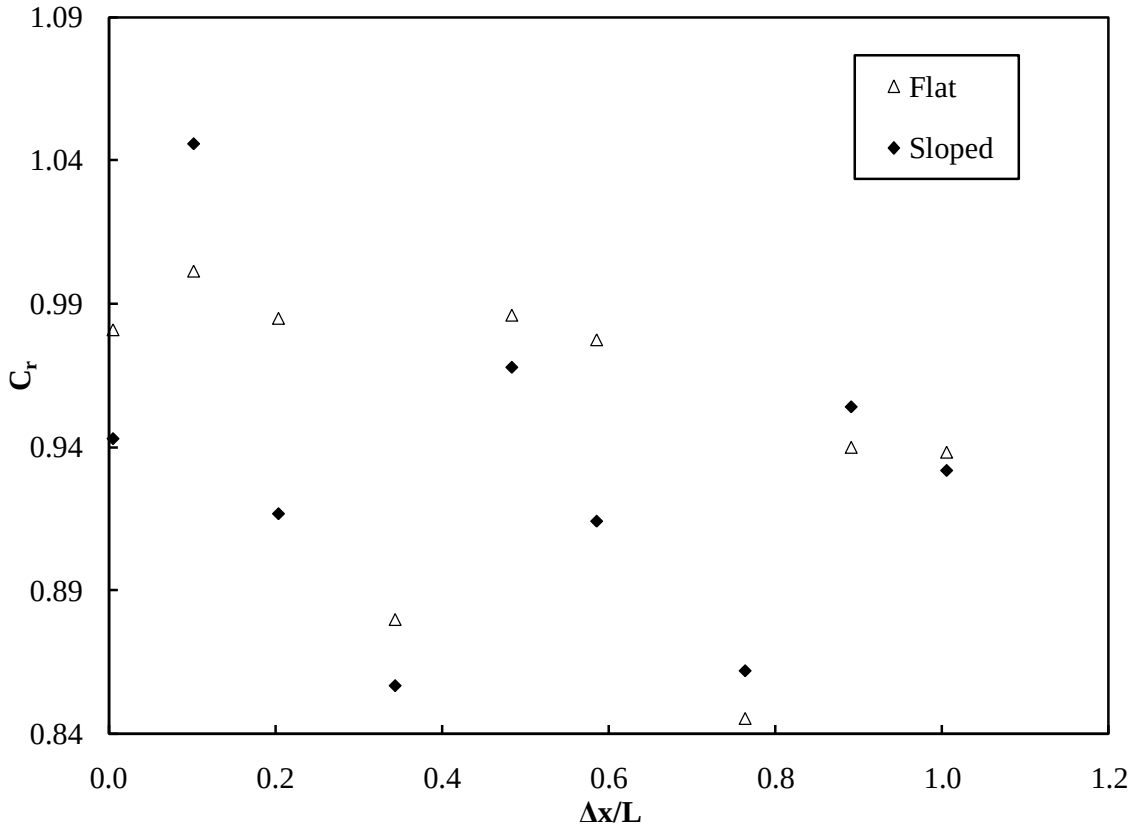

Figure 3.9. Barrier test comparison of a flat vs. sloped sandy beach. Experiment (81) from Table 3.2.

Test duration was also examined and it was found that longer tests did not produce significantly different results; therefore the testing period was held to 10 minutes (300 waves) per test. 3 minutes of a test run were given for the wave field to develop, and then elevation data was collected by the wave gages for the final 7 minutes of testing. Once the desired tests were completed for a particular breakwater, the tank was drained and the breakwater was removed from the tank.

3.4 DATA ANALYSIS

Once wave elevation data is collected, MATLAB codes are used for calculating incident wave heights and reflection coefficients. Incident wave heights are calculated by averaging the wave gage measurements from background tests. C_r is calculated by the reflection method of Goda and Suzuki (1976), which presupposes a superposition of multi-reflected waves within a testing environment, and resolves the components using the Fast Fourier Transform (FFT) technique. Jeon and Cho (2006) provide a summary of the frequency range presented by Goda and Suzuki (1976). A complete explanation of this method and its calculations are demonstrated by Goda and Suzuki (1976). Background C_r values determined from the sloped beach only ranged from 0.03 to 0.09 and could be a source of error in the total reflection values given in Chapter 4 (Table 4.2).

3.5 EXPERIMENTAL PARAMETERS

Table 3.2. Experimental conditions: NBW – no breakwater installed; X_c – distance from center of breakwater to wave paddle. Other terms defined in Figure 3.5.

EXP #	BW ID	h (cm)	T (s)	H_i (cm)	L (cm)	h_c/H_i	X_c (cm)
1	BW-1	17.5	2	6.58	283.4	0.11	473.5
2	BW-1	18	2	8.54	276.8	0.16	473.5
3	BW-1	19	2	8.73	296.8	0.27	473.5
4	BW-1	22	2	5.47	289.7	1.01	473.5
5	BW-1	22	2	6.76	278.5	0.80	473.5
6	BW-1	21	2	7.98	291.9	0.46	473.5
7	BW-1	22	2	5.94	295.5	0.84	473.5
8	BW-1	24.5	2	7.80	333.9	1.18	523.5

EXP #	BW ID	h (cm)	T (s)	H_i (cm)	L (cm)	h_c/H_i	X_c (cm)
9	BW-1	20.5	2	8.97	314.2	0.57	523.5
10	BW-1	22.5	2	5.08	320.8	1.42	523.5
11	BW-1	23.5	2	6.30	326.5	1.30	523.5
12	BW-1	24.5	2	6.45	314.2	1.43	523.5
13	BW-1	24.5	2	5.37	318.9	1.71	523.5
14	BW-1	20.5	2	6.03	321.3	0.88	523.5
15	BW-1	21.5	2	6.23	333.3	1.04	523.5
16	BW-1	22.5	2	6.40	326.5	1.17	523.5
17	BW-2	17.5	2	6.58	283.4	0.14	473.5
18	BW-2	18	2	8.54	276.8	0.16	473.5
19	BW-2	20	2	9.96	301.4	0.34	473.5
20	BW-2	22	2	5.47	289.7	0.99	473.5
21	BW-2	23	2	7.31	301.9	0.86	473.5
22	BW-2	22	2	6.76	278.5	0.72	473.5
23	BW-2	19.5	2	8.21	311.5	0.51	523.5
24	BW-2	20.5	2	8.97	314.2	0.59	523.5
25	BW-2	23.5	2	6.30	326.5	1.33	523.5
26	BW-2	24.5	2	6.45	314.2	1.46	523.5
27	BW-2	24.5	2	5.37	318.9	1.77	523.5
28	BW-2	20.5	2	6.03	321.3	0.90	523.5
29	BW-2	21.5	2	6.23	333.3	1.03	523.5
30	BW-2	22.5	2	6.40	326.5	1.17	523.5
31	BW-2	17.5	2	9.96	301.4	0.23	523.5
32	BW-2	19.5	2	5.47	289.7	0.82	523.5
33	BW-3	17.5	2	6.58	283.4	0.04	473.5
34	BW-3	18	2	8.54	276.8	0.09	473.5

EXP #	BW ID	h (cm)	T (s)	H_i (cm)	L (cm)	h_c/H_i	X_c (cm)
35	BW-3	22	2	6.76	278.5	0.71	473.5
36	BW-3	17.5	2	9.96	301.4	0.30	523.5
37	BW-3	19.5	2	6.87	300.3	0.74	523.5
38	BW-3	20.5	2	7.31	301.9	0.83	523.5
39	BW-3	19.5	2	8.21	311.5	0.61	523.5
40	BW-3	20.5	2	8.97	314.2	0.66	523.5
41	BW-3	20.5	2	6.03	321.3	0.96	523.5
42	BW-3	21.5	2	6.23	333.3	1.09	523.5
43	BW-3	22.5	2	6.40	326.5	1.22	523.5
44	BW-3	18.5	2	7.98	291.9	0.48	523.5
45	BW-3	16.5	2	8.73	296.8	0.23	523.5
46	BW-3	24.5	2	5.01	342.1	1.97	523.5
47	BW-3	24.5	2	6.45	314.2	1.54	523.5
48	BW-3	24.5	2	5.37	318.9	1.84	523.5
49	BW-4	15	2	6.58	283.4	0.03	523.5
50	BW-4	15.5	2	8.54	276.8	0.09	523.5
51	BW-4	17.5	2	9.96	301.4	0.29	523.5
52	BW-4	19.5	2	5.47	289.7	0.90	523.5
53	BW-4	19.5	2	6.76	278.5	0.71	523.5
54	BW-4	19.5	2	8.21	311.5	0.61	523.5
55	BW-4	20.5	2	6.03	321.3	0.98	523.5
56	BW-4	20.5	2	8.97	314.2	0.66	523.5
57	BW-4	21.5	2	6.23	333.3	1.12	523.5
58	BW-4	22.5	2	6.40	326.5	1.25	523.5
59	BW-4	23.5	2	6.30	326.5	1.44	523.5
60	BW-4	24.5	2	5.37	318.9	1.86	523.5

EXP #	BW ID	h (cm)	T (s)	H_i (cm)	L (cm)	h_c/H_i	X_c (cm)
61	BW-4	24.5	2	6.45	314.2	1.55	523.5
62	BW-4	15	2	6.58	283.4	0.09	523.5
63	BW-4	19.5	2	5.47	289.7	0.99	523.5
64	BW-4	19.5	2	6.76	278.5	0.96	523.5
65	BW-4	20.5	2	7.31	301.9	0.75	523.5
66	BW-5	15	2	6.58	283.4	0.08	523.5
67	BW-5	15.5	2	8.54	276.8	0.12	523.5
68	BW-5	17.5	2	9.96	301.4	0.31	523.5
69	BW-5	19.5	2	5.47	289.7	0.95	523.5
70	BW-5	19.5	2	6.76	278.5	0.77	523.5
71	BW-5	19.5	2	8.21	311.5	0.63	523.5
72	BW-5	20.5	2	6.03	321.3	1.01	523.5
73	BW-5	20.5	2	7.31	301.9	0.85	523.5
74	BW-5	20.5	2	8.97	314.2	0.69	523.5
75	BW-5	21.5	2	6.23	333.3	1.16	523.5
76	BW-5	22.5	2	6.40	326.5	1.28	523.5
77	BW-5	23.5	2	6.30	326.5	1.46	523.5
78	BW-5	24.5	2	5.37	318.9	1.90	523.5
79	BW-5	24.5	2	6.45	314.2	1.58	523.5
80	NBW	25	1.7	3.50	265.2	-	-
81	NBW	32.5	2	2.91	392.8	-	-

CHAPTER FOUR

WAVE REFLECTION ANALYSIS

4.1 INTRODUCTION

The central focus of this study is to examine the wave reflection characteristics around submerged impermeable and permeable trapezoidal breakwaters. This chapter is split into four parts: a discussion of significant parameters, a presentation of the experimental results, a comparison to existing equations, and a proposal for future design considerations. First, an analysis of dimensionless parameters governing reflection coefficients demonstrates the dependence or lack thereof on various parameters, followed by a section presenting and discussing experimental results. The third part then compares existing equations determined through other laboratory studies with the data collected in the Clemson Flow Physics Laboratory in order to substantiate a need for further examination. Finally, the last section proposes future design considerations in reference to the given results.

4.2 DIMENSIONLESS PARAMETERS GOVERNING WAVE REFLECTION

Figure 4.1 is given to assist in explaining the parameters used in the following dimensional analysis.

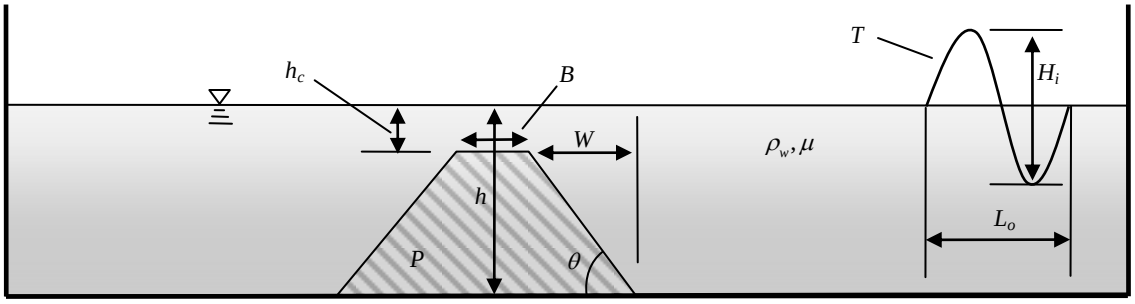

Figure 4.1. Dimensional analysis parameter definitions: h_c – depth of submergence (freeboard), B – crest width, W – horizontal width of the offshore face of the breakwater, h – water depth at the center of breakwater, θ – angle of breakwater slope, H_i – incident wave height, T – wave period, L_o – deepwater wavelength, P – porosity of structure, ρ_w – water density, μ – dynamic viscosity.

In this section, a dimensional analysis is performed to obtain the dimensionless parameters governing the reflection of waves around a submerged breakwater as follows:

Consider a submerged breakwater of crest width, B, and a submergence depth of h_c. Each breakwater is located at a depth of h where the incident wave height at the breakwater is H_i, deep water wavelength is L_o, and wave period is T. Other important parameters to consider are gravitational acceleration (g), breakwater face slope angle (θ), porosity (P), exposed breakwater slope width (W), water density (ρ_w), and dynamic viscosity (μ). A complete set of parameters determining the reflection coefficient, C_r, is given by:

$$C_r = \phi\left(h_c, B, h, H_i, L_o, T, g, W, \rho_w, \mu, \theta, P\right) \tag{4.1}$$

where ϕ is a function. In this analysis, it is assumed that the breakwater is of infinite length and is also perpendicular to the wave direction, because of the 2-D nature of the study. H_i implicitly accounts for the sloping effects of the beach. Therefore, the wave incidence angle, beach slope angle, and breakwater length are excluded from the set of important parameters. Out of the ten dimensional parameters in Equation (4.1), L_o and T are related through the deep water wavelength equation, $L_o = gT^2/2\pi$, and therefore are interchangeable, leaving 9 governing dimensional parameters as follows:

$$C_r = \phi\left(h_c, B, h, H_i, T, g, W, \rho_w, \mu, \theta, P\right) \tag{4.2}$$

The set of repeating variables should represent all three basic dimensions [M-mass, L-length, T-time] included in the set of dimensional parameters, and cannot themselves form a dimensionless group. For this set of parameters, the repeating variables can be selected as H_i = [L], T = [T], and ρ_w = [ML^{-3}]. The following dimensionless groups are then formed:

$$C_r = Y\left(\frac{h_c}{H_i}, \frac{B}{H_i}, \frac{h}{H_i}, \frac{gT^2}{H_i}, \frac{W}{H_i}, \frac{\mu T}{\rho_w H_i^2}, \theta, P\right) \tag{4.3}$$

where Y is a function. After rearranging the presented dimensionless groups, several commonly used dimensionless groups can be formed from those listed above. Adjusting the fourth group and replacing gT^2 with L_o can produce the term H_i/L_o. Generating this term is necessary for deriving other commonly applied terms. Understanding that the breakwater Reynolds number incorporates a velocity term defined as $H_i\pi/T$, the fourth group may also be manipulated by multiplying it with $H_i/H_i\pi^2$ to give the Richardson

number, $Ri = \frac{gH_i}{u^2}$, where u represents velocity. By inverting and taking the square root of Ri, the Froude number is obtained as $\mathrm{Fr} = \frac{u}{\sqrt{gH_i}}$. Showing the connection between H_i/L_o and these two dimensionless numbers is intended to explain why Ri and Fr are not considered as dimensionless groups in Equation (4.4). Combining H_i/L_o with θ yields the well-known surf similarity parameter, $\xi = \frac{\tan\theta}{\sqrt{H_i/L_o}}$. Additionally, multiplying H_i/L_o by the fifth term gives W/L_o, a more sensible parameter when considering the effects of phase shift on the reflection coefficient. Lastly, the sixth group can be transformed into the breakwater Reynolds number, $\mathrm{Re}_{bw} = \frac{\left(H_i\pi/T\right)B}{\nu}$, primarily by inverting the sixth group and multiplying it with the second group. The final collection of dimensionless groups can be given as:

$$C_r = Y\left(\frac{h_c}{H_i}, \frac{B}{H_i}, \frac{h}{H_i}, \frac{H_i}{L_o}, \frac{W}{L_o}, \frac{\left(H_i\pi/T\right)B}{\nu}, \frac{\tan\theta}{\sqrt{H_i/L_o}}, P\right) \tag{4.4}$$

or

$$C_r = Y\left(\frac{h_c}{H_i}, \frac{B}{H_i}, \frac{h}{H_i}, \frac{H_i}{L_o}, \frac{W}{L_o}, \mathrm{Re}_{bw}, \xi, P\right) \tag{4.5}$$

For these groups, plots representing their relationship with the reflection coefficient are presented in Figure 4.2. Other parameters are not held constant in Figure 4.2, but are still influencing the reflection coefficient values. Displaying these figures demonstrates that h_c/H_i is the only dominant dimensionless group given in Equation (4.5). The deep

water wavelength has been replaced by the local wavelength, L, in this figure as both are determined by wave period and water depth. Substituting the local wavelength, the third term may be transformed to produce the relative depth of h/L which can be modified to give the common parameter kh. Manipulating the dimensionless groups in Equation (4.3) also allows the formation of the phase shift on the reflection coefficient for submerged breakwaters given in Equation (2.19). Several key dimensionless groups (ξ, W/L, h_c/H_i, and θ) are discussed further in this Section. Notably, H_i/L is plotted in 4.2.d and displays no significant relationship with the reflection coefficient. However, H_i/L_o could have a significant influence on the reflection coefficient for a particular range of wave conditions, as will be discussed later.

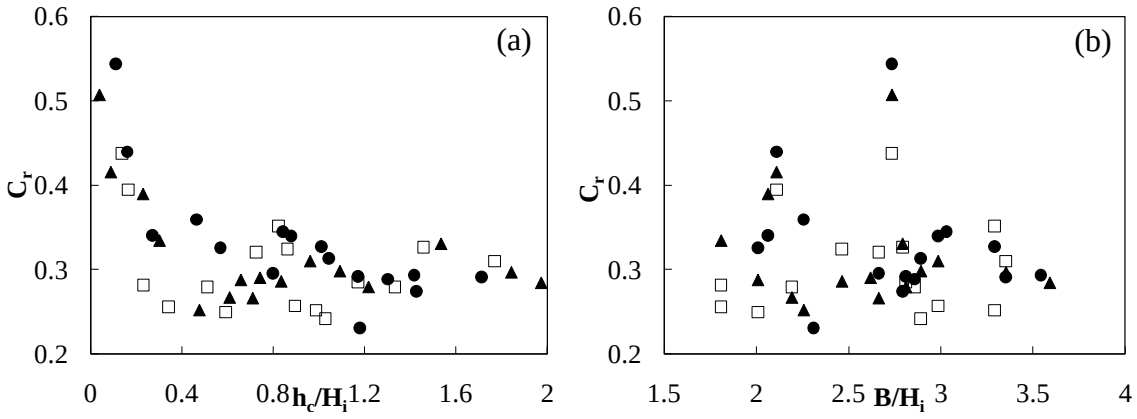

Figure 4.2. Comparison of dimensionless groups and their effect on the reflection coefficient. (●) – BW-1; (□) – BW-2; (▲) – BW-3.

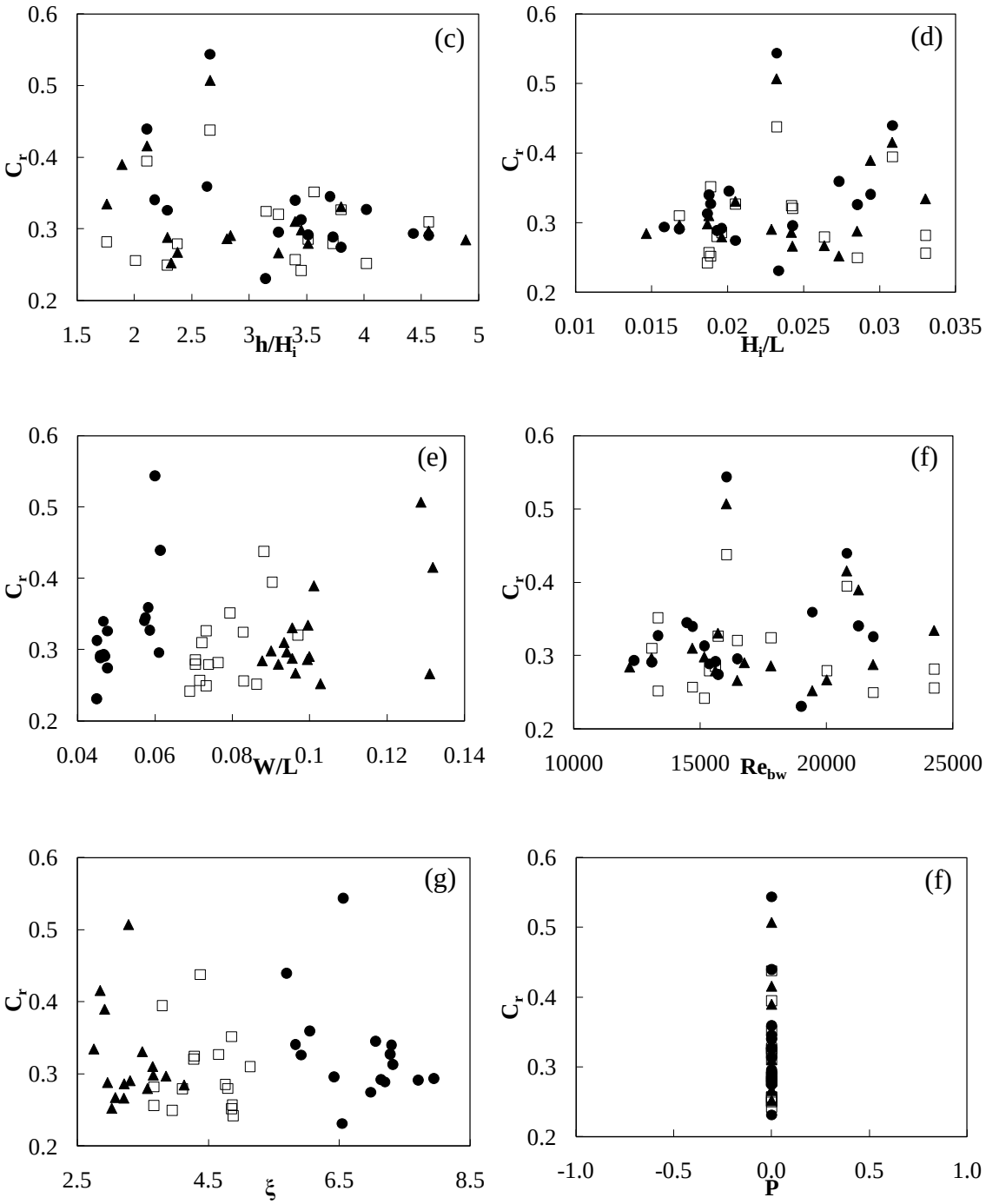

Figure 4.2. (cont.) Comparison of dimensionless groups and their effect on the reflection coefficient. (●) – BW-1; (□) – BW-2; (▲) – BW-3.

Figure 4.3 presents the reflection coefficient data of Melito and Melby (2002) plotted against the surf similarity parameter of a submerged structure. The faint relationship depicted in Figure 4.2.g is supported by the research of Melito and Melby (2002). From the figure, it is apparent that the dependency of reflection coefficients on the surf similarity parameter for submerged structures is weak in their case, if present at all. However, the surf similarity parameter and W/L, two parameters that describe the sloped face of the breakwater, show the greatest potential of all the groups displayed in Figure 4.2, that are not h_c/H_i. In future parameterizations both of these dimensionless groups will be thoroughly considered.

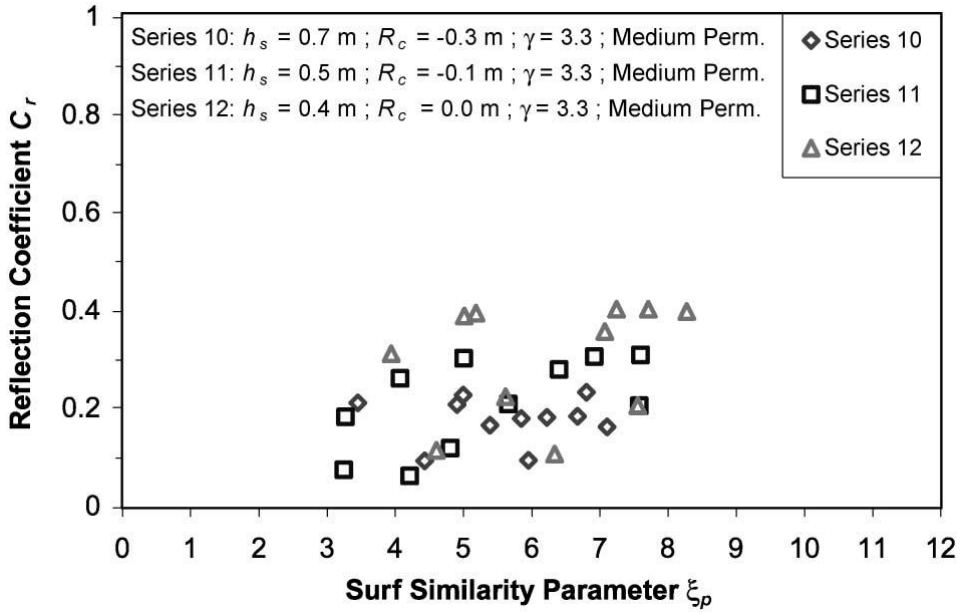

Figure 4.3. C_r versus ξ for submerged structures (Melito and Melby, 2002).

Neelamani and Sandhya (2003) studied the correlation between several different parameters and the wave reflection from seawalls. Their experiments involved three different forms of seawalls: plane, dentated, and serrated. Only results from their plane seawall experiments are presented because the dentated and serrated seawalls do not directly relate to the current research. For the range of model breakwater slopes tested in this study (see Table 3.1), Figures 4.4 through 4.6 indicate that the slope of the breakwater face has minimal to no effect on the reflection coefficient. Figure 4.6 represents similar parameters to those waves tested in this study (h/L ~ 0.10), but Figure 4.5 depicts the testing of shorter waves (h/L = 0.45), showing that under such conditions the breakwater slope should still remain an insignificant parameter for the tested slopes. Figure 4.4 displays reflection coefficient values for several different relative water depths, h/L. Looking at Figure 4.4, were the relative water depths greater than 0.17, h/L effects on the reflection coefficient would have to be considered.

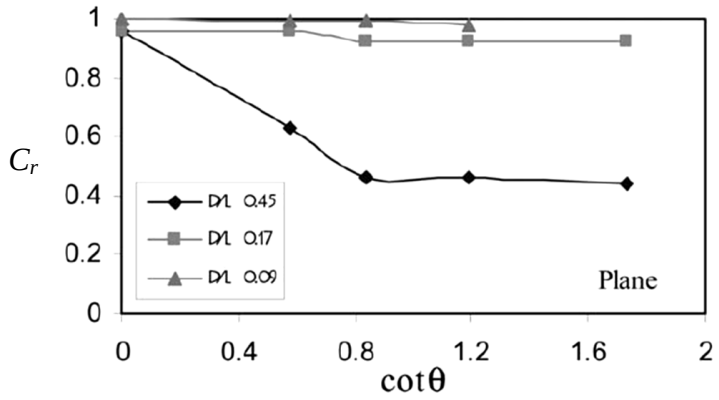

Figure 4.4. Effect of seawall slope on C_r for different wave periods (H_i/h = 0.21). D/L is the relative water depth, equivalent to h/L (Neelamani and Sandhya, 2003).

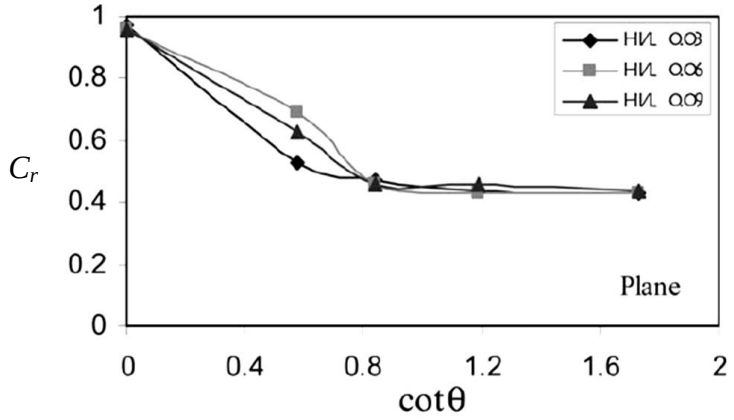

Figure 4.5. Effect of seawall slope on C_r for different wave heights (h/L = 0.45). H_i/L is the relative wave steepness (Neelamani and Sandhya, 2003).

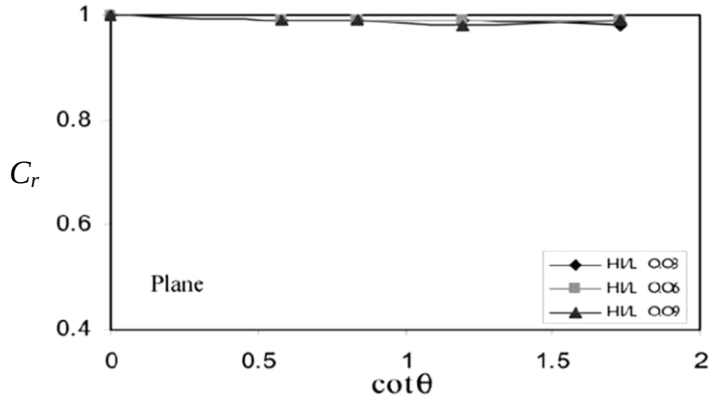

Figure 4.6. Effect of seawall slope on C_r for different wave heights (h/L = 0.09). H_i/L is the relative wave steepness (Neelamani and Sandhya, 2003).

Submerged breakwaters have experienced a growing interest as coastal communities seek to protect and preserve their beaches without affecting their inherent aesthetic beauty. The depth of water above a bottom-founded submerged breakwater constantly changes throughout the tidal cycle, and therefore it is advantageous to predict the response that such a structure will have on surrounding wave motions as tidal elevations shift. Hence,

h_c/H_i is a sensible parameter to use when measuring wave reflection from submerged breakwaters. This parameter has been used by previous researchers (D'Angremond et al., 1996; Seabrook and Hall, 1998, etc.) to study transmission coefficients over emerged and submerged breakwaters. Zanuttigh and van der Meer (2008) incorporate this term into their proposed reflection coefficient equation (Equation 2.16) for low-crested structures. The term h_c/H_i is plotted against the experimental reflection coefficient values in Section 4.3 to demonstrate their relationship. Parameters for each experimental test are given at the end of the chapter in Table 4.2.

4.3 EXPERIMENTAL RESULTS

Impermeable Breakwaters

Figure 4.7 presents the reflection coefficients determined for each of the impermeable breakwater models. Within the figure several different regions appear, each demonstrating a different dependency on the parameter h_c/H_i. When h_c/H_i values are less than roughly 0.5, the submerged crest is relatively close to the mean water level and waves are breaking on the structures. As the troughs approach the structure a drawback effect is created and the waves directly impact a segment of the breakwater face. This direct impact, similar to striking an emerged structure, yields an initial large reflection coefficient value. The intense wave breaking that occurs at lower submergence depths coupled with a heightening of wave transmission, as the depth increases, results in the initial strong decay of the reflection coefficient. The conclusion of this decay region comes with the transition from plunging to spilling breakers. Theoretically, in this region

of h_c/H_i values, some portion of the surface wave remains in contact with the structure, since the depth is less than or equal to half of the wave height. In this region, the breakwater with the steepest slope (BW-1 – 1:1) shows larger reflection coefficient values when compared with milder slopes, but the difference is minimal. Overall, wave reflection coefficients from impermeable submerged trapezoidal breakwaters appear to decay with increasing values of h_c/H_i, settling at a constant value of around 0.25.

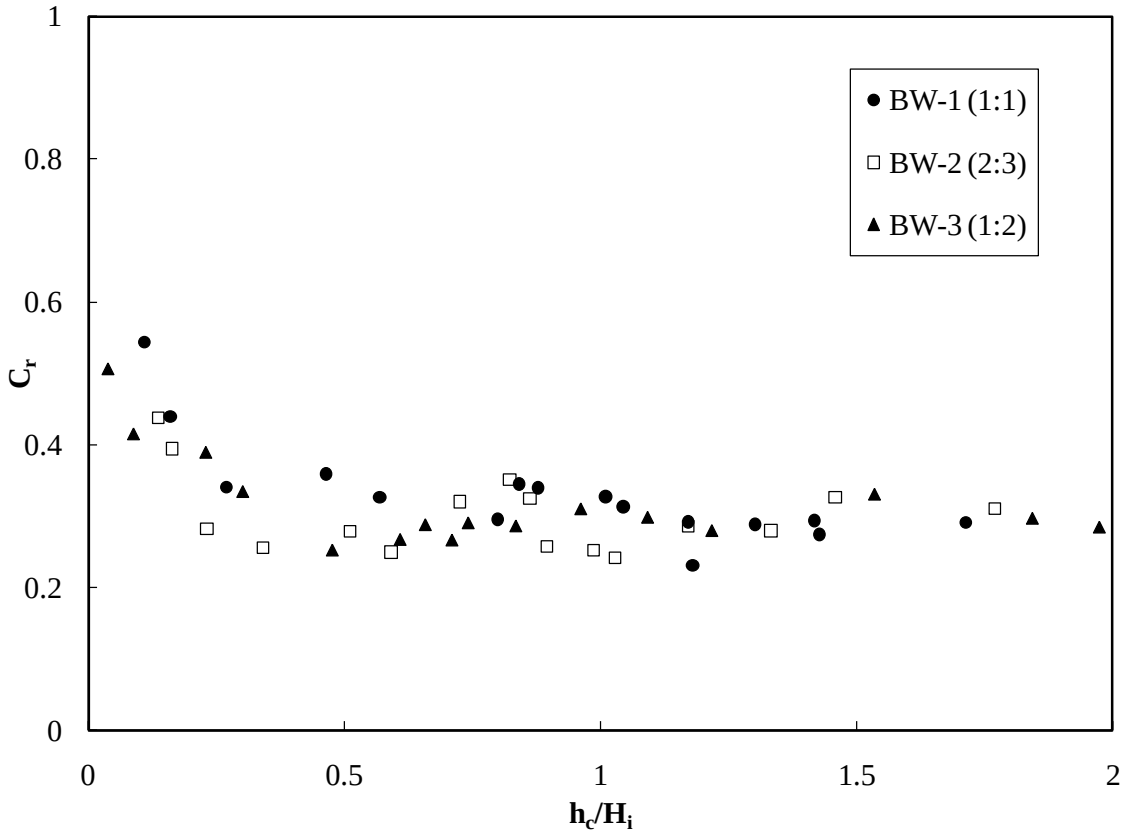

Figure 4.7. Reflection coefficients of impermeable breakwater tests. Breakwater slopes in parentheses (V:H).

Wave reflection coefficients in deeper water (h_c/H_i values larger than approximately 0.75) are larger than those predicted by the impermeable submerged vertical breakwater reflection coefficient equation proposed by Young and Testik (2011), shown in Figure 4.8, given as

$$C_{r-vertical} = 0.53e^{-0.85\frac{h_c}{H_i}} \tag{4.6}$$

Equation (4.6) is derived from the research presented in the master's thesis of Young (2008). An increase of this type could be explained by a shoaling effect that occurs across the width of the trapezoidal breakwaters. As waves pass over the sloped faces of trapezoidal breakwaters, wave height continually increases due to shoaling. Naturally a larger wave then breaks over the structure, in comparison to a vertical or semicircular breakwater. Greater wave heights at the structure may produce larger reflected waves. This discrepancy would be the most notable when waves cease to break. Waves that fail to break maintain a larger wave height while continuing to shoal across the sloped beach in the lee of the breakwater. This process produces a greater wave height that impacts the shoreline which leads to a larger reflected wave height from the shore, of which a portion may return over the structure.

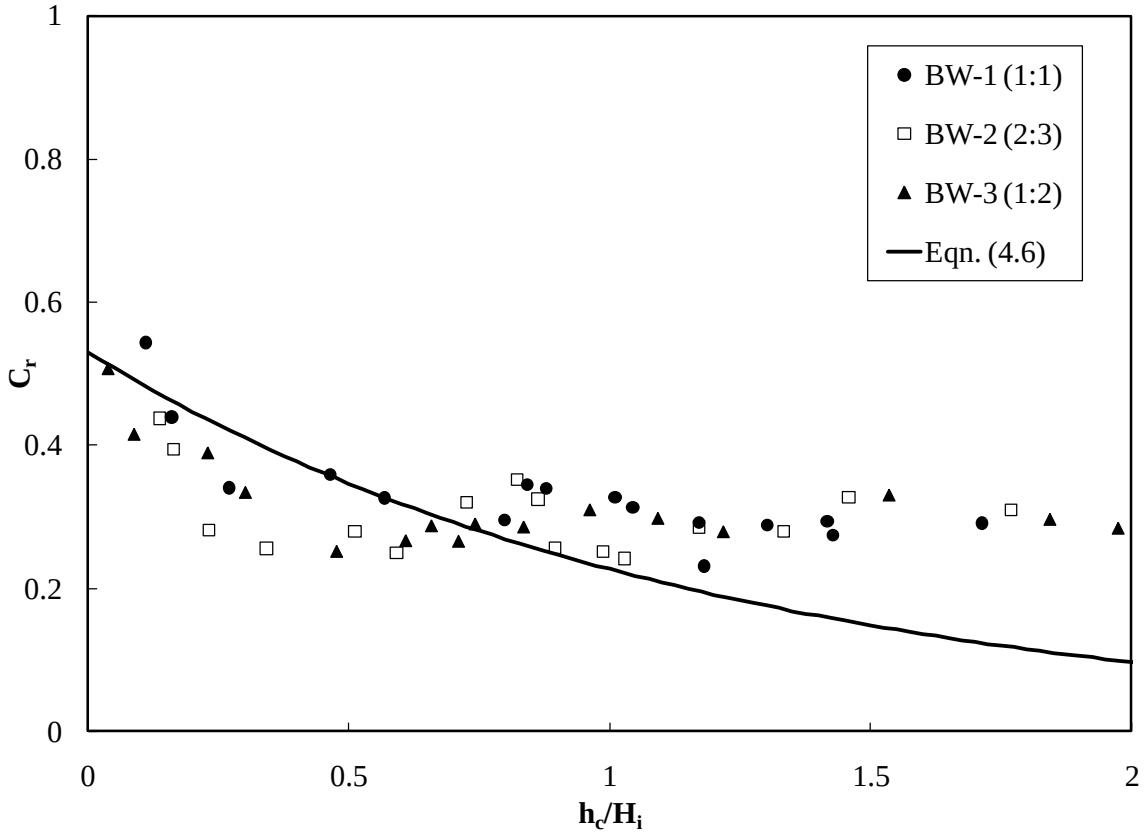

Figure 4.8. Comparison of experimental reflection coefficient values of impermeable submerged breakwaters with the Young and Testik (2011) parameterization. Breakwater slopes in parentheses (V:H).

While the breakwater models become increasingly submerged, an unusual bulge occurs between h_c/H_i values of approximately 0.5 and 1.0. As h_c/H_i approaches 0.5, the depth of submergence nears half of the incident wave height. At larger h_c/H_i values the wave is theoretically able to pass completely over the crest, assuming no wave-breaking. This could initiate a transitional region (evident by the bulge) in the wave reflection coefficient values as the structures respond to an increasing relative submergence depth and a decreasing intensity of wave-breaking. Most likely, this region begins in response to the wave breaker type changing, as shown in Figure 4.9. Figure 4.10 shows that the

region of strong decay is extended for breakwaters of a milder sloped face. Figure 4.10.c, representing BW-3, shows lower values within the strong decay region, and a slightly delayed beginning for the bulge region. As far as the conclusion of the bulge region, wave-breaking theoretically terminates when the wave height approaches 0.8 of the water depth (Equation 2.36), pertaining to an h_c/H_i value of 1.25. This value provides a potential physical condition for the conclusion of this transitional region. Defining this connection between wave-breaking conditions and the reflection coefficient is the aim of a future parameterization involving h_c/H_i.

A similar observation is reported by Blenkinsopp and Chaplin (2008) through experimental wave tank tests determining reflection coefficients from a submerged sloping structure. Blenkinsopp and Chaplin (2008) explain how each incident wave has an energy budget, or a certain amount of energy that must be allotted between energy dissipation, reflection, and transmission. This energy budget can be quickly depleted by heightened dissipation during large wave-breaking events at relatively low levels of crest submergence, leaving less energy to be reflected or transmitted from the structure. As wave-breaking intensity decreases (or plunging breakers turn to spilling breakers) and the sloping structure becomes increasingly submerged, it is possible for the structure to reflect more wave energy since it is not being dissipated through wave-breaking.

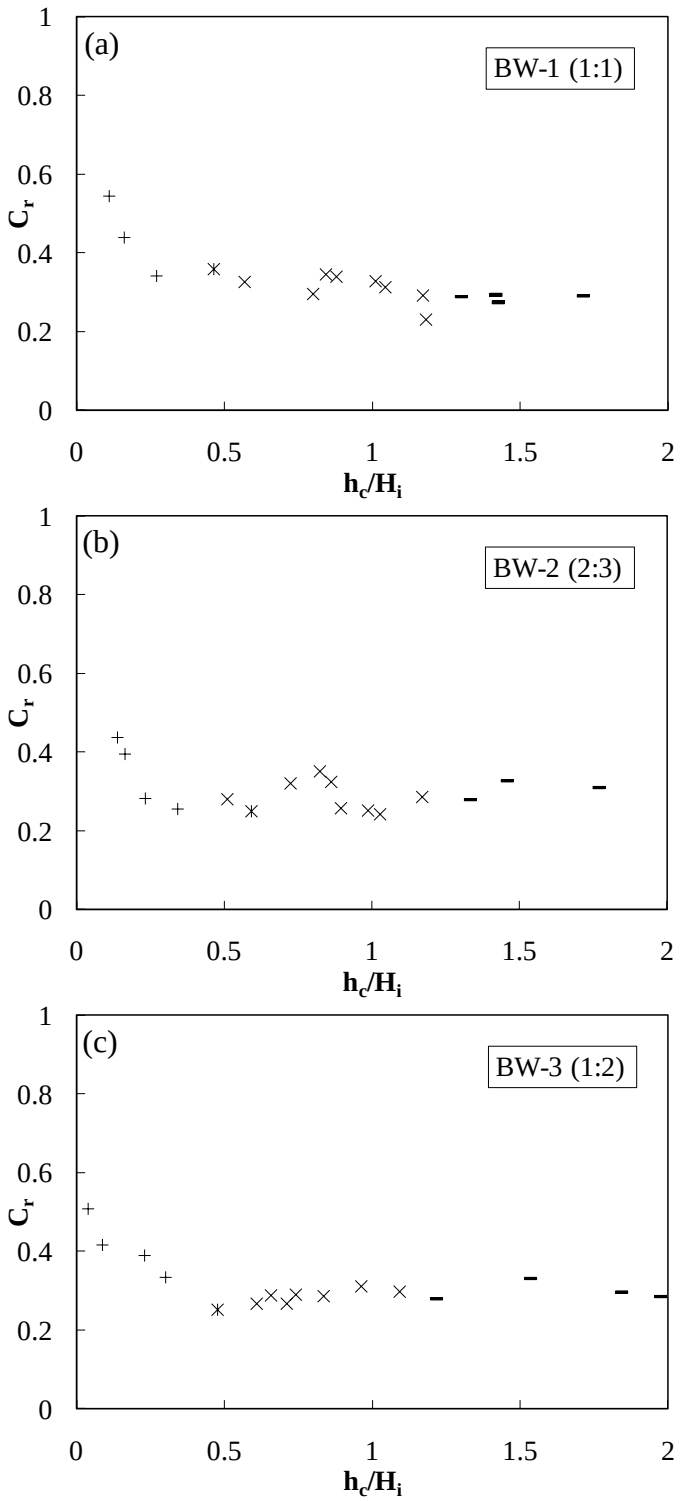

Figure 4.9. Breaker type of each experiment as observed at the impermeable breakwater. Symbols used: (+) – plunging breaker; (⨯) – plunging – spilling transitional breaker; (×) – spilling breaker; (−) – no wave-breaking. Breakwater slopes in parentheses (V:H).

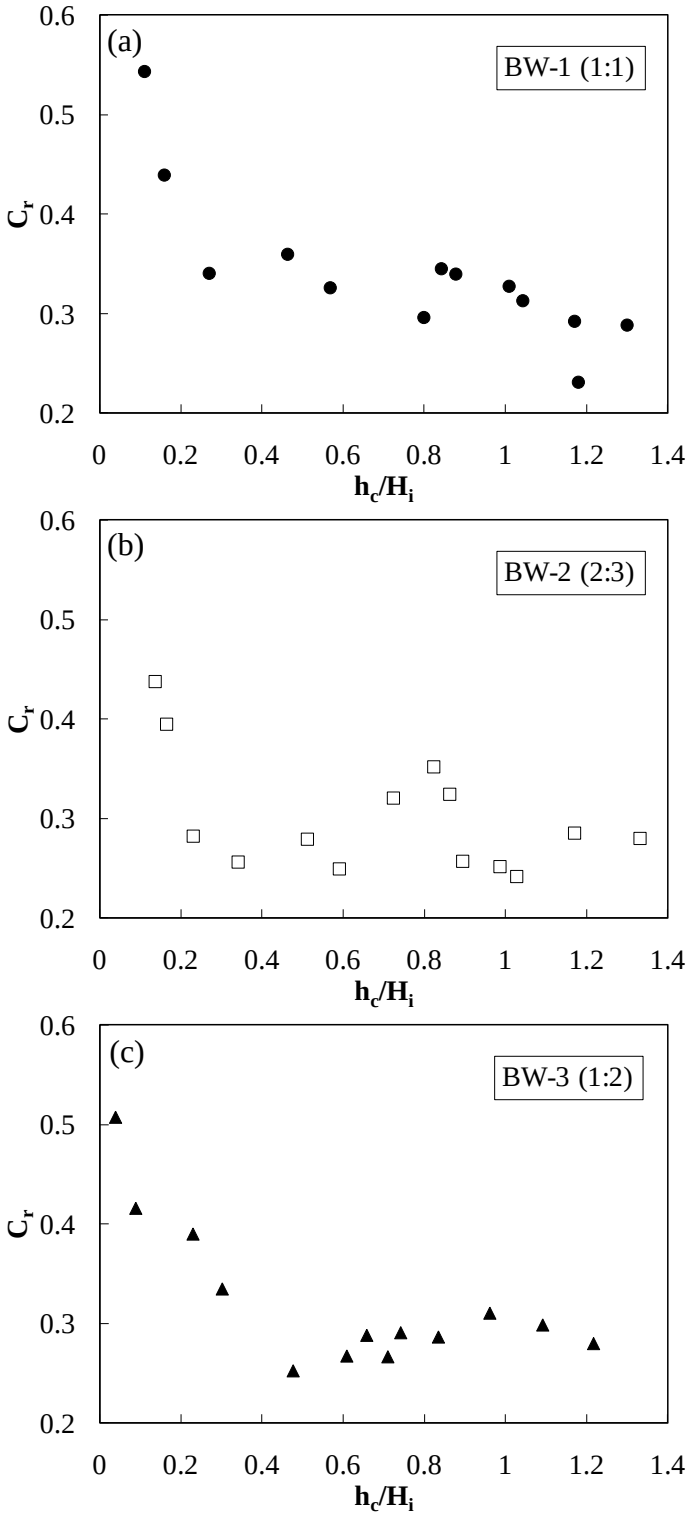

Figure 4.10. Enhanced presentation of bulge region for each breakwater. Note that several data points have been removed in each figure to focus on the bulge region. Breakwater slopes in parentheses (V:H).

Breaker type is indicated throughout the full spectrum of h_c/H_i values, for each breakwater, in Figure 4.9. Each figure shows a transition from plunging to spilling breakers occurring at the bulge region. For the given values, wave reflection coefficients strongly decay as the submergence depth increases, until eventually displaying a mild increase through the bulge region, likely due to the phenomenon described by Blenkinsopp and Chaplin (2008). Figure 4.10 gives a closer look at the bulge region for each breakwater, individually.

In Figure 4.10, the graphs from top to bottom (a-c) correspond to breakwaters with increasing exposed slope widths. As the exposed breakwater width extends, the clarity of the bulge is enhanced, indicating that W/L plays an important role in influencing the shape of the bulge region. For the bulge, as W/L increases, spilling breakers will dissipate more wave energy before reflecting off of the breakwater. For BW-1 (Figure 4.10.a), there is minimal travel over the breakwater and therefore an almost constant reflection coefficient value is observed. In the case of BW-2 (Figure 4.10.b) and BW-3 (Figure 4.10.c), waves travel less over BW-2 and therefore larger reflection coefficient values are observed than in the case of BW-3. Energy dissipation is the highest in BW-3 and so lower reflection coefficient values are observed and the bulge is best defined.

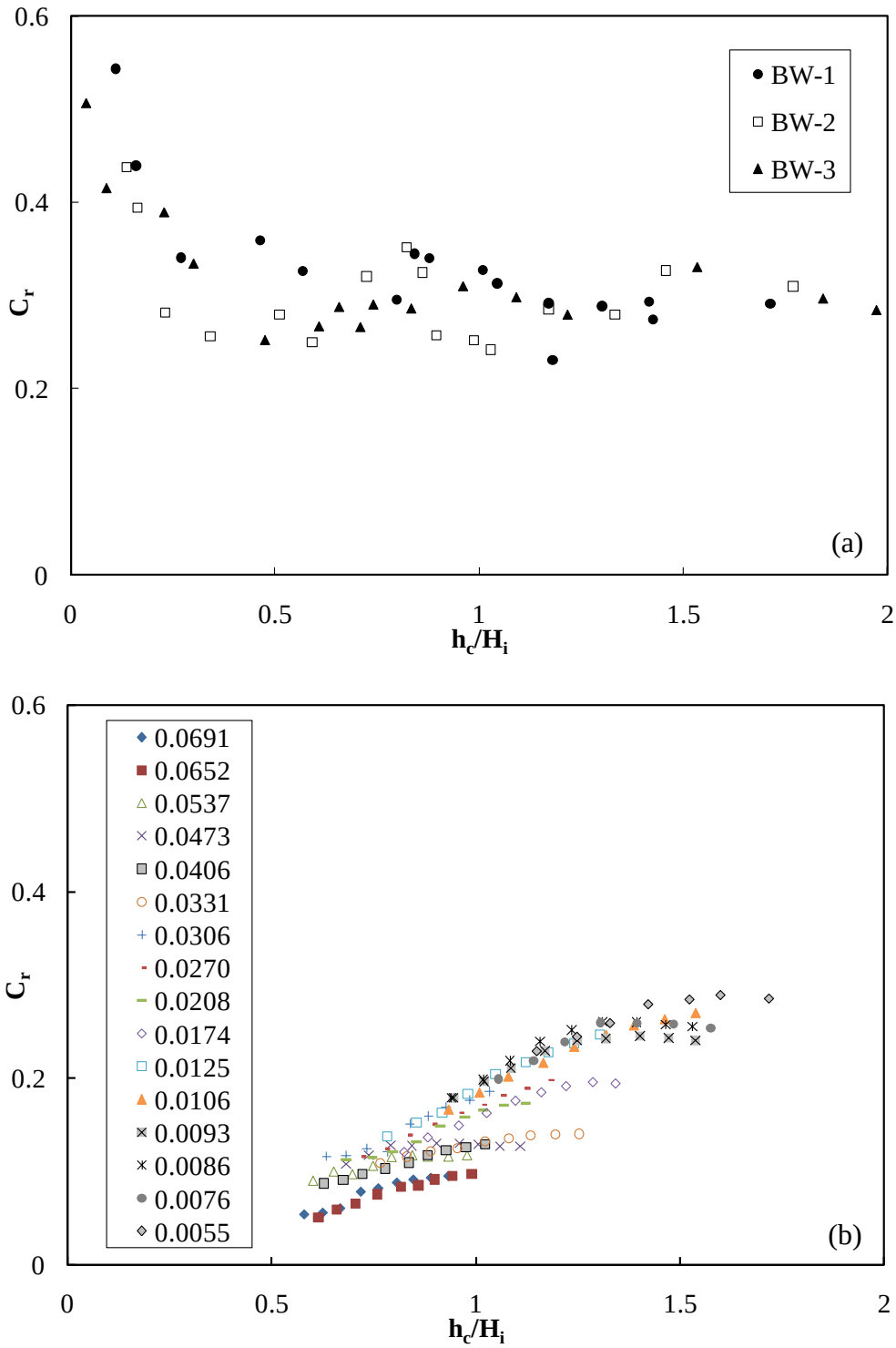

Figure 4.11. Visualization of bulge in reflection coefficient data: (a) data from present study; (b) data of Blenkinsopp and Chaplin (2008). Legend in (b) gives H_i/L_o values of tests.

Figure 4.11 displays the similarities between the experimental data of this study and that of Blenkinsopp and Chaplin (2008). The testing conditions of Blenkinsopp and Chaplin (2008) were limited to an h_c/H_i range of around 0.5 to 1.4. In addition to testing the effect of h_c/H_i on the reflection coefficient, they also considered the effect of wave steepness, H_i/L_o, on the reflection coefficient (see Figure 4.11.b). These curves correspond to the bulges similar to those in the experimental data of this study, presented in Figures 4.7 and 4.11.a. Their impermeable breakwater was 6 meters long and had a slope of 1:10, making it 60 cm tall. It must also be noted that Blenkinsopp and Chaplin (2008) incorporate the same method as the current study for measuring reflection coefficients from their structure. Figure 4.11.b portrays a clear, distinct bulge region for each separate H_i/L_o value, due to a lengthened milder slope. This supports the premise that W/L and H_i/L_o are important dimensionless parameters governing the characteristics of the bulge region. When superimposing data from the current study over the data of Blenkinsopp and Chaplin (2008) it is noticed that the reflection coefficient values of the current study are larger than the values observed through the experiments of Blenkinsopp and Chaplin (2008). There are several differences between the setup employed in the current study and that used by Blenkinsopp and Chaplin (2008). The shape tested in their experiments is a wedge with no crest width, no onshore sloping face, and also no sandy beach. The wedge is simply placed into a wave tank, leaving a horizontal bed onshore and offshore of the structure. The reasoning behind such a design is that waves are able to break at the peak of the structure and then reform in the lee to

produce clear transmitted waves. After passing the breakwater, a layer of polyether foam is used as an absorbing beach to prevent multiple reflected waves. The typical background reflection coefficients observed from the absorbing beach itself were between 0.008 and 0.085, similar to the background reflection values of roughly 0.03 to 0.09 observed in the present study. With a different setup it is understandable that the reflection coefficient values could have different magnitudes. There are more areas with a potential to reflect incident waves in the setup used in the current study. Also, the crest width could affect the dissimilarities between the bulges in each study. Having an actual crest and onshore slope extends the distance that a wave must travel through shallower depths, more likely inducing wave-breaking. Also, the inclusion of a sloping beach for the present study could further reduce the clarity of the bulge in reflection coefficients. Another possible explanation for the observed differences is the long, mild slope used by Blenkinsopp and Chaplin (2008). This would cause the bulge observed by Blenkinsopp and Chaplin (2008) to be more pronounced because the waves with spilling breakers travel a longer distance over the sloped face. While it was shown by Neelamani and Sandhya (2003) that the slope of a plane seawall does not affect the reflection coefficients induced by the structure, an extremely mild and long slope may cause some difference in the observed reflection values from a submerged breakwater (the findings of Neelamani and Sandhya (2003) presented in Figures 4.4 through 4.6 cover the slope range for our tests, but do not cover a 1:10 slope). As previously discussed, the actual exposed width has a noticeable effect on the measured reflection coefficients, so a bulge as such would become increasingly clearer and more evident as the exposed width increases. Data

presented in Figure 4.7 was measured from a range of breakwater face widths of 15.0 to 36.5 cm and heights of 15.0 to 17.0 cm. In order to test this hypothesis, a full range of experiments were performed where BW-1 and BW-2 were installed directly on the tank bottom, all other setup conditions remaining constant. This produced exposed widths and heights as small as 5 cm. The results from these tests are displayed in Figures 4.12 and 4.13.

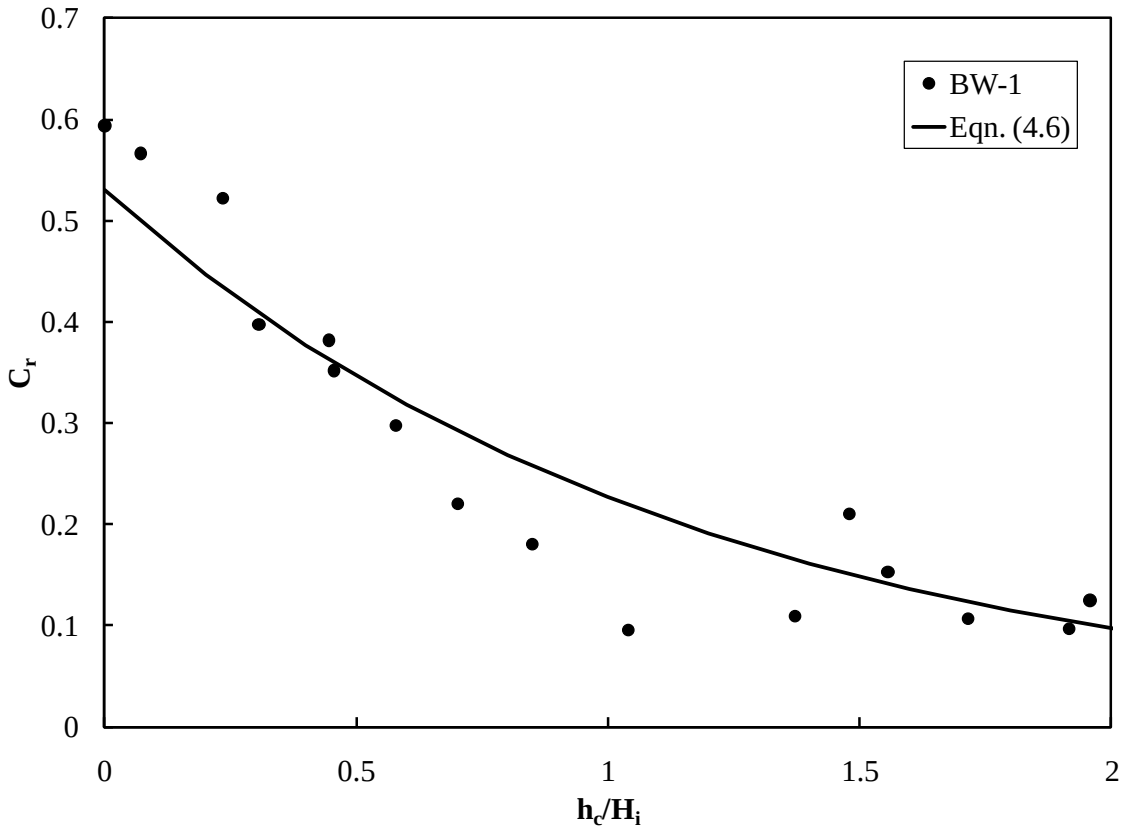

Figure 4.12. Comparison of BW-1 reflection coefficients measured from tests with exposed breakwater width reduction (i.e. $W/L \ll$, $W = 5\,\text{cm}$, see Table 4.2 for L values) with Young and Testik (2011) parameterization.

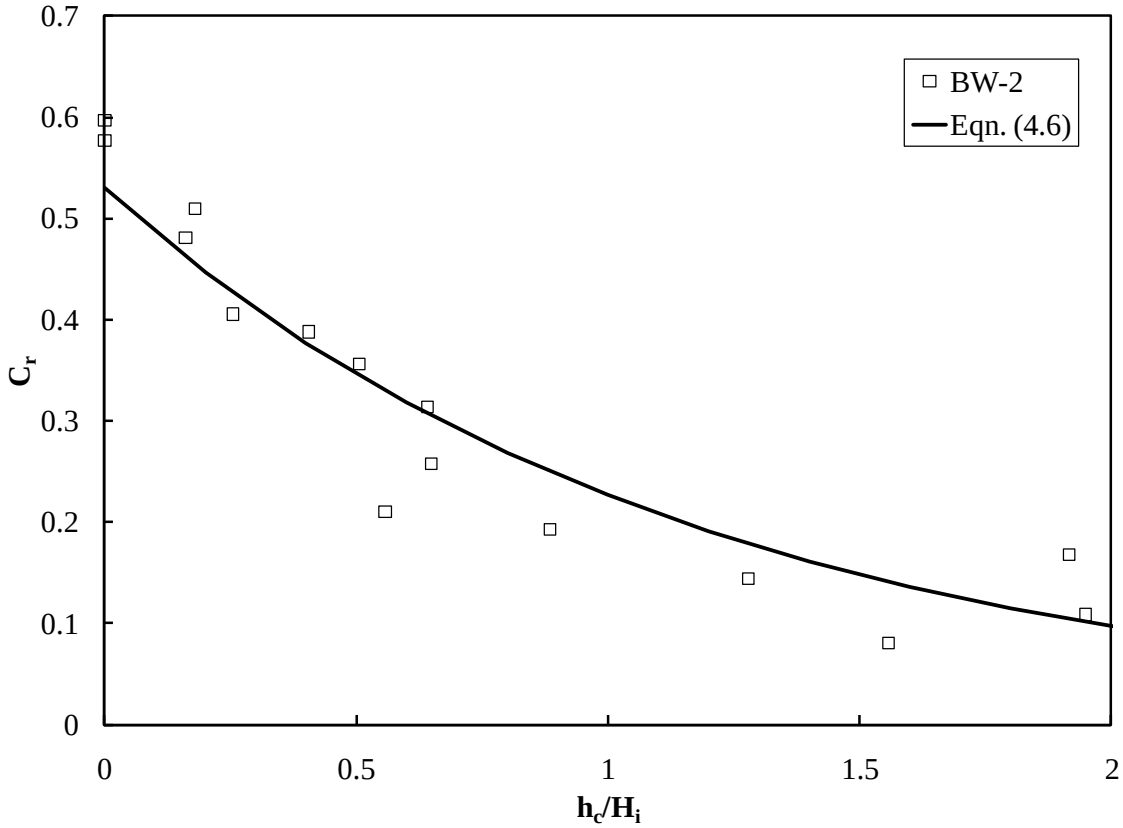

Figure 4.13. Comparison of BW-2 reflection coefficients measured from tests with exposed breakwater width reduction (i.e. $W/L \ll$, $W = 7.5\,\text{cm}$, see Table 4.2 for L values) with Young and Testik (2011) parameterization.

In Figures 4.12 and 4.13, the measured reflection coefficient values are plotted for comparison with the parameterization proposed by Young and Testik (2011) for impermeable submerged vertical breakwaters. Not only do the observed reflection coefficient values match the proposed vertical breakwater parameterization by Young and Testik (2011), but they also fail to exhibit any bulge formation. Looking at the presented data in this section, the unique bulge region in the reflection coefficient values for impermeable submerged breakwaters is shown to increase in clarity as the exposed width of the breakwater face extends. The parameter that includes the exposed width, W/L,

can also be connected to the phase shift angle, γ, because the exposed width of breakwaters with similar crest heights determines the slope angle of the breakwater face. This slope angle, along with H_i/L_o, connects W/L to the surf similarity parameter as well. These dimensionless groups are to be analyzed further in future parameterizations to quantify and explain the bulge region.

Permeable Breakwaters

Two permeable breakwater models are tested and experimental data is presented below. Figure 4.14 compares the reflection coefficient data for two separate permeable breakwaters, BW-4 and BW-5. BW-5 is composed of golf balls at a porosity of 0.39, whereas BW-4 has a higher porosity, being specifically designed with a porosity of 0.49 by placing PVC pipes at calculated intervals. BW-2 is included later in order to compare the impermeable breakwater of the same geometry to the permeable breakwaters. The observed breaker types during each permeable breakwater experiment are displayed later in the section as well.

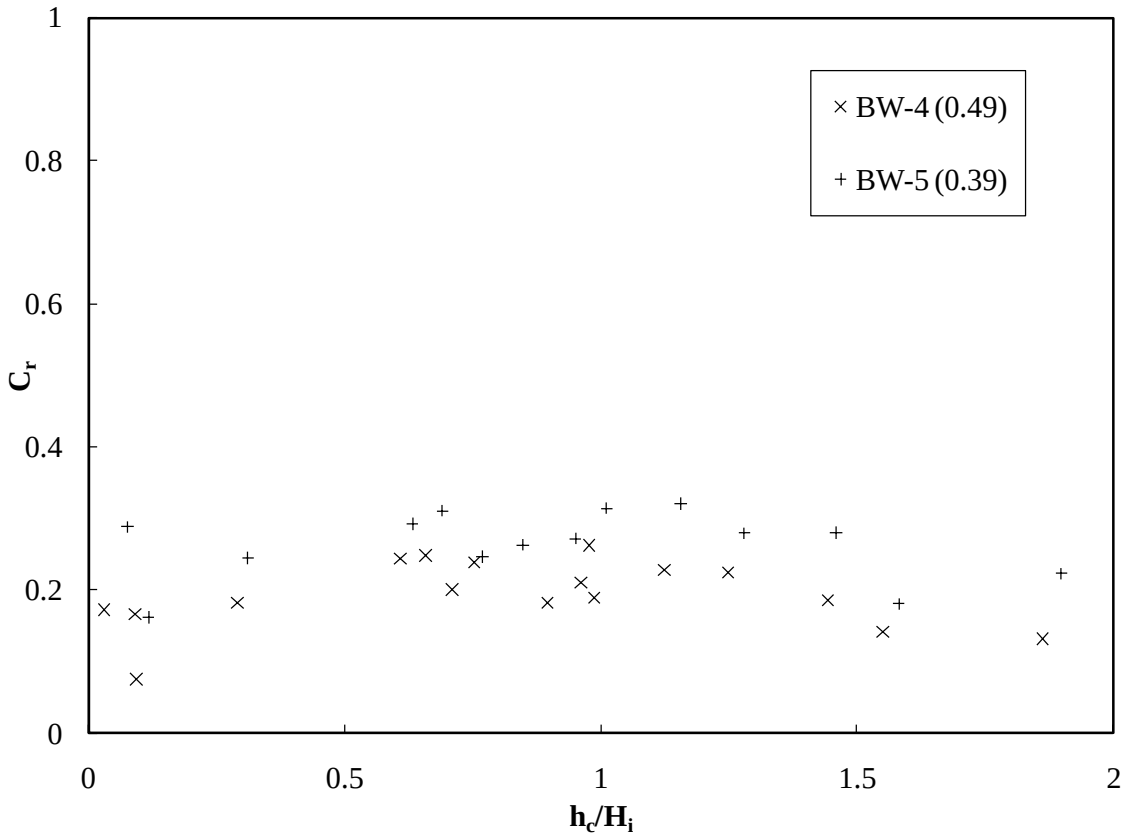

Figure 4.14. Reflection coefficients of permeable breakwater tests. Breakwater porosities in parentheses.

For the permeable breakwater data presented in Figure 4.14, the less porous structure (BW-5) displays greater reflection. As the porosity of a structure increases, its reflection capabilities typically decrease as there is a greater permissible area for waves to transmit through the structure. An important observation from Figure 4.14 is that the permeable breakwaters do not exhibit a strong decay in the reflection coefficient for h_c/H_i values less than around 0.5. This is because instead of the wave impacting a solid object, in the case of the impermeable structures, the wave is able to transmit a portion of its energy through voids in the permeable models. For the plunging breakers that are occurring,

wave-breaking is confined to a narrow area over the breakwater and the jet of water associated with this particular type of breaker forces water through the voids, transmitting and dissipating energy. Aside from the dissipation due to breaking, additional energy may be dissipated through frictional forces within the breakwater. However, the permeable breakwaters then show an increase in the reflection coefficient values past this point, displaying a trend similar to the impermeable breakwaters. The permeable breakwaters are compared to the impermeable one of the same geometry in Figure 4.15. It is observed that for low values of h_c/H_i ($<$ approximately 0.4) the porosity plays a key role in determining the reflection coefficient. However, as h_c/H_i becomes greater than roughly 0.4, BW-2 and BW-5 produce similar reflection coefficients. This may be attributed to the porosity being insignificant such that surface waves are only affected by the structure shape through the step change in water depth. Reflection coefficients from the structure with greater porosity, BW-4, still exhibit some dependence on its permeability. Overall, each permeable breakwater produces a relatively constant value for the reflection coefficient before eventually decaying past an h_c/H_i value of around 1.5. Breaker types observed during each permeable breakwater experiment are presented in Figure 4.16.

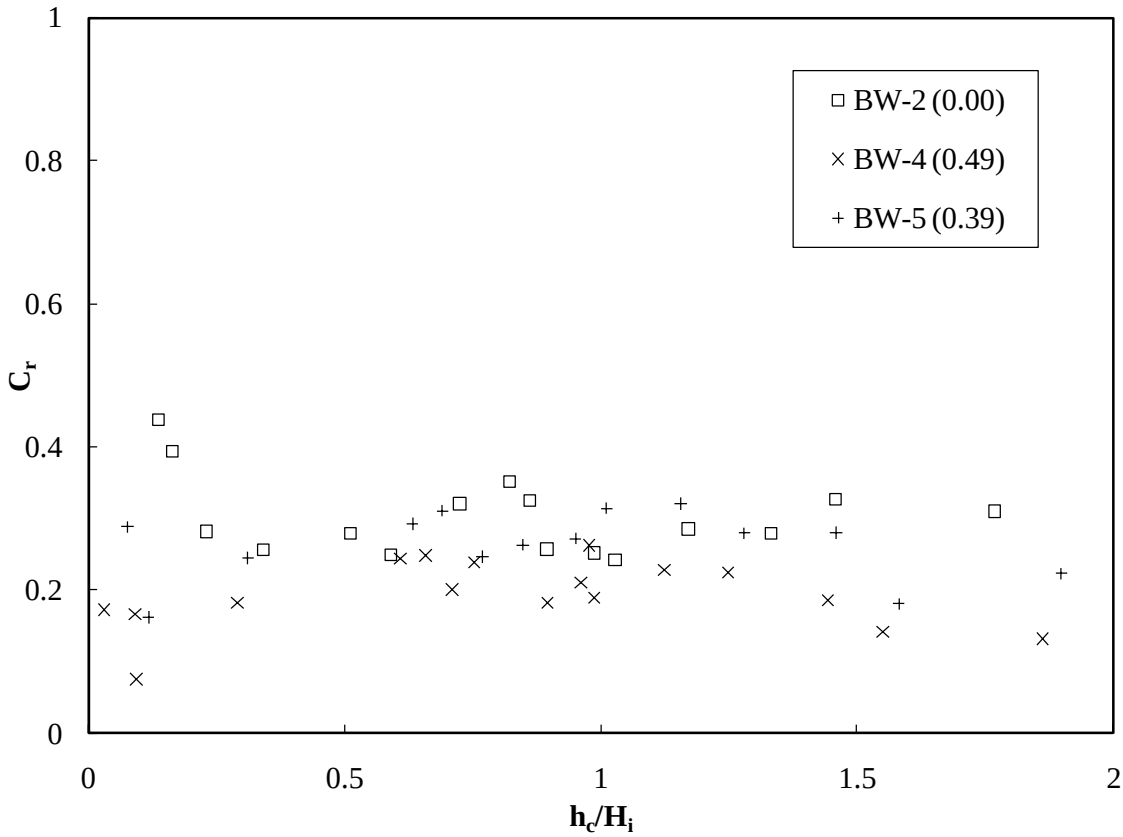

Figure 4.15. Comparison of reflection coefficients from impermeable (BW-2) and permeable (BW-4 and 5) breakwaters of the same shape. Breakwater porosities in parentheses.

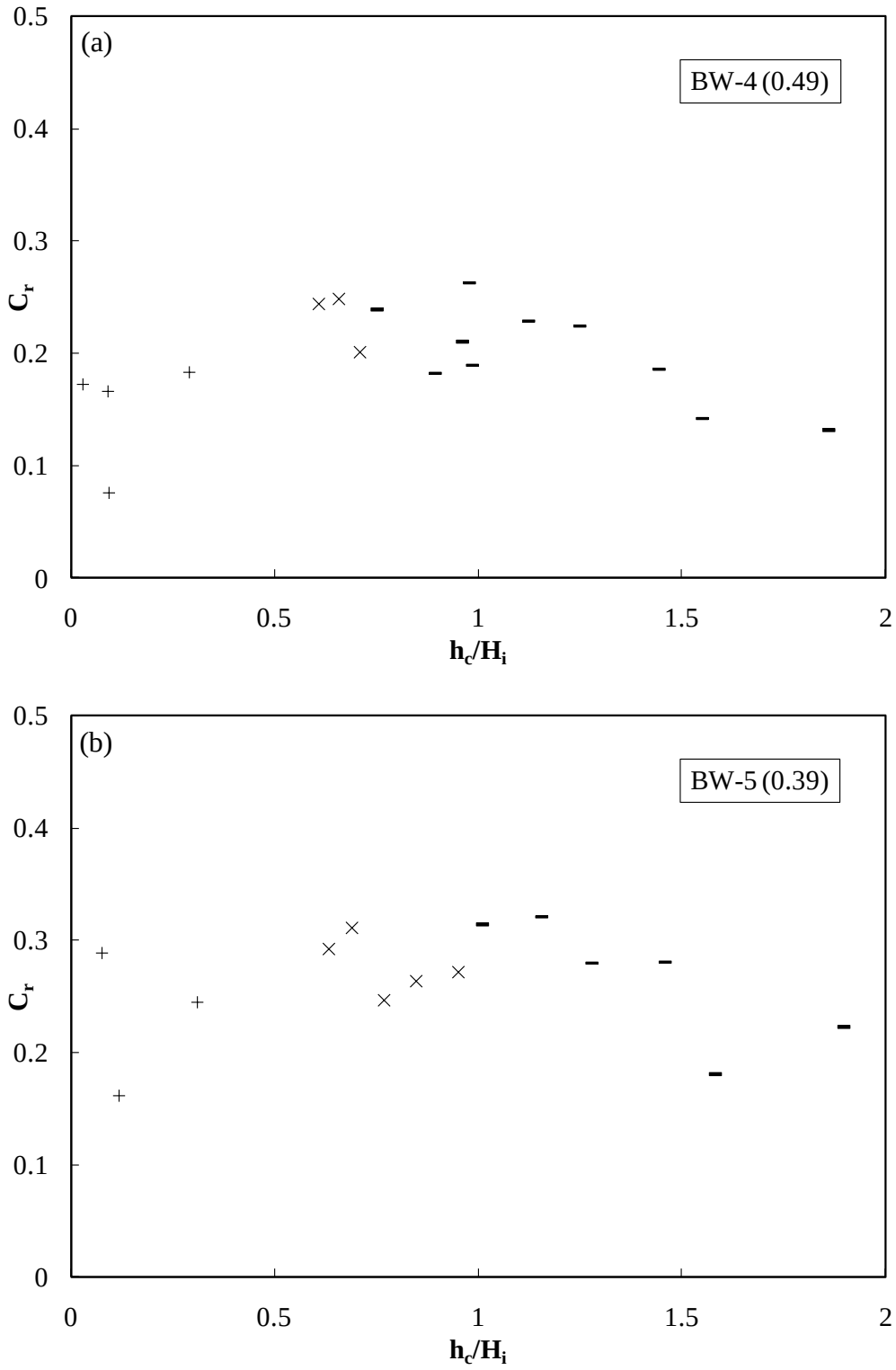

Figure 4.16. Breaker type of each experiment as observed at the permeable breakwaters. Symbols used: (+) – plunging breaker; (╳) – spilling breaker; (━) – no wave-breaking. Breakwater porosities in parentheses.

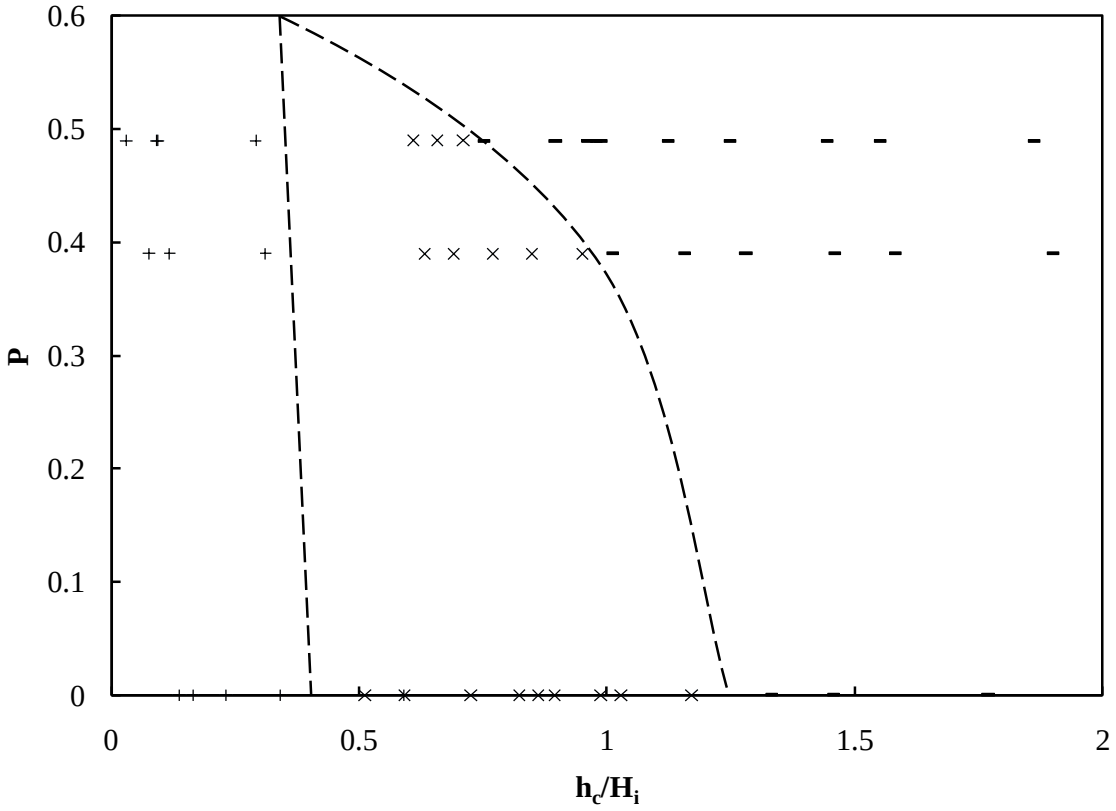

Figure 4.17. Breaker type regime diagram. BW-2, BW-4, and BW-5 breaker types are plotted. Symbols used: (+) – plunging breaker; (╳) – spilling breaker; (—) – no wave-breaking. Dashed lines are qualitative.

A regime diagram is shown in Figure 4.17 to contrast the breaker transitions across a range of h_c/H_i values for breakwaters of different porosities. Transitions between breaker types occur at lower h_c/H_i values for breakwaters of greater porosity. Dashed lines represent transition zones between structures of different porosities.

4.4 EVALUATION OF REFLECTION COEFFICIENT EQUATIONS

While several equations for the transmission coefficient have been proposed for submerged breakwaters, reflection coefficients from submerged trapezoidal breakwaters

have received considerably less attention. This is especially true for the impermeable case, where mostly impermeable emerged seawalls have been studied. Reflection coefficient data was collected and examined by Blenkinsopp and Chaplin (2008) for a submerged wedge-shaped structure but no equation was proposed from their experimental data. Therefore, this extensive study on reflection coefficients of submerged trapezoidal breakwaters provides a large set of data to the coastal engineering community that will enable a more thorough insight on this topic.

Prior researchers that examined reflection coefficients focused on emerged breakwaters (e.g. Battjes, 1974; Seelig and Ahrens, 1981; Postma, 1989; see Section 2.3). Zanuttigh and van der Meer (2008) recently proposed a parameterization for submerged structures, given in Equation (2.16), but concede that further investigation is needed to confirm and improve their proposed parameterization. Figure 4.18 compares the existing equations with experimental data from this study to prove their ineffectiveness in predicting the measured reflection coefficients for submerged structures. Several negative values (4.2% of total impermeable, 6.5% of total permeable) were predicted by Equation (2.16) proposed by Zanuttigh and van der Meer (2008) and were removed from the respective plots due to obvious physical reasoning. Additionally, 87.5% of total impermeable and all permeable values predicted by Equation (2.5) from Battjes (1974) were removed from the respective plots due to unreasonable predictions.

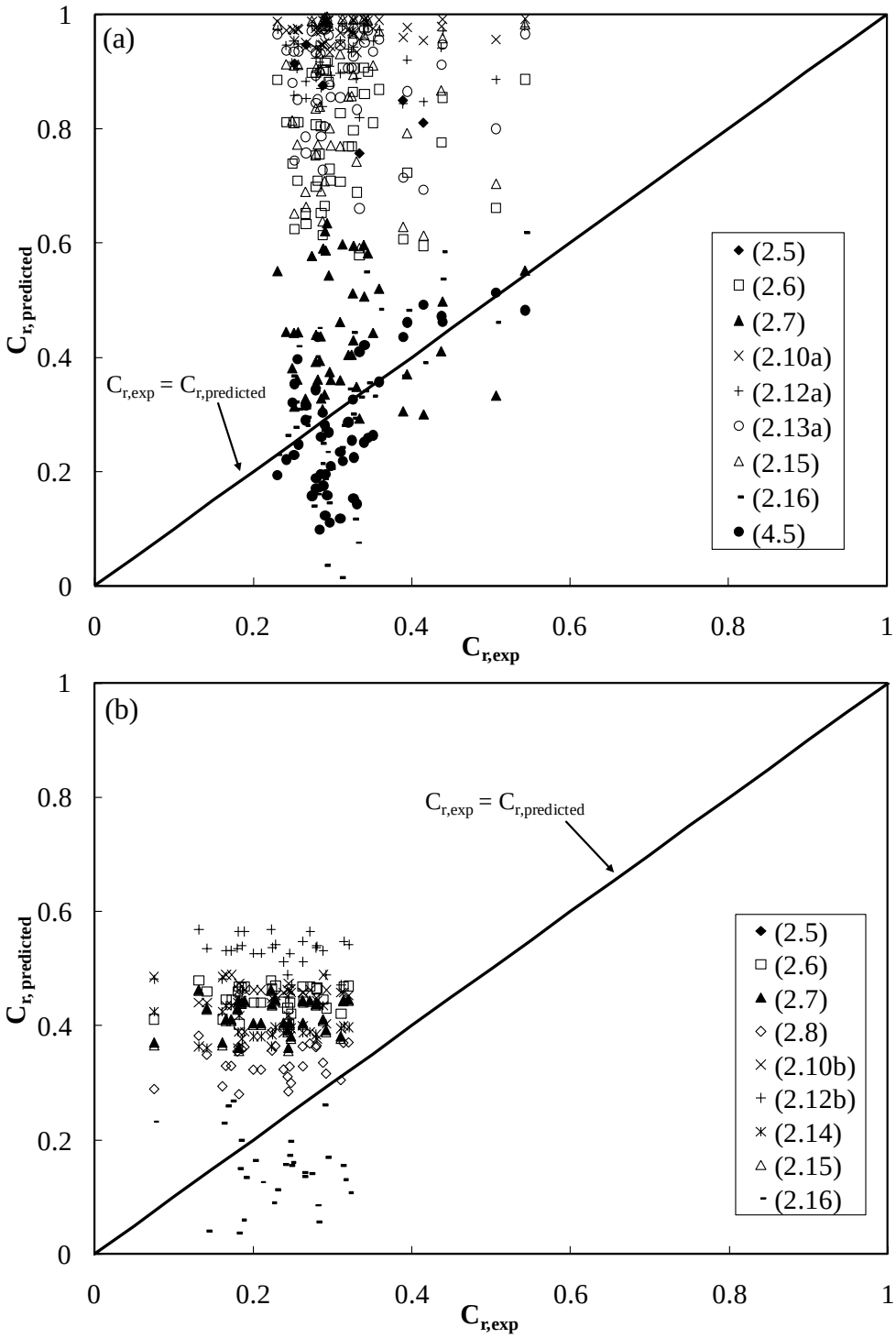

Figure 4.18. Predictions of the reflection coefficient values by the equations tabulated in Table 4.1 compared to C_r values measured in the experiments conducted for submerged trapezoidal breakwaters: (a) – impermeable; (b) – permeable. Legends relate the symbols with equation numbers given in Table 4.1.

Table 4.1. Compilation of available C_r equations for permeable and impermeable breakwaters. Coefficients of interest are defined in Chapter 2. Columns 4 and 5 represent the mean error, $\frac{1}{n}\sum_{i=1}^{n}\frac{C_{r,predicted}}{C_{r,experimental}}$, of predicted C_r values by each equation.

Eqn. #	Reference	Equation	Fig. 4.18.a	Fig. 4.18.b
(2.5)	Battjes (1974)	$0.1\xi^2$	*8.40*	*9.69*
(2.6)	Seelig & Ahrens (1981)	$\frac{a\xi^2}{\xi^2+b}$	*2.53*	*2.18*
(2.7)	Postma (1989)	$0.14\xi^{0.73}$	*1.43*	*2.03*
(2.8)	Postma (1989)	$0.071P^{-0.082}\cot\theta^{-0.62}s^{-0.46}$	-	*1.64*
(2.10a)	Hughes & Fowler (1995)	$\frac{0.1176}{0.1176+\xi_h^{2.6}}$	*3.16*	-
(2.10b)	Hughes & Fowler (1995)	$\frac{0.1415}{0.1415+\xi_h^{0.804}}$	-	*2.26*
(2.12a)	Sutherland & O'Donoghue (1998b)	$\frac{\xi_f^{2.58}}{7.64+\xi_f^{2.58}}$	*3.02*	-
(2.12b)	Sutherland & O'Donoghue (1998b)	$\frac{0.82\xi_f^2}{22.85+\xi_f^2}$	-	*2.55*
(2.13a)	Muttray & Oumeraci (2002)	$1-\left(H_i/H_{i,crit}\right)^{3/2}\left(1-\left(2/\pi\right)\right)$	*2.90*	-
(2.14)	Muttray et al. (2006)	$\frac{1}{1.3+3h\frac{2\pi}{L}}$	-	*1.93*
(2.15)	Zanuttigh & van der Meer (2008)	$\tanh\left(a\xi^b\right)$	*2.77*	*2.01*
(2.16)	Zanuttigh & van der Meer (2008)	$\tanh\left(a\xi^b\right)\left(0.67+0.37\frac{R_c}{H_i}\right)$	*0.92*	*0.69*
(4.6)	Young and Testik (2011)	$0.53e^{-0.85\frac{h_c}{H_i}}$	*0.88*	-

Table 4.1 displays the mean error of predicted reflection coefficients by each available C_r equation. Equation (2.16) under-predicts the values for permeable breakwater data points, but still offers the most accurate prediction of reflection coefficient values for both impermeable and permeable breakwaters, combined. This equation fits best because it was actually developed for the case of submerged breakwaters, but used a small sample and needs further confirmation. Equation (2.5) developed by Battjes (1974) over-predicts the values of both to the worst degree as the equation is unbounded of itself because the surf similarity parameter could have infinite values. For the impermeable case alone, Equation (4.6) of Young and Testik (2011), even though derived for submerged vertical breakwaters, provides the closest relationship, most likely due to similar testing conditions. The rest of the equations all poorly fit the data set as they were intended for application with emerged breakwaters. While assuming the submerged structures to be emerged, the predicted values are expected to be greater than measured because most of these equations assume no overtopping, thus no transmission. Therefore, only the slope of the structure and the wave height and length are taken into consideration, ignoring that for a submerged structure a significant portion of the wave energy may be transmitted past the breakwater. The wave transmission, and also the wave dissipation through breaking that may occur on a submerged breakwater, provides for a lower measured reflection coefficient value than predicted by these equations.

Similar research prior to this study has been performed by Davies (1991) and Smith and Kraus (1990). Davies (1991) tested similar impermeable structures on a small scale, but

did not display any data from the reflection coefficient tests. Davies (1991) used the same method as the current study of calculating reflection coefficients; however, Davies (1991) used a different setup, placing structures on a flat sandy beach. Among many other things, Smith and Kraus (1990) studied wave reflection from submerged bars, or artificial reefs. In their tests they used a 1:30 solid concrete sloping beach to prevent any possible shoreline transformations from affecting their test results. Structure slopes were mild, intending to emulate offshore bars in the field, with an average tested offshore bar slope angle of 20 degrees and an overall range between 4 and 37 degrees. Wave reflection was measured by the method of Goda and Suzuki (1976), the same method as the current study, using two gages offshore of the structure. They began collecting wave data after waves reflected off the concrete slope (to include the slope in the reflection coefficient) but before the reflected waves from the wave board returned to the sand bar. Having a very long wave tank (150 feet long) made such a method possible. They found through their testing that the measured reflection coefficients did not fit the proposed equations given by Battjes (1974) or Seelig and Ahrens (1981). This is understandable and agrees with the observations of the current study. Their reflection coefficients ranged from 0.1 to 0.35 without exhibiting much of a trend. Reflection coefficients were plotted against the seaward bar angle and did not exhibit the strong decay trend shown in this study.

Wave reflection has not been extensively examined for impermeable submerged slopes. Reflection coefficients of submerged structures have only been significantly studied for

rock permeable slopes (Zanuttigh and van der Meer, 2008). Findings from the experimentation presented herein provide a thorough basis for further research of impermeable submerged slopes. Examining reflection coefficients across a more complete range of relative submergence depths will provide future insight into the placing of breakwater constructions. With a proven bulge in reflection at certain relative submergence depths, breakwater placement could be set to ensure that the energy reflection capacity of a structure is maximized throughout its local tidal range. Applying the experimental results in order to maximize the efficiency of a breakwater is the pursuit of this study, and a brief discussion on breakwater design considerations based upon the experimental findings are discussed in the following section.

4.5 DESIGN CONSIDERATIONS

Several design considerations can be drawn from the wave reflection data assembled into this chapter. Most notably, the bulge region discovered from the reflection coefficient measurements, affirmed through prior research by Blenkinsopp and Chaplin (2008), should be taken into account, along with the present breaker type at the breakwater. When placing a breakwater into a coastal zone, these two factors can play a major role in saving money not only through beach retention, but also in construction costs.

The presence of the bulge in reflection coefficients cannot be overlooked when deciding the proper placement of a breakwater construction. As the breakwater becomes more submerged it is expected that the reflection coefficient, along with its ability to shelter a

coastline, will decay. Therefore, placing the breakwater such that its crest is as close to mean water level as possible seems preferred. However, the bulge provides relief in that the breakwater may be placed at a position such that it remains submerged throughout the entire tidal cycle, providing no impact on the horizon. Being submerged to a greater depth also reduces the volume of material necessary for construction, cutting down on costs (less material, machinery, labor, etc.).

Discovering that the bulge results from the transition to spilling breakers is also important as spilling breakers will dissipate energy over a longer period of time. When a breakwater is placed to perform within the bulge region, the reflection coefficient from the breakwater may only be in the range of 0.3 to 0.4, not necessarily desirable. However, not only are these reflection coefficient values larger than those immediately outside of the bulge region, but inducing spilling breakers allows transmitted wave energy to continually dissipate past the breakwater. This turbulent process reduces the overall energy reaching the shore and may help further maintain the protected coastline.

If transmission levels prove undesirably high, there are several ways that wave dissipation may be increased at a breakwater. Seabrook and Hall (1998) conclude that while the transmission coefficient of a breakwater is most sensitive to its relative submergence, the relative crest width is also very important. Therefore, adjusting the crest width of the breakwater may reduce the transmitted wave energy. Also, the tests of Neelamani and Sandhya (2003) have shown that dentated and serrated seawalls produce a

significant reduction in their observed wave reflection, so an impermeable trapezoidal breakwater, or a modified design for a permeable breakwater, may have a modified face that is serrated or dentated in order to increase the wave dissipation and potentially reduce wave transmission. Finally, roughness elements may be added to a submerged breakwater, while also providing a "green" aspect to its design, in order to reduce wave transmission past a breakwater. These roughness elements may consist of something similar to seagrass, or other simulated natural elements, to conform the breakwater to a structure that is more conducive to the habitat of nearby marine life.

Table 4.2. Parameters of testing. Experimental numbers correlate with Table 3.2. BT – breaker type; within breaker type column: P – plunging breaker; P/S – breaker exhibiting transition from plunging to spilling characteristics; S – spilling breaker; NB – no breaker. Breaker type is determined at the breakwater.

EXP #	BW ID	h (cm)	H_i (cm)	L (cm)	h_c/H_i	C_r	W (cm)	BT
1	BW-1	17.5	6.58	283.4	0.11	0.544	17.0	P
2	BW-1	18	8.54	276.8	0.16	0.439	17.0	P
3	BW-1	19	8.73	296.8	0.27	0.341	17.0	P
4	BW-1	22	5.47	289.7	1.01	0.327	17.0	S
5	BW-1	22	6.76	278.5	0.80	0.296	17.0	S
6	BW-1	21	7.98	291.9	0.46	0.359	17.0	P/S
7	BW-1	22	5.94	295.5	0.84	0.345	17.0	S
8	BW-1	24.5	7.80	333.9	1.18	0.231	15.0	S
9	BW-1	20.5	8.97	314.2	0.57	0.326	15.0	S
10	BW-1	22.5	5.08	320.8	1.42	0.294	15.0	NB
11	BW-1	23.5	6.30	326.5	1.30	0.289	15.0	NB
12	BW-1	24.5	6.45	314.2	1.43	0.274	15.0	NB

EXP #	BW ID	h (cm)	H_i (cm)	L (cm)	h_c/H_i	C_r	W (cm)	BT
13	BW-1	24.5	5.37	318.9	1.71	0.291	15.0	NB
14	BW-1	20.5	6.03	321.3	0.88	0.340	15.0	S
15	BW-1	21.5	6.23	333.3	1.04	0.313	15.0	S
16	BW-1	22.5	6.40	326.5	1.17	0.292	15.0	S
17	BW-2	17.5	6.58	283.4	0.14	0.438	25.0	P
18	BW-2	18	8.54	276.8	0.16	0.3945	25.0	P
19	BW-2	20	9.96	301.4	0.34	0.256	25.0	P
20	BW-2	22	5.47	289.7	0.99	0.252	25.0	S
21	BW-2	23	7.31	301.9	0.86	0.3245	25.0	S
22	BW-2	22	6.76	278.5	0.72	0.320	27.0	S
23	BW-2	19.5	8.21	311.5	0.51	0.279	23.0	S
24	BW-2	20.5	8.97	314.2	0.59	0.250	23.0	P/S
25	BW-2	23.5	6.30	326.5	1.33	0.280	23.0	NB
26	BW-2	24.5	6.45	314.2	1.46	0.327	23.0	NB
27	BW-2	24.5	5.37	318.9	1.77	0.310	23.0	NB
28	BW-2	20.5	6.03	321.3	0.90	0.257	23.0	S
29	BW-2	21.5	6.23	333.3	1.03	0.242	23.0	S
30	BW-2	22.5	6.40	326.5	1.17	0.285	23.0	S
31	BW-2	17.5	9.96	301.4	0.23	0.282	23.0	P
32	BW-2	19.5	5.47	289.7	0.82	0.352	23.0	S
33	BW-3	17.5	6.58	283.4	0.04	0.507	36.5	P
34	BW-3	18	8.54	276.8	0.09	0.416	36.5	P
35	BW-3	22	6.76	278.5	0.71	0.266	36.5	S
36	BW-3	17.5	9.96	301.4	0.30	0.334	30.0	P
37	BW-3	19.5	6.87	300.3	0.74	0.290	30.0	S
38	BW-3	20.5	7.31	301.9	0.83	0.286	30.0	S

EXP #	BW ID	h (cm)	H_i (cm)	L (cm)	h_c/H_i	C_r	W (cm)	BT
39	BW-3	19.5	8.21	311.5	0.61	0.267	30.0	S
40	BW-3	20.5	8.97	314.2	0.66	0.288	30.0	S
41	BW-3	20.5	6.03	321.3	0.96	0.310	30.0	S
42	BW-3	21.5	6.23	333.3	1.09	0.298	30.0	S
43	BW-3	22.5	6.40	326.5	1.22	0.280	30.0	NB
44	BW-3	18.5	7.98	291.9	0.48	0.252	30.0	P/S
45	BW-3	16.5	8.73	296.8	0.23	0.390	30.0	P
46	BW-3	24.5	5.01	342.1	1.97	0.284	30.0	NB
47	BW-3	24.5	6.45	314.2	1.54	0.331	30.0	NB
48	BW-3	24.5	5.37	318.9	1.84	0.297	30.0	NB
49	BW-4	15	6.58	283.4	0.03	0.173	24.0	P
50	BW-4	15.5	8.54	276.8	0.09	0.075	24.0	P
51	BW-4	17.5	9.96	301.4	0.29	0.183	24.0	P
52	BW-4	19.5	5.47	289.7	0.90	0.182	24.0	NB
53	BW-4	19.5	6.76	278.5	0.71	0.201	24.0	S
54	BW-4	19.5	8.21	311.5	0.61	0.244	24.0	S
55	BW-4	20.5	6.03	321.3	0.98	0.263	24.0	NB
56	BW-4	20.5	8.97	314.2	0.66	0.248	24.0	S
57	BW-4	21.5	6.23	333.3	1.12	0.228	24.0	NB
58	BW-4	22.5	6.40	326.5	1.25	0.224	24.0	NB
59	BW-4	23.5	6.30	326.5	1.44	0.186	24.0	NB
60	BW-4	24.5	5.37	318.9	1.86	0.132	24.0	NB
61	BW-4	24.5	6.45	314.2	1.55	0.142	24.0	NB
62	BW-4	15	6.58	283.4	0.09	0.166	24.0	P
63	BW-4	19.5	5.47	289.7	0.99	0.189	24.0	NB
64	BW-4	19.5	6.76	278.5	0.96	0.210	24.0	NB

EXP #	BW ID	h (cm)	H_i (cm)	L (cm)	h_c/H_i	C_r	W (cm)	BT
65	BW-4	20.5	7.31	301.9	0.75	0.239	24.0	NB
66	BW-5	15	6.58	283.4	0.08	0.289	24.0	P
67	BW-5	15.5	8.54	276.8	0.12	0.162	24.0	P
68	BW-5	17.5	9.96	301.4	0.31	0.2448	24.0	P
69	BW-5	19.5	5.47	289.7	0.95	0.272	24.0	S
70	BW-5	19.5	6.76	278.5	0.77	0.246	24.0	S
71	BW-5	19.5	8.21	311.5	0.63	0.292	24.0	S
72	BW-5	20.5	6.03	321.3	1.01	0.314	24.0	NB
73	BW-5	20.5	7.31	301.9	0.85	0.263	24.0	S
74	BW-5	20.5	8.97	314.2	0.69	0.311	24.0	S
75	BW-5	21.5	6.23	333.3	1.16	0.321	24.0	NB
76	BW-5	22.5	6.40	326.5	1.28	0.280	24.0	NB
77	BW-5	23.5	6.30	326.5	1.46	0.280	24.0	NB
78	BW-5	24.5	5.37	318.9	1.90	0.223	24.0	NB
79	BW-5	24.5	6.45	314.2	1.58	0.181	24.0	NB

CHAPTER FIVE

CONCLUSIONS

5.1 CONCLUSIONS

Breakwaters are placed into a wave field with the goal of protecting a specified area by reducing the transmitted energy of an approaching wave through reflection and dissipation. Having their critics, none can doubt that when breakwaters fulfill their intended purpose they can be economically and environmentally beneficial to surrounding coastal communities. Advances continue in the study of submerged breakwaters to determine models that are not only effective but also progressive. Research such as presented in this manuscript and performed worldwide can combine to provide the information needed to accomplish this task.

This study examines the reflective characteristics of impermeable and permeable submerged trapezoidal breakwaters. The impermeable breakwater models are constructed from oriented strand board while one permeable breakwater is constructed from PVC pipes and the other consists of a wire cage filled with golf balls. A dimensional analysis is performed to obtain the dimensionless parameters governing wave reflection around an impermeable submerged breakwater. Sloping effects on reflection coefficient values are studied by varying the offshore slope of a submerged trapezoidal breakwater between three separate impermeable models, each with unique slopes. The reflection coefficient is not found to be significantly dependent upon the breakwater face slopes. Thus, a single slope, common to BW-2 of the impermeable tests,

is selected for both of the permeable breakwaters. Doing so provides consistency between their tests and the ability to compare permeable and impermeable breakwaters of the same geometry. The chosen slope for the permeable breakwater tests (same as BW-2) is a more common slope for practical applications of rubble-mound breakwaters than the steeper one (BW-1) and takes up less volume than the milder slope (BW-3). With 79 experiments formally presented herein, and numerous others ran (as shown in Figures 4.12 and 4.13), minimizing the volume of the test structure is important to ensure the ability to quickly fill and remove golf balls from the wire caged. Experimental results are compared to available reflection coefficient equations to determine their relevance to this study, and also to prove the need for a new parameterization. The Young and Testik (2011) parameterization (Equation 4.6) for impermeable submerged vertical breakwaters is found to be the best fit for the impermeable case, whereas Equation (2.16), proposed by Zanuttigh and van der Meer (2008), is discovered to fit both the impermeable and the permeable case well.

This study is necessary because it provides additional research and insight into a relatively undeveloped area of breakwater research. Practically no applicable comparisons with a full range of reflection coefficient values are available in the case of impermeable submerged trapezoidal breakwaters. The expectation of this study is that further analysis of the given data will provide a parameterization that complements those installing breakwaters. With such, the construction and design tasks related to submerged

trapezoidal breakwaters will be simplified and their execution allowed to be carried out more efficiently.

A discussion on design considerations is presented in Section 4.5 and highlights the impact of the bulge region on the placement of future breakwaters. Using the presented results, breakwaters may be placed accordingly to maximize their potential for wave sheltering. As the crest height of a submerged structure approaches the mean water level, the reflection coefficients it can produce are shown to increase. For maximum reflection, structures would thus be placed at the mean water level. However, other factors should be considered. Throughout the tidal cycle, water surface elevation fluctuations will eventually expose a breakwater whose crest is placed too closely to the mean water level. Also, the length and volume of a higher crested breakwater should be considered as these all can lead to higher overall project costs. The results of the study display a region with a peculiar bulge in the reflection coefficient values. This region is compared to similar findings from the tests described by Blenkinsopp and Chaplin (2008). In this region, it is expected that reflection values would continue the initially observed strong decay. However, values in this region exhibit an increase explained through the energy conservation (Equation 2.31) during different forms of wave-breaking. Initially, the dominant breaker type is a highly dissipative plunging breaker and a significant portion of the wave is reflected. Wave reflection strongly decays as the breakwater becomes further submerged and within the bulge region the breaker type transitions to spilling breakers, where less energy is dissipated and more energy is available to be divided

between the transmission and reflection coefficients of the breakwater. Such a region allows for submerged trapezoidal breakwaters to potentially be placed at depths where they will remain submerged throughout the tidal cycle, and yet still provide sufficient wave sheltering for a particular area. While observed reflection coefficient values within the bulge region (C_r ~ 0.3-0.4) are not as high as one may expect from a wave sheltering structure, the ability to induce spilling breakers allows the turbulence of such a breaker to continually dissipate energy past the breakwater until breaking at the shore. Beyond the bulge region, reflection coefficient values appear to slowly decay. Further testing will be needed if data points in the region past the bulge are required.

5.2 FUTURE WORK

There are several potential extensions of the work presented herein. Some of the aspirations for future work are as follows: comparing reflection coefficient measurement methodologies, defining a parameterization for the reflection coefficients of submerged trapezoidal breakwaters, producing a more efficient artificial reef structure and an accompanying parameterization, and concluding the effect of a wide range of slopes on the reflection coefficients from submerged breakwaters.

One example of future work could involve comparing different methods of reflection coefficient measurement over a sloping beach, similar to the procedures of Isaacson (1991). Reflection coefficient values may be questioned based off the methodology used in their determination. Performing this analysis would help eliminate any suspicions

surrounding the accuracy of certain methods when determining reflection coefficient values in laboratory wave tank tests over a sloping beach. Although a preliminary such investigation has been presented here in Chapter 2 for the method of Goda and Suzuki (1976), an extension of this is desirable. Also, several methods for measuring wave reflection coefficients (i.e. Chang and Hsu, 2003) over a slope have been developed but have not had extensive laboratory testing and confirmation.

Primarily, a parameterization is to be pursued in order to assist future engineers with their task of efficiently designing successful erosion prevention systems. Designers will benefit through the streamlined design process that such a parameterization would offer. The results offered in this manuscript are unlike those seen elsewhere, but its correlation with the data of Blenkinsopp and Chaplin (2008) provides a basis for credibility which cannot be ignored. Thus, further research should be taken to supplement the existing data set and confirm present findings as well as possibly improve their reliability.

Additional testing should include different structures, preferably focusing on sustainable artificial reef-type structures. There are few easily applicable equations for such structures, thus an extensive study to analyze typical reflection coefficients at a wide range of porosities, shapes, and design styles would enhance the present knowledge available for these structures. Testing could also include the development of a unique structure with the intent to enhance the protective capabilities of submerged breakwaters

while also maximizing the recreational potential and aquatic-friendly behavior of such a structure.

Along with the development of a new structure, an extensive range of slopes should be tested to further illustrate the impact a slope has on the reflection coefficient, similar to Neelamani and Sandhya (2003) but would instead be focused on submerged breakwaters rather than emerged seawalls. Such testing would describe whether the reflection coefficient decays, increases, or remains the same as the slope of a structure changes as this could provide insight into the relationship between different studies. For instance, Blenkinsopp and Chaplin (2008) employ a 1:10 slope for their structure which could explain why the bulge region of their data is more clearly defined and why their reflection coefficient values are reported to be smaller overall in comparison to the present study. The completion of these proposed tasks, in conjunction with the supplied results, will equip future researchers and engineers with a trustworthy understanding of the reflective behaviors of impermeable and permeable submerged trapezoidal breakwaters.

APPENDIX

A: PERMISSIONS FOR REUSE

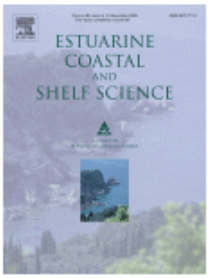

Title: Beach response to shore-parallel breakwaters at Sea Palling, Norfolk, UK
Author: F. Thomalla, C. E. Vincent
Publication: Estuarine, Coastal and Shelf Science
Publisher: Elsevier
Date: February 2003

Logged in as:
Mathew Hornack
Account #:
3000351944

LOGOUT

License Number	2533470686671
License date	Oct 21, 2010
Licensed content publisher	Elsevier
Licensed content publication	Estuarine, Coastal and Shelf Science
Licensed content title	Beach response to shore-parallel breakwaters at Sea Palling, Norfolk, UK
Licensed content author	F. Thomalla, C. E. Vincent
Licensed content date	February 2003
Licensed content volume number	56
Licensed content issue number	2
Number of pages	10
Type of Use	reuse in a thesis/dissertation
Intended publisher of new work	other
Portion	figures/tables/illustrations
Number of figures/tables /illustrations	5
Format	both print and electronic
Are you the author of this Elsevier article?	No
Will you be translating?	No
Order reference number	
Title of your thesis/dissertation	Wave Reflection Characteristics of Permeable and Impermeable Submerged Trapezoidal Breakwaters
Expected completion date	Nov 2010
Estimated size (number of pages)	80
Elsevier VAT number	GB 494 6272 12
Permissions price	0.00 USD
Value added tax 0.0%	0.0 USD / 0.0 GBP
Total	0.00 USD

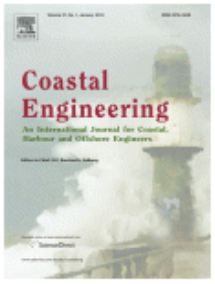

Title: Wave runup, transmission, and reflection for structures armored with CORE-LOC®
Author: Ivano Melito, Jeffrey A. Melby
Publication: Coastal Engineering
Publisher: Elsevier
Date: March 2002

License Number	2533470860062
License date	Oct 21, 2010
Licensed content publisher	Elsevier
Licensed content publication	Coastal Engineering
Licensed content title	Wave runup, transmission, and reflection for structures armored with CORE-LOC®
Licensed content author	Ivano Melito, Jeffrey A. Melby
Licensed content date	March 2002
Licensed content volume number	45
Licensed content issue number	1
Number of pages	20
Type of Use	reuse in a thesis/dissertation
Intended publisher of new work	other
Portion	figures/tables/illustrations
Number of figures/tables /illustrations	2
Format	both print and electronic
Are you the author of this Elsevier article?	No
Will you be translating?	No
Order reference number	
Title of your thesis/dissertation	Wave Reflection Characteristics of Permeable and Impermeable Submerged Trapezoidal Breakwaters
Expected completion date	Nov 2010
Estimated size (number of pages)	80
Elsevier VAT number	GB 494 6272 12
Permissions price	0.00 USD
Value added tax 0.0%	0.0 USD / 0.0 GBP
Total	0.00 USD

Title: Wave reflection characteristics of plane, dentated and serrated seawalls
Author: S. Neelamani, N. Sandhya
Publication: Ocean Engineering
Publisher: Elsevier
Date: August 2003

License Number	2533470504062
License date	Oct 21, 2010
Licensed content publisher	Elsevier
Licensed content publication	Ocean Engineering
Licensed content title	Wave reflection characteristics of plane, dentated and serrated seawalls
Licensed content author	S. Neelamani, N. Sandhya
Licensed content date	August 2003
Licensed content volume number	30
Licensed content issue number	12
Number of pages	27
Type of Use	reuse in a thesis/dissertation
Intended publisher of new work	other
Portion	figures/tables/illustrations
Number of figures/tables /illustrations	5
Format	both print and electronic
Are you the author of this Elsevier article?	No
Will you be translating?	No
Order reference number	
Title of your thesis/dissertation	Wave Reflection Characteristics of Permeable and Impermeable Submerged Trapezoidal Breakwaters
Expected completion date	Nov 2010
Estimated size (number of pages)	80
Elsevier VAT number	GB 494 6272 12
Permissions price	0.00 USD
Value added tax 0.0%	0.0 USD / 0.0 GBP
Total	0.00 USD

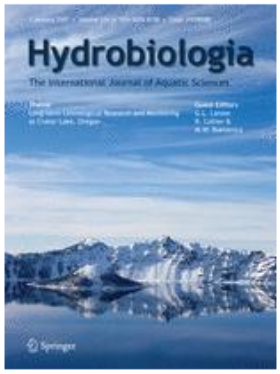

Title: Effects of an artificial protection structure on the sandy shore macrofaunal community: the special case of Lido di Dante (Northern Adriatic Sea)
Author: Fabio Bertasi
Publication: Hydrobiologia
Publisher: Springer
Date: Jul 1, 2007

Logged in as:
Mathew Hornack
Account #:
3000351944
LOGOUT

License Number	2533471134452
License date	Oct 21, 2010
Licensed content publisher	Springer
Licensed content publication	Hydrobiologia
Licensed content title	Effects of an artificial protection structure on the sandy shore macrofaunal community: the special case of Lido di Dante (Northern Adriatic Sea)
Licensed content author	Fabio Bertasi
Licensed content date	Jul 1, 2007
Volume number	586
Issue number	1
Type of Use	Thesis/Dissertation
Portion	Figures
Author of this Springer article	No
Title of your thesis / dissertation	Wave Reflection Characteristics of Permeable and Impermeable Submerged Trapezoidal Breakwaters
Expected completion date	Nov 2010
Estimated size(pages)	80
Total	0.00 USD

Title: Wave Phase Shift at Coastal Structures
Author: James SutherlandTom O'Donoghue
Publication: Journal of Waterway, Port, Coastal, and Ocean Engineering
Publisher: American Society of Civil Engineers
Date: 03/01/1998

Logged in as:
Mathew Hornack
Account #:
3000351944
LOGOUT

Type of use: Dissertation/Thesis

Portion: figures/tables/illustrations

Format: print and electronic

Use of this content will make up more than 25% of the new work: no

Author of this ASCE work or ASCE will publish the new work: no

Title: Investigation of the effects of offshore breakwater parameters on sediment accumulation
Author: Ali Remzi Birben, İsmail Hakkı Özölçer, Servet Karasu, Murat İhsan Kömürcü
Publication: Ocean Engineering
Publisher: Elsevier
Date: February 2007

License Number	2542761256918
License date	Nov 05, 2010
Licensed content publisher	Elsevier
Licensed content publication	Ocean Engineering
Licensed content title	Investigation of the effects of offshore breakwater parameters on sediment accumulation
Licensed content author	Ali Remzi Birben, İsmail Hakkı Özölçer, Servet Karasu, Murat İhsan Kömürcü
Licensed content date	February 2007
Licensed content volume number	34
Licensed content issue number	2
Number of pages	19
Type of Use	reuse in a thesis/dissertation
Intended publisher of new work	other
Portion	figures/tables/illustrations
Number of figures/tables /illustrations	2
Format	both print and electronic
Are you the author of this Elsevier article?	No
Will you be translating?	No
Order reference number	
Title of your thesis/dissertation	Wave Reflection Characteristics of Permeable and Impermeable Submerged Trapezoidal Breakwaters
Expected completion date	Nov 2010
Estimated size (number of pages)	80
Elsevier VAT number	GB 494 6272 12
Permissions price	0.00 USD
Value added tax 0.0%	0.0 USD / 0.0 GBP
Total	0.00 USD

Title: Scour at the head of a vertical-wall breakwater
Author: B. M. Sumer, J. Fredsøe
Publication: Coastal Engineering
Publisher: Elsevier
Date: January 1997

License Number	2644841376014
License date	Apr 09, 2011
Licensed content publisher	Elsevier
Licensed content publication	Coastal Engineering
Licensed content title	Scour at the head of a vertical-wall breakwater
Licensed content author	B. M. Sumer, J. Fredsøe
Licensed content date	January 1997
Licensed content volume number	29
Licensed content issue number	3-4
Number of pages	30
Type of Use	reuse in a thesis/dissertation
Portion	figures/tables/illustrations
Number of figures/tables /illustrations	1
Format	both print and electronic
Are you the author of this Elsevier article?	No
Will you be translating?	No
Order reference number	
Title of your thesis/dissertation	Wave Reflection Characteristics of Permeable and Impermeable Submerged Trapezoidal Breakwaters
Expected completion date	Apr 2011
Estimated size (number of pages)	124
Elsevier VAT number	GB 494 6272 12
Permissions price	0.00 USD
VAT/Local Sales Tax	0.0 USD / 0.0 GBP
Total	0.00 USD

Title: The effect of relative crest submergence on wave breaking over submerged slopes
Author: C.E. Blenkinsopp, J.R. Chaplin
Publication: Coastal Engineering
Publisher: Elsevier
Date: December 2008

Logged in as:
Mathew Hornack
Account #:
3000351944

LOGOUT

License Number	2644850204016
License date	Apr 09, 2011
Licensed content publisher	Elsevier
Licensed content publication	Coastal Engineering
Licensed content title	The effect of relative crest submergence on wave breaking over submerged slopes
Licensed content author	C.E. Blenkinsopp, J.R. Chaplin
Licensed content date	December 2008
Licensed content volume number	55
Licensed content issue number	12
Number of pages	8
Type of Use	reuse in a thesis/dissertation
Portion	figures/tables/illustrations
Number of figures/tables /illustrations	1
Format	both print and electronic
Are you the author of this Elsevier article?	No
Will you be translating?	No
Order reference number	
Title of your thesis/dissertation	Wave Reflection Characteristics of Permeable and Impermeable Submerged Trapezoidal Breakwaters
Expected completion date	Apr 2011
Estimated size (number of pages)	124
Elsevier VAT number	GB 494 6272 12
Permissions price	0.00 USD
VAT/Local Sales Tax	0.0 USD / 0.0 GBP
Total	0.00 USD

REFERENCES

ASR Limited. A review of existing multi-purpose artificial surfing reefs and the physical properties behind their function. ASR America, Marine Consulting and Research. Cocoa Beach, FL. 2008.

Basco, D.R. Beach monitoring results and management plan FCTCLANT, Dam Neck, Virginia Beach, VA. Final Report, Beach Consultants, Inc. Norfolk, VA. 2000.

Battjes, J.A. Computation of set-up, longshore currents, run-up, and overtopping due to wind-generated waves. Comm. on Hydraulics, Department of Civil Engineering, Delft University of Technology, Report 74-2. 1974.

Bertasi, F., Colangelo, M.A., Abbiati, M., Ceccherelli, V.U. Effects of an artificial protection structure on the sandy shore macrofaunal community: the special case of Lido di Dante (Northern Adriatic Sea). Hydrobiologia (586). 2007. pp. 277-290.

Birben, A.R., Özölçer, İ.H., Karasu, S., Kömürcü, M.İ. Investigation of the effects of offshore breakwater parameters on sediment accumulation. Ocean Engineering (34). 2007. pp. 284-302.

Blenkinsopp, C.E., Chaplin, J.R. The effect of relative crest submergence on wave breaking over submerged slopes. Coastal Engineering (55). 2008. pp. 967-974.

Chakrabarti, S.K. Wave interaction with an upright breakwater structure. Ocean Engineering (26). 1999. pp. 1003-1021.

Chang, H.-K., Hsu, T.-W. A two-point method for estimating wave reflection over a sloping beach. Ocean Engineering (30). 2003. pp. 1833-1847.

Cokgor, S., Kapdasli, M.S. Performance of submerged breakwaters as environmental friendly coastal structures. Environmentally Friendly Coastal Protection (53). 2005. pp. 211-218.

D'Angremond, K., van der Meer, J.W., De Jong, R.J. Wave transmission at low-crested structures. Proc. of 25th ICCE. 1996. pp. 2418-2427.

Dally, W.R., Pope, J. Detached breakwaters for shore protection. Technical Report CERC-86-1, US Army Corps of Engineers WES. 1986.

Daniil, E.I., Tsoukala, V.K., Moutzouris, C.I. The beneficial role of rubble mound coastal structures on seawater oxygenation. Annales Geophysicae (18). 2000. pp. 1360-1371.

Davies, B.L. Model testing of low-crested breakwaters. Trident Scholar Project Report no. 177, U.S. Naval Academy. Annapolis, Maryland. 1991.

Dong, G.H., Zheng, Y.N., Li, Y.C., Teng, B., Guan, C.T., Lin, D.F. Experiments on wave transmission coefficients of floating breakwaters. Ocean Engineering (35). 2008. pp. 931-938.

Frihy, O.E., El Ganaini, M.A., El Sayed, W.R., Iskander, M.M. The role of fringing coral reef in beach protection of Hurghada, Gulf of Suez, Red Sea of Egypt. Ecological Engineering (22). 2004. pp. 17-25.

Goda, Y., Suzuki, Y. Estimation of incident and reflected waves in random wave experiments. Proc. of 15th ICCE. 1976. pp. 828-845.

Hughes, S.A., Fowler, J.E. Estimating wave-induced kinematics at sloping structures. Journal of Waterway, Port, Coastal, and Ocean Engineering (121). 1995. pp. 209-215.

Hur, D.-S., Kawashima, N., Iwata, K. Experimental study of the breaking limit of multi-directional random waves passing over an impermeable submerged breakwater. Ocean Engineering (30). 2003. pp. 1923-1940.

Isaacson, M. Measurement of regular wave reflection. Journal of Waterway, Port, Coastal, and Ocean Engineering (117). 1991. pp. 553-569.

Jeon, C.-H., Cho, Y.-S. Bragg reflection of sinusoidal waves due to trapezoidal submerged breakwaters. Ocean Engineering (33). 2006. pp. 2067-2082.

Johnson, H. K. Wave modeling in the vicinity of submerged breakwaters. Coastal Engineering (53). 2006. pp. 39-48

Kajima, R. Estimation of incident wave spectrum in the sea area influenced by reflection. Coastal Engineering in Japan (12). 1969. pp. 9-16.

Koftis, T., Prinos, P. 2DV hydrodynamics of a catamaran-shaped floating structure. IASME Transactions (2). 2005. pp. 1180-1189.

Kriebel, D.L. Vertical wave barriers: wave transmission and wave forces. Proc. of 23rd ICCE. 1992. pp. 1313-1326.

Kuo, C.A., Hwung, H.H., Chien, C.H. Using time-stack overlooking images to separate incident and reflected waves in wave flume. Wave Motion (46). 2009. pp. 189-199.

Loi, T. Environmental assemblages and intertidal assemblages on hard substrates in the port of Long Beach, California, USA. Marine Biology (63). 1981. pp. 197-211.

Madsen, P.A. Wave reflection from a vertical permeable wave absorber. Coastal Engineering (7). 1983. pp. 381-396.

Mani, J.S. Experimental and numerical investigations on zigzag porous screen breakwater. Natural Hazards (49). 2009. pp. 401-409.

Mansard, E.P.D., Funke, E.R. The measurement of incident and reflected spectra using a least squares method. Proc. of 17th ICCE. 1980. pp. 154-172.

Martin, T.R., Smith, J.B. Analysis of the performance of the prefabrication erosion prevention (P.E.P.) reef system, Town of Palm Beach, Florida. CERC Technical Note, CETN-II-36. Vicksburg, Mississippi, USA. 1997.

McCartney, B.L. Floating Breakwater Design. Journal of Waterway, Port, Coastal, and Ocean Engineering (3). 1985. pp. 304-318.

Melito, I., Melby, J. A. Wave runup, transmission, and reflection for structures armored with CORE-LOC. Coastal Engineering (45). 2002. pp. 33-52.

Moraes, CDE C. Experiments of wave reflexion on impermeable slopes. Proc. of 12th ICCE. 1970. pp. 509-521.

Muttray, M., Oumeraci, H., Zeimmerman, C., Partenscky, H.W. Wave energy dissipation on and in rubble mound structures. Proc. of 23rd ICCE. 1992. pp. 1434-1447.

Muttray, M., Oumeraci, H. Wave transformation at sloping perforated walls. Proc. of 28th ICCE. 2002. pp. 2031-2043.

Muttray, M., Oumeraci, H., Oever, E. Wave reflection and wave run-up at rubble mound breakwaters. Proc. of 30th ICCE. 2006. pp. 4313-4324.

Nagashima, H. Reflection and breaking of internal waves on a sloping beach. J. Oceanogr. Soc. Japan (27). 1971. pp. 1-6.

Neelamani, S., Sandhya, N. Wave reflection characteristics of plane, dentated and serrated seawalls. Ocean Engineering (30). 2003. pp. 1507-1533.

Palmer, G.N., Christian, C.D. Design and construction of rubble mound breakwaters. IPENZ Transactions (25). 1998. pp. 19-33.

Pilarczyk, K.W. Design of low-crested (submerged) structures – an overview. 6th International Conference on Coastal and Port Engineering in Developing Countries. 2003. pp. 1-19.

Pope, J. Segmented offshore breakwaters: an alternative for beach erosion control. Proceedings of the 9th Annual Conference of the Coastal Society. 1985. pp. 287-292.

Postma, G.M. Wave reflection from rock slopes under random wave attack. M. Sc. Thesis. Faculty of Civil Engineering, Delft University of Technology, Delft, The Netherlands. 1989.

Ranasinghe, R., Larson, M., Savioli, J. Shoreline response to a single shore-parallel submerged breakwater. Coastal Engineering (57). 2010. pp. 1006-1017.

Reish, D.J., Soule, D.F., Soule, J.D. The benthic biological conditions of Los Angeles – Long Beach harbors: Results of 28 years of investigations and monitoring. Helgoländer Meeresunters (34). 1980. pp. 193-205.

Saengsupavanich, C., Chonwattana, S., Naimsampao, T. Coastal erosion through integrated management: A case of Southern Thailand. Ocean & Coastal Management (52). 2009. pp. 307-316.

Seabrook, S.R., Hall, K.R. Wave transmission at submerged rubble mound breakwaters. Proc. of 26th ICCE. 1998. pp. 2000-2013.

Seelig, W.N., Ahrens, J.P. Estimation of Wave Reflection and Energy Dissipation Coefficients for Beaches, Revetments, and Breakwaters. CERC Technical Report No. 81-1. Fort Belvoir, Virginia, USA. 1981.

Shore Protection Manual. Coastal Engineering Research Center. U.S. Army Corps of Engineers. 1984.

Silva, R., Govaere, G., Salles, P. Wave interaction with cylindrical porous piles. Ocean Engineering (30). 2003. pp. 1719-1740.

Smith, E.R., Kraus, N.C. Laboratory study on macro-features of wave breaking over bars and artificial reefs. CERC Technical Report No. 90-12. Vicksburg, Mississippi, USA. 1990.

Stamos, D.G., Hajj, M.R. Reflection and transmission of waves over submerged breakwaters. Journal of Engineering Mechanics (127). 2001. pp. 99-105.

Sumer, B.M., Fredsøe, J. Scour at the head of a vertical-wall breakwater. Coastal Engineering (29). 1997. pp. 201-230.

Sumer, B.M., Fredsøe, J. Experimental study of 2D scour and its protection at a rubble-mound breakwater. Coastal Engineering (40). 2000. pp. 59-87.

Sutherland, J., O'Donoghue, T. Wave phase shift at coastal structures. Journal of Waterway, Port, Coastal, and Ocean Engineering (124). 1998a. pp. 90-98.

Sutherland, J., O'Donoghue, T. Characteristics of wave reflection spectra. Journal of Waterway, Port, Coastal, and Ocean Engineering (124). 1998b. pp. 303-311.

Taira, K., Nagata, Y. Experimental study of wave reflection by a sloping beach. J. Oceanogr. Soc. Japan (24). 1968. pp. 242-252.

Thomalla, F., Vincent, C.E. Beach response to shore-parallel breakwaters at Sea Palling, Norfolk, UK. Estuarine, Coastal and Shelf Science (56). 2003. pp. 203-212.

Twu, S.-W., Chieu, C.-C. A highly wave dissipation offshore breakwater. Ocean Engineering (27). 2000. pp. 315-330.

U.S. Army Corps of Engineers. Coastal Engineering Manual. Engineer Manual 1110-2-1100, U.S. Army Corps of Engineers, Washington, D.C. 2006. (in 6 volumes).

van der Meer, J.W. Conceptual design of rubble mound breakwaters. Advances in Coastal and Ocean Engineering. 1995. pp. 221-315.

Vidal, C., Losada, M.A., Medina, R., Mansard, E.P.D., Gomez-Pina, G. A universal analysis for the stability of both low-crested and submerged breakwaters. Proc. of 23rd ICCE. 1992. pp. 1680-1692.

Young, D.M. A laboratory study on the effects of submerged vertical and semicircular breakwaters on near-field coastal hydrodynamics and morphodynamics. M. Sc. Thesis. Department of Civil Engineering, Clemson University, Clemson, South Carolina, USA. 2008.

Young, D.M., Testik, F.Y. Wave reflection by submerged vertical and semicircular breakwaters. Ocean Engineering. 2011. (under review)

Zanuttigh, B., van der Meer, J.W. Wave reflection from coastal structures in design conditions. Coastal Engineering (55). 2008. pp. 771-779.